



US 20150118972A1

(19) **United States**
(12) **Patent Application Publication**
Montgomery et al.

(10) **Pub. No.: US 2015/0118972 A1**
(43) **Pub. Date: Apr. 30, 2015**

(54) **ANTENNA STRUCTURES AND METHODS THEREOF**

Publication Classification

(71) Applicant: **Skycross, Inc.**, Fremont, CA (US)
(72) Inventors: **Mark T. Montgomery**, Melbourne Beach, FL (US); **Frank M. Caimi**, Vero Beach, FL (US); **Duane Rabe**, Hawthorn Woods, IL (US)
(73) Assignee: **Skycross, Inc.**, Fremont, CA (US)

(51) **Int. Cl.**
H04B 1/40 (2006.01)
H01Q 1/52 (2006.01)
H01Q 1/50 (2006.01)
G01R 29/08 (2006.01)
(52) **U.S. Cl.**
CPC **H04B 1/401** (2013.01); **G01R 29/0807** (2013.01); **H01Q 1/521** (2013.01); **H01Q 1/50** (2013.01)

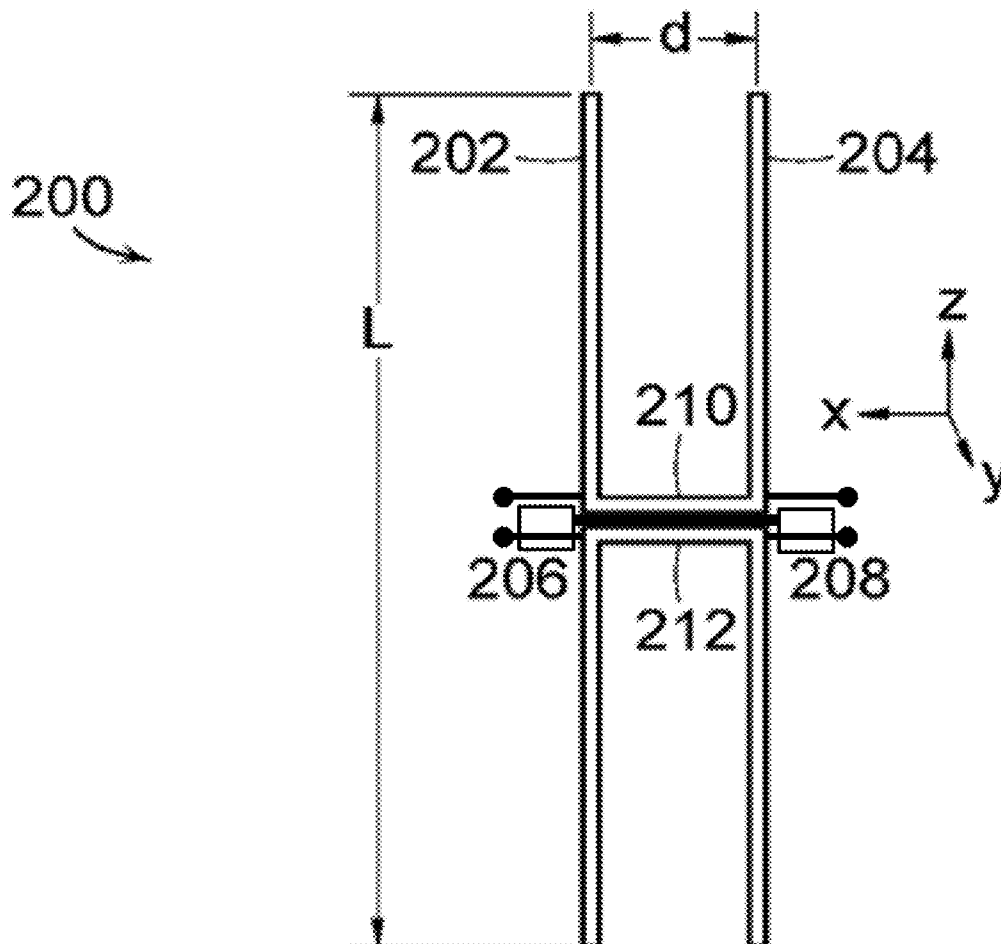
(21) Appl. No.: **14/266,008**

(22) Filed: **Apr. 30, 2014**

Related U.S. Application Data

(60) Provisional application No. 61/896,233, filed on Oct. 28, 2013, provisional application No. 61/932,831, filed on Jan. 29, 2014, provisional application No. 61/941,888, filed on Feb. 19, 2014.

(57) **ABSTRACT**
A system that incorporates the subject disclosure may include, for example, a circuit for measuring from a near field sensor a first signal representing radiated energy from an antenna structure, measuring from a probe a second signal supplied to the antenna structure, determining a phase differential from a first phase of the first signal and a second phase of the second signal, detecting a frequency offset of the antenna structure based on the phase differential, and adjusting an operating frequency of the antenna structure to mitigate the frequency offset. Other embodiments are disclosed.



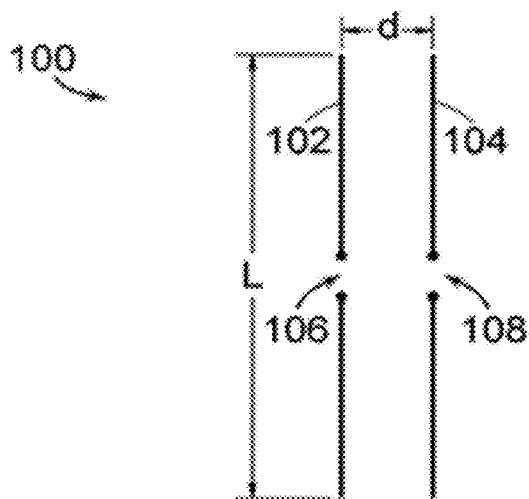


FIG. 1A

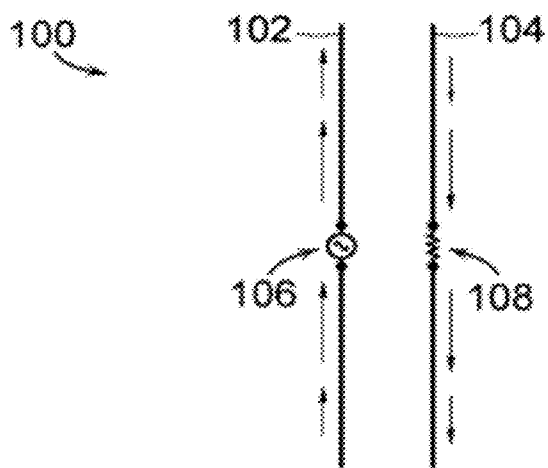


FIG. 1B

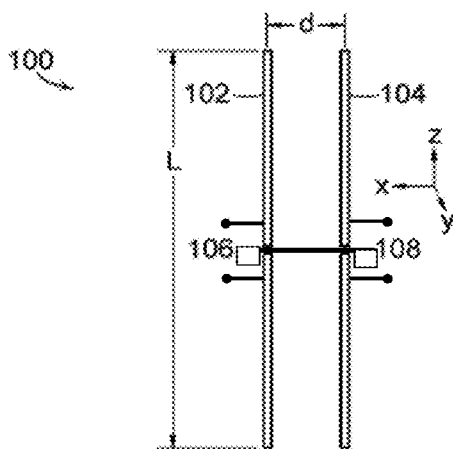


FIG. 1C

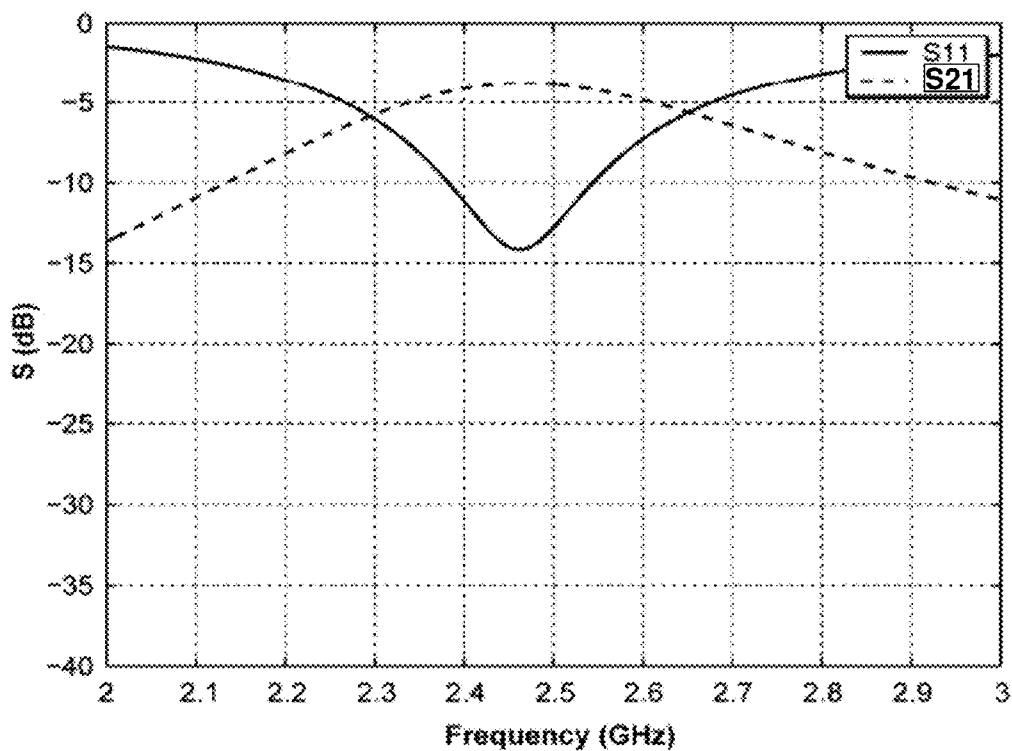


FIG. 1D

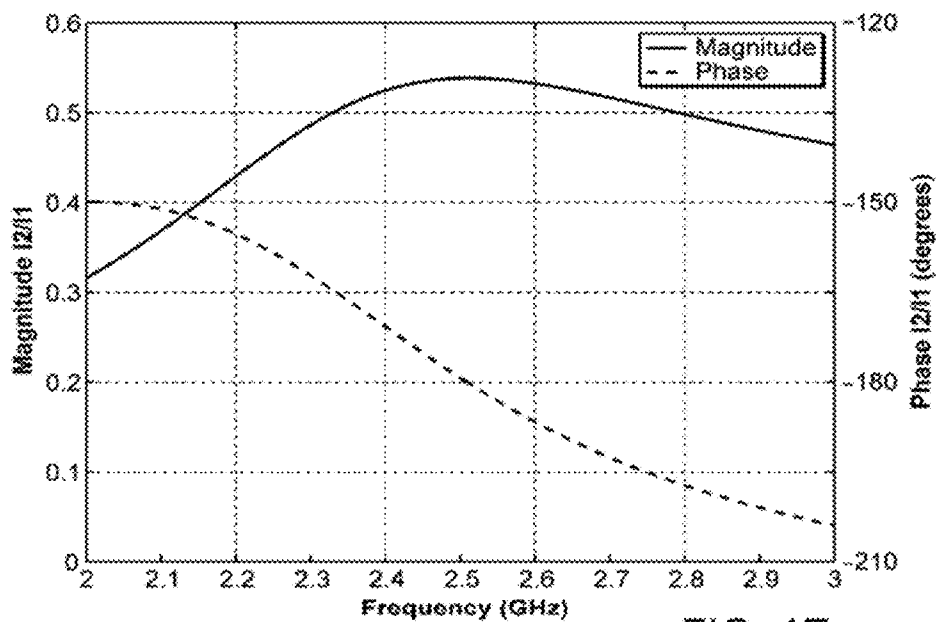


FIG. 1E

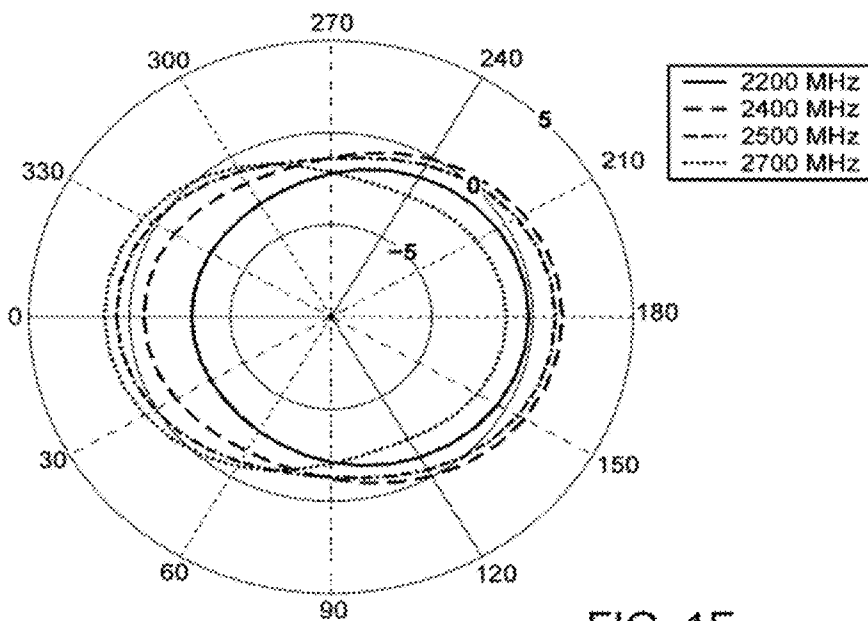


FIG. 1F

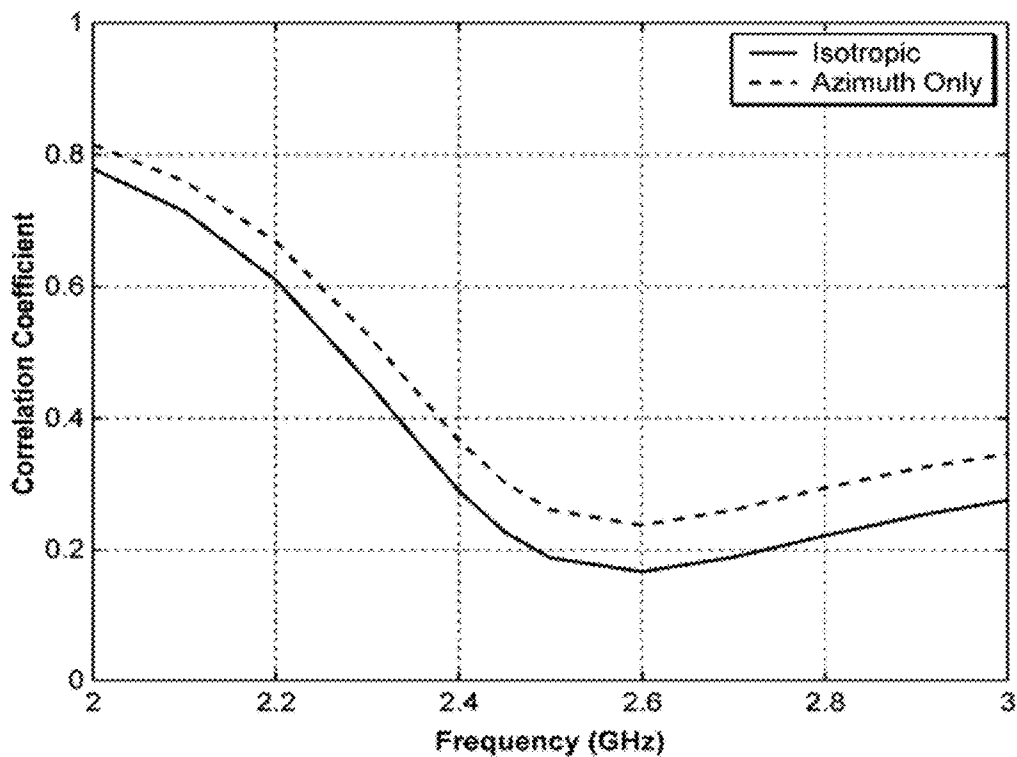


FIG. 1G

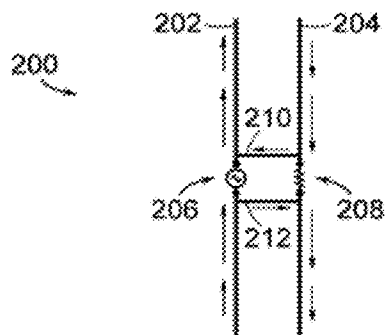


FIG. 2A

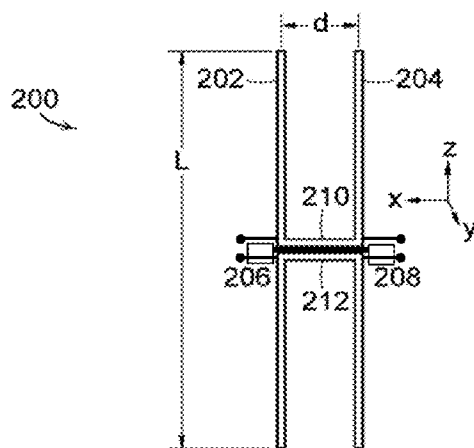


FIG. 2B

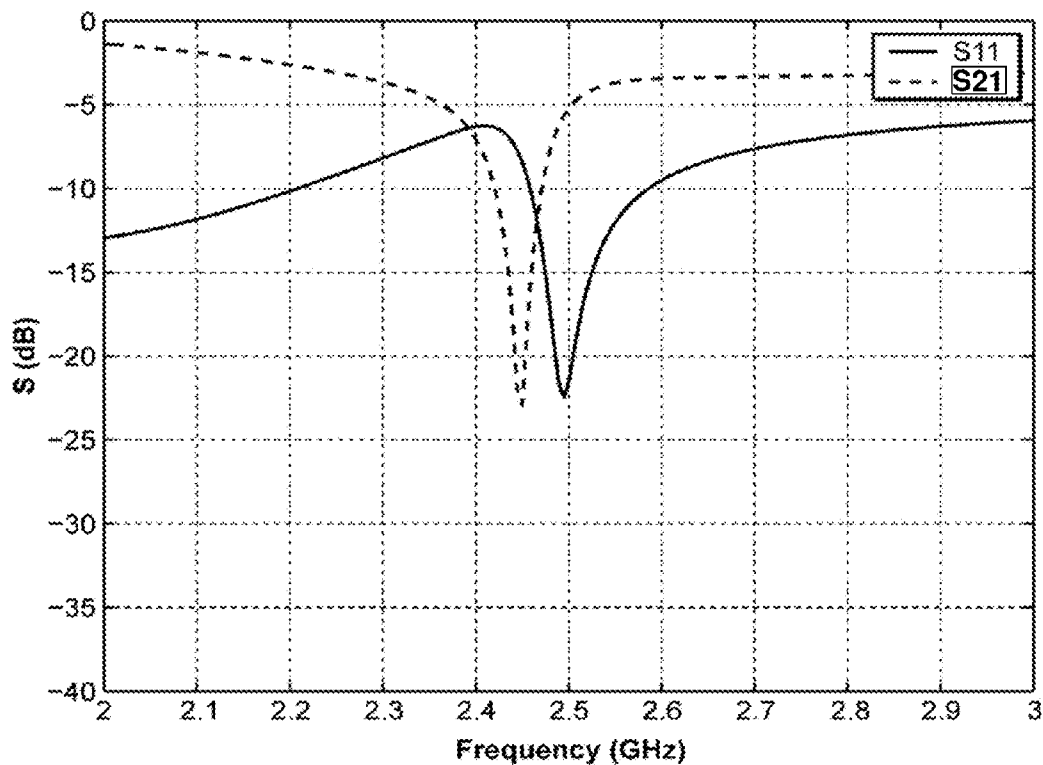


FIG. 2C

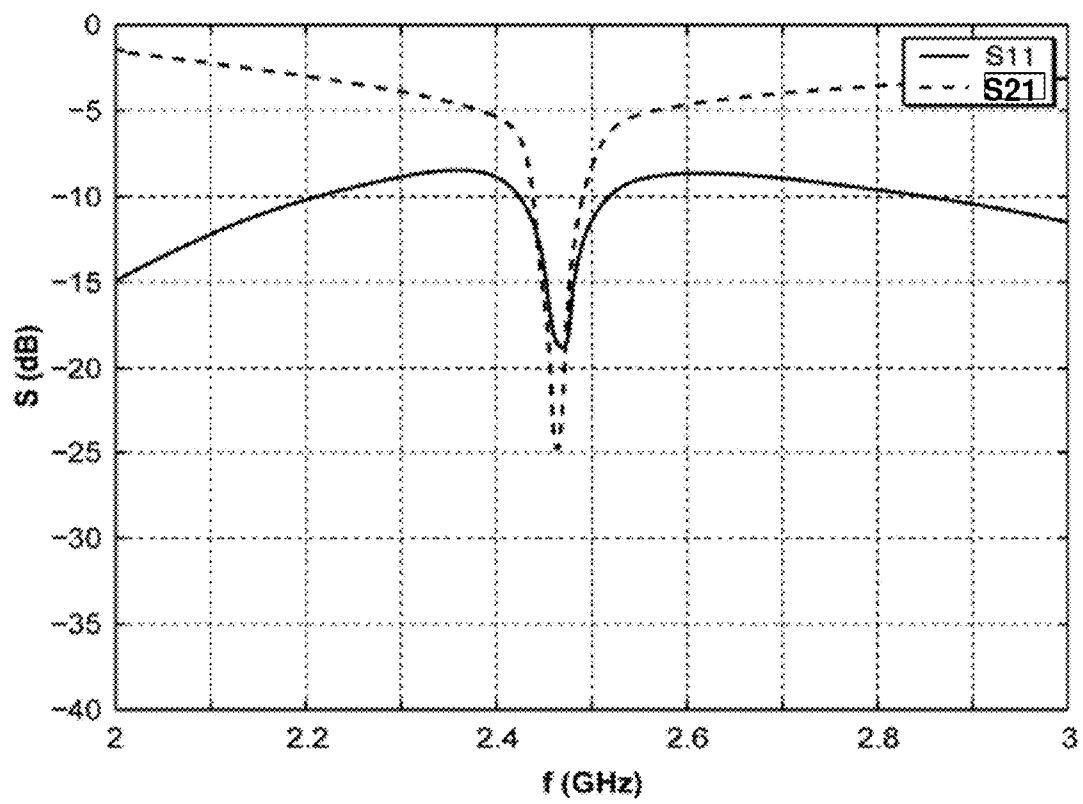


FIG. 2D

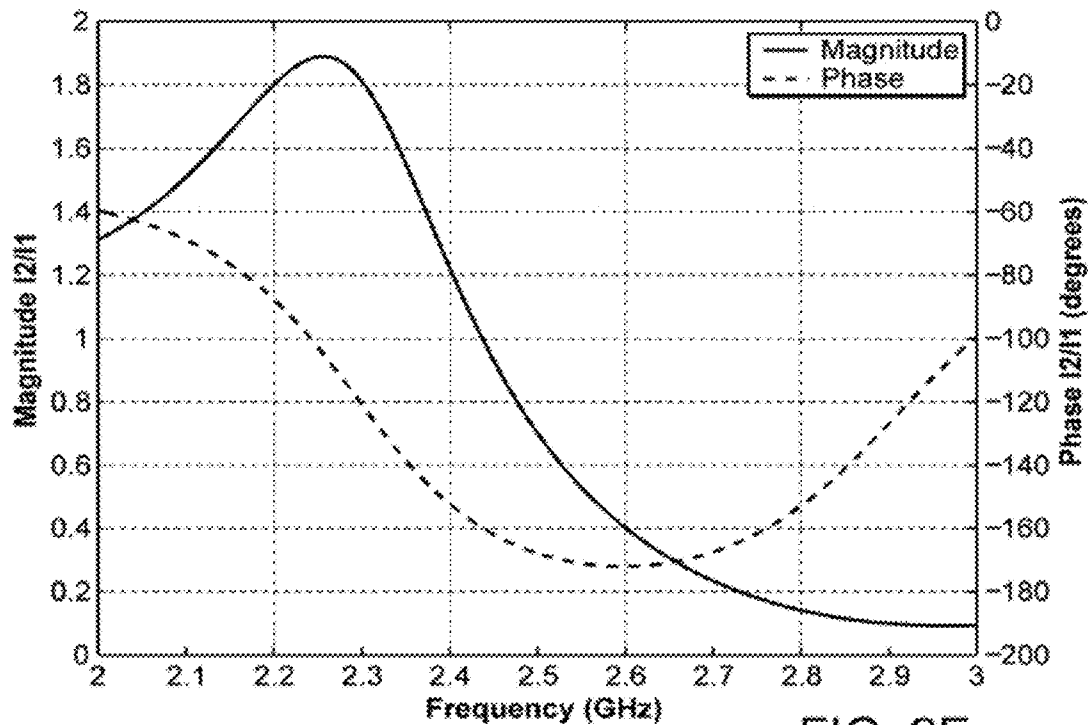


FIG. 2E

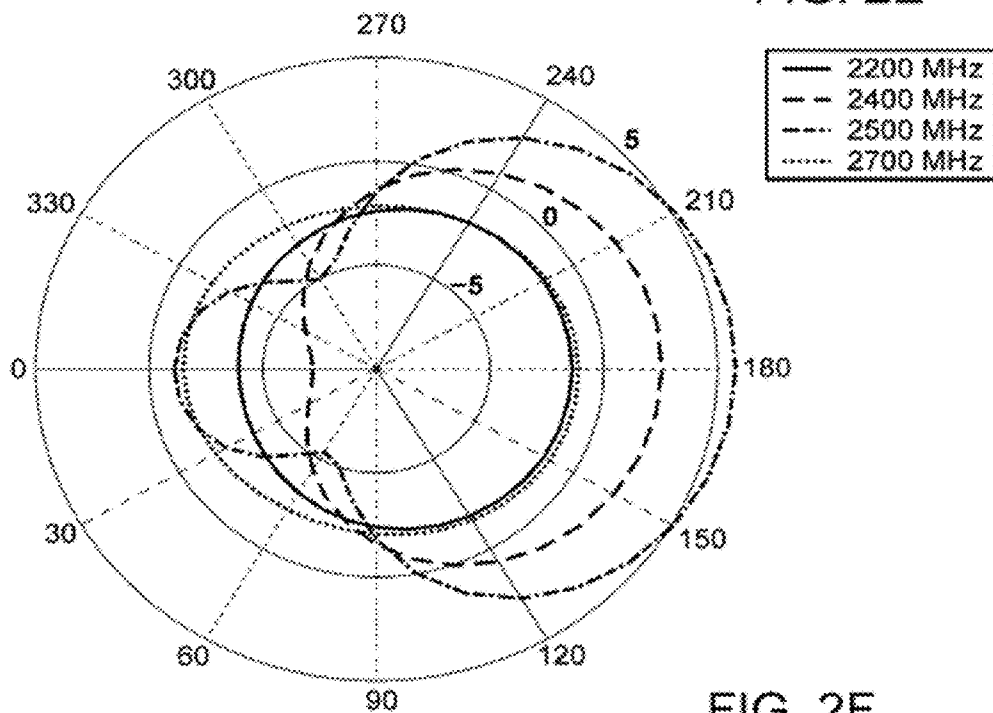


FIG. 2F

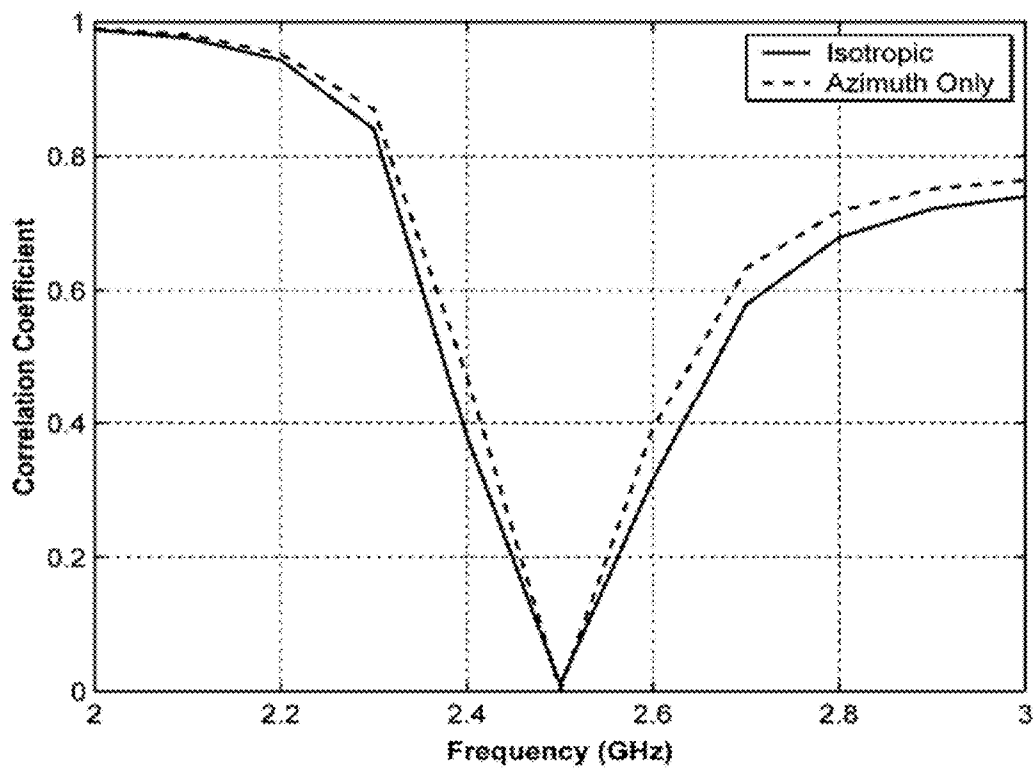


FIG. 2G

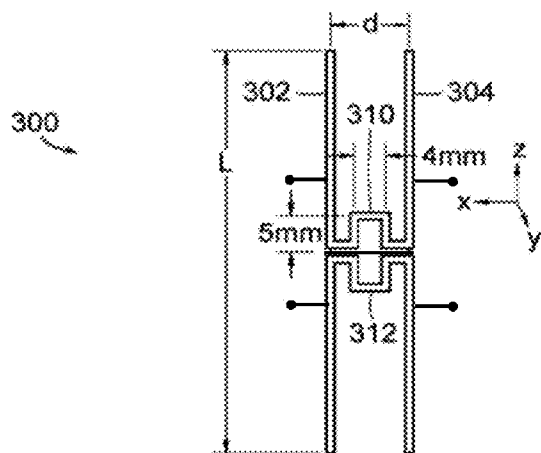


FIG. 3A

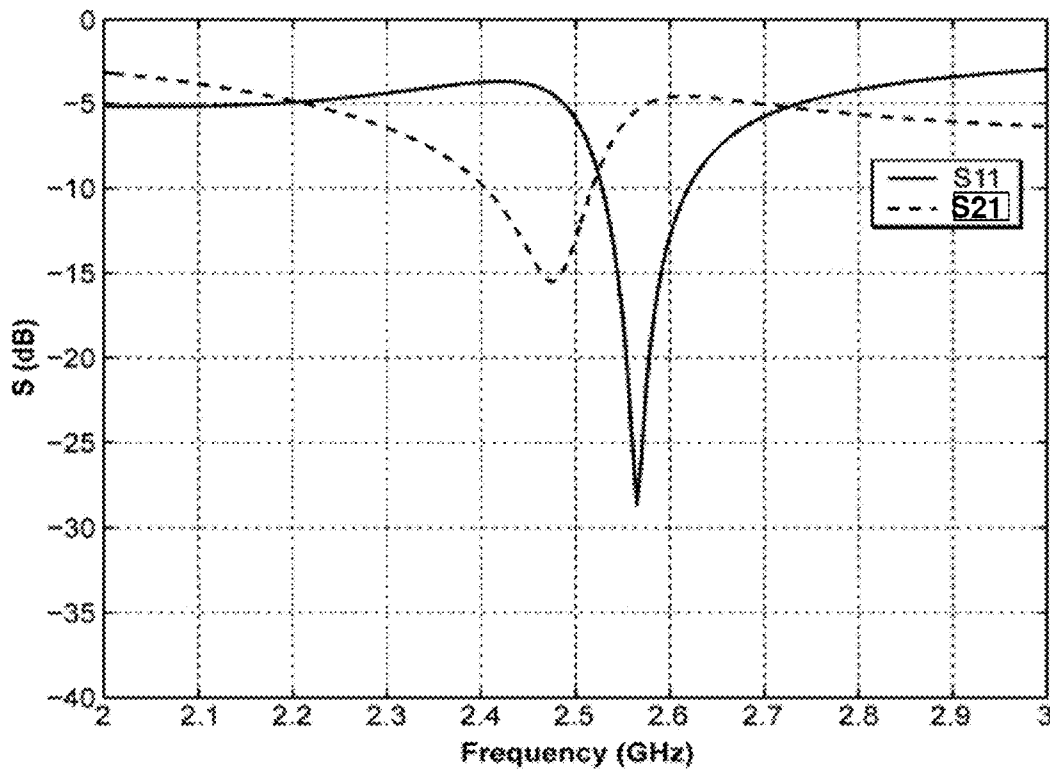


FIG. 3B

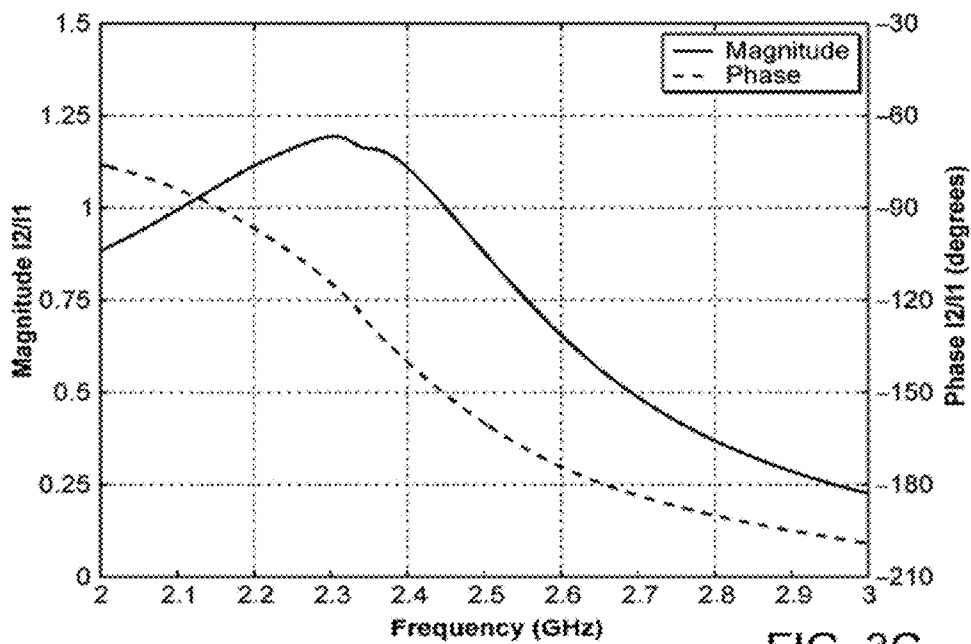


FIG. 3C

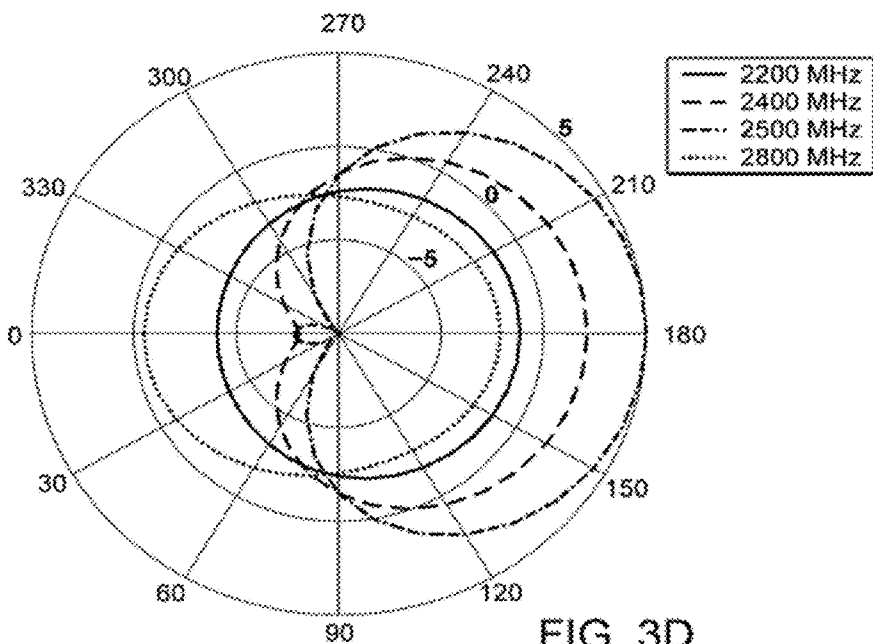


FIG. 3D

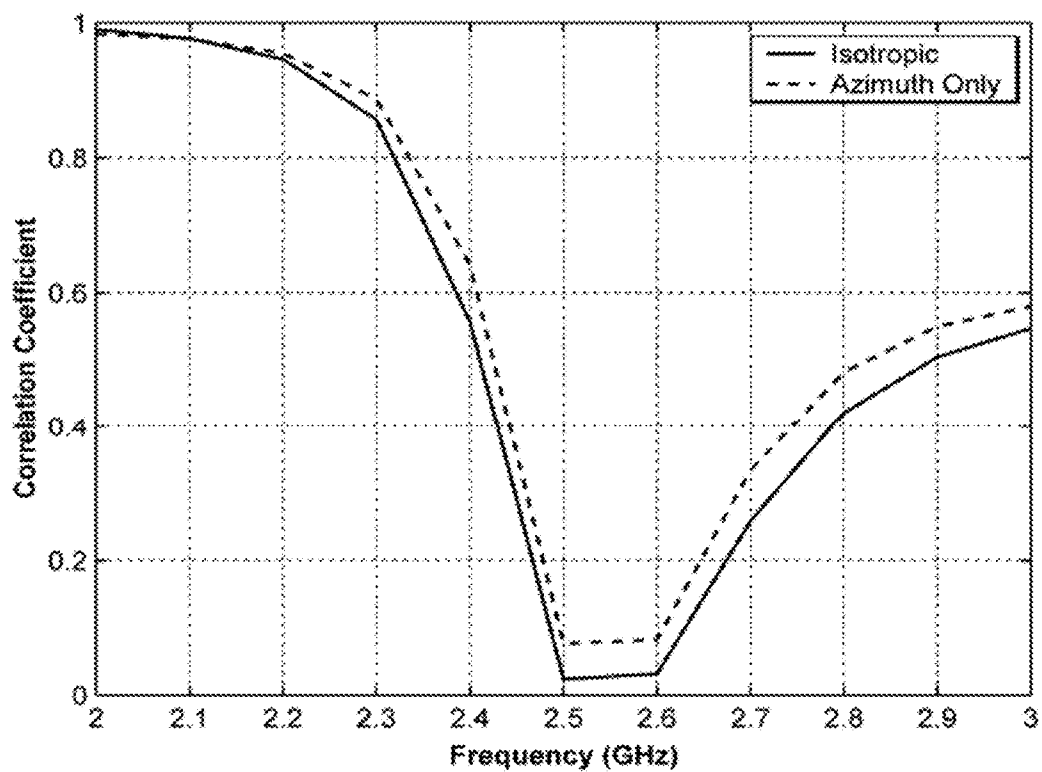


FIG. 3E

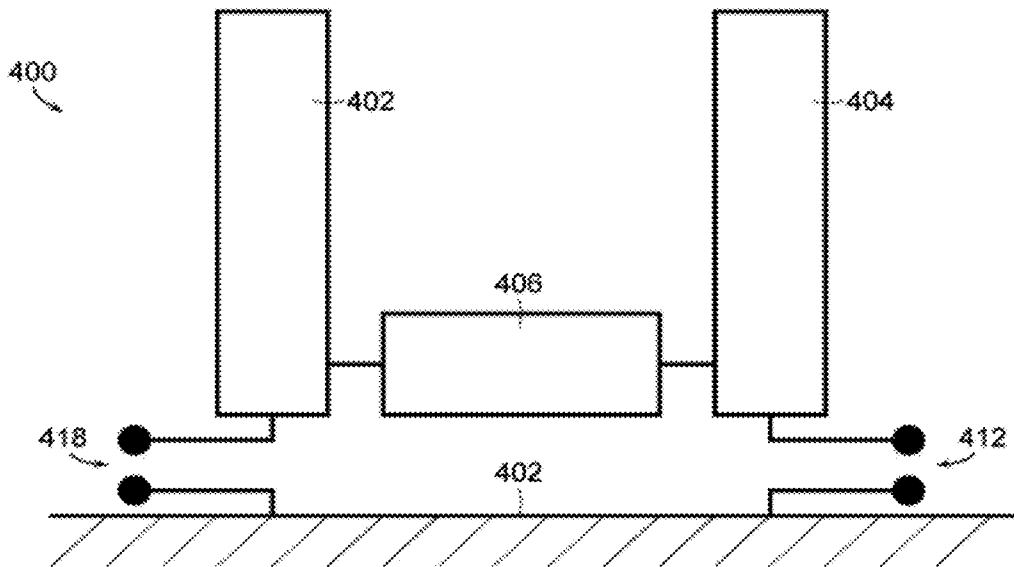


FIG. 4

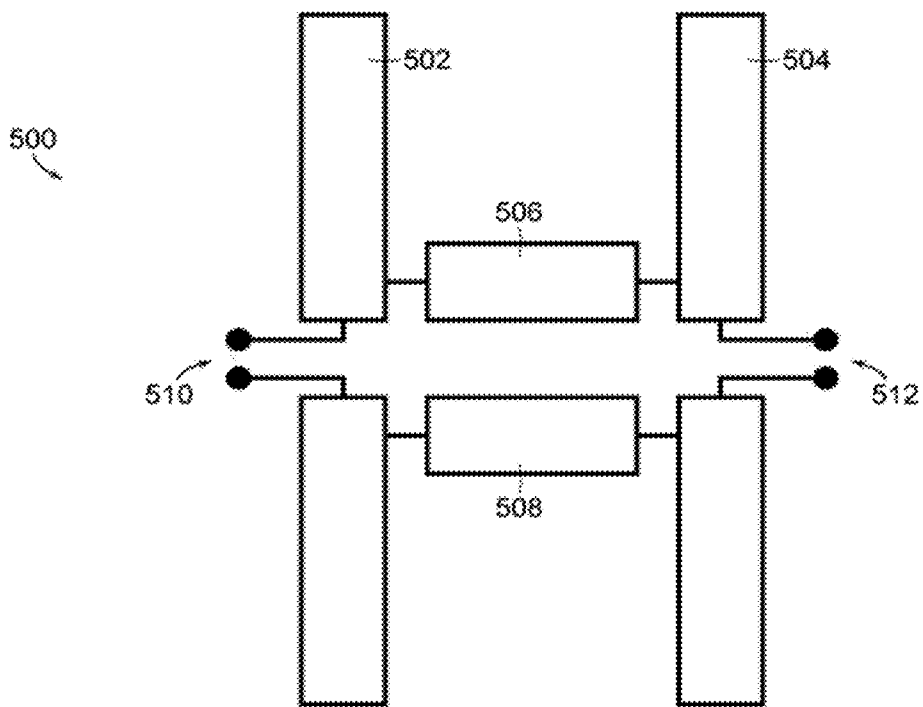


FIG. 5

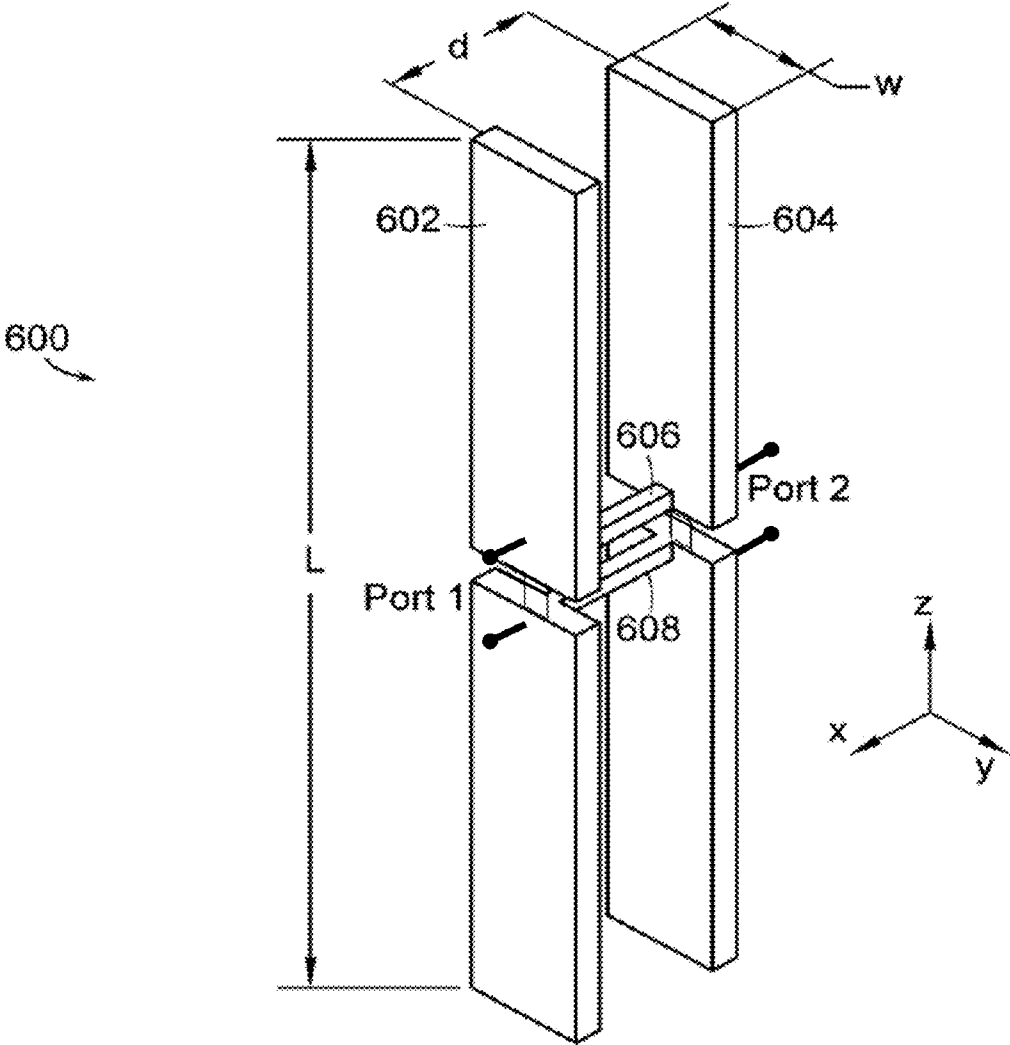


FIG. 6A

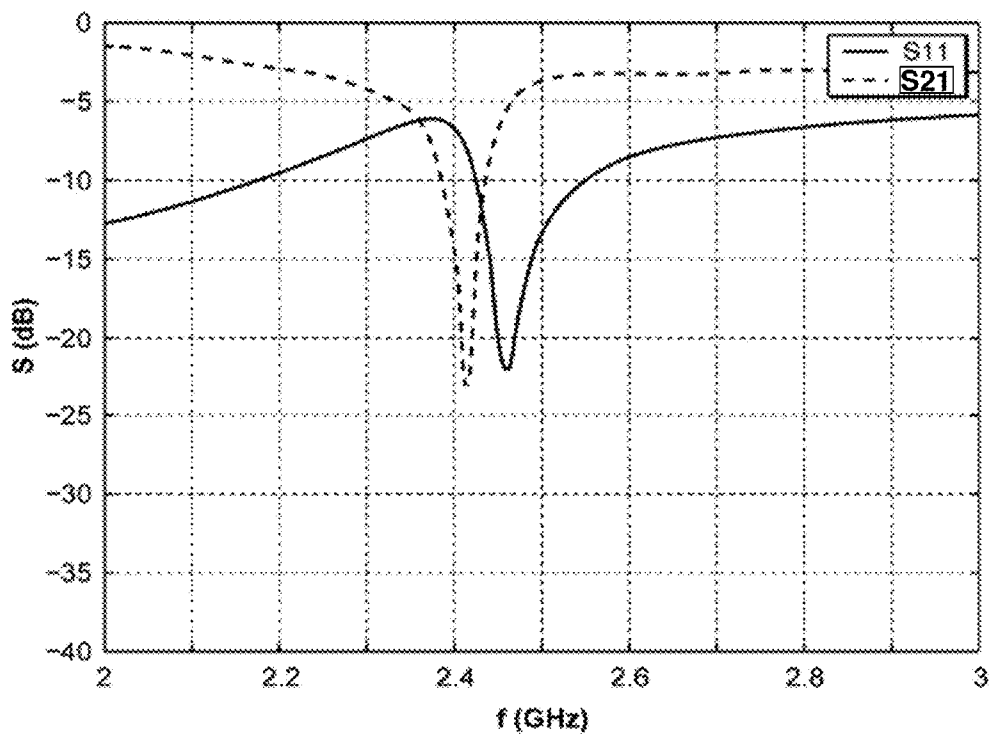


FIG. 6B

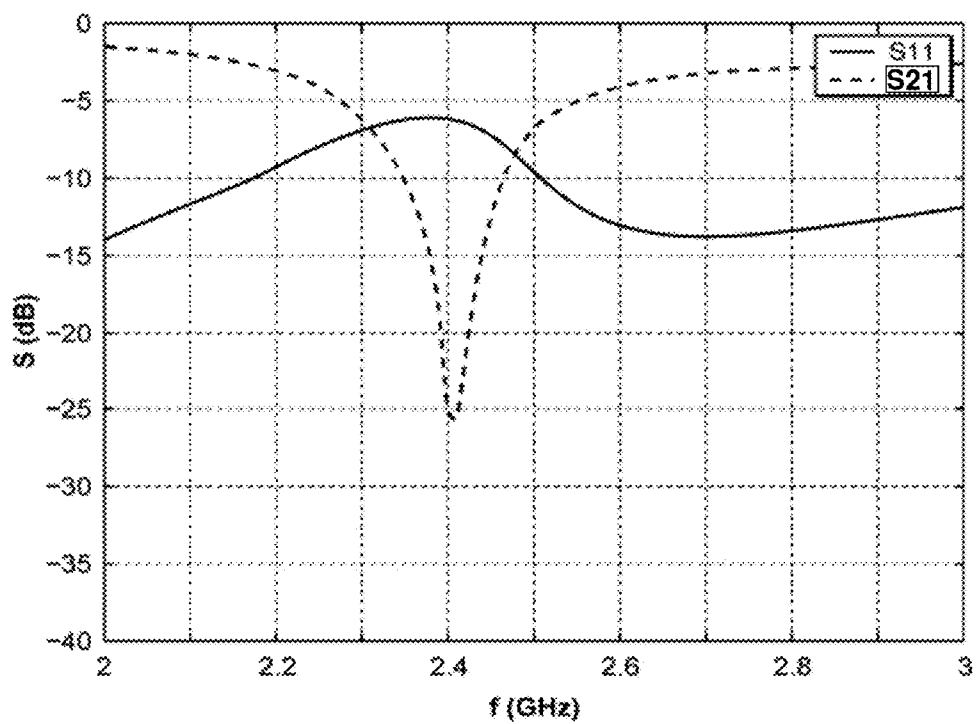


FIG. 6C

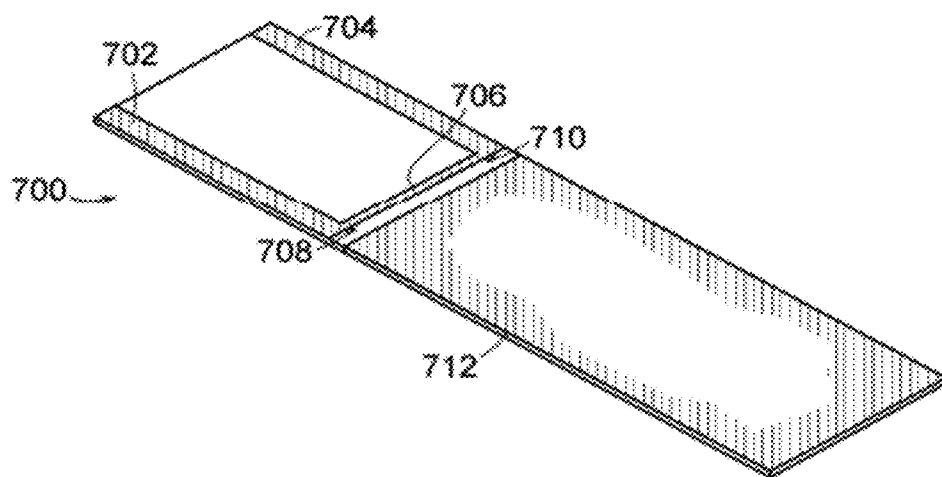


FIG. 7

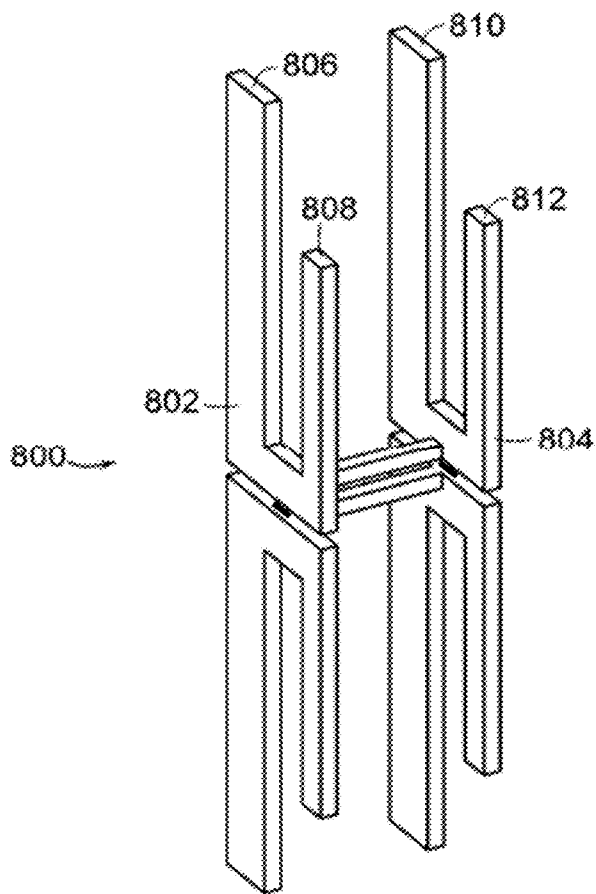


FIG. 8A

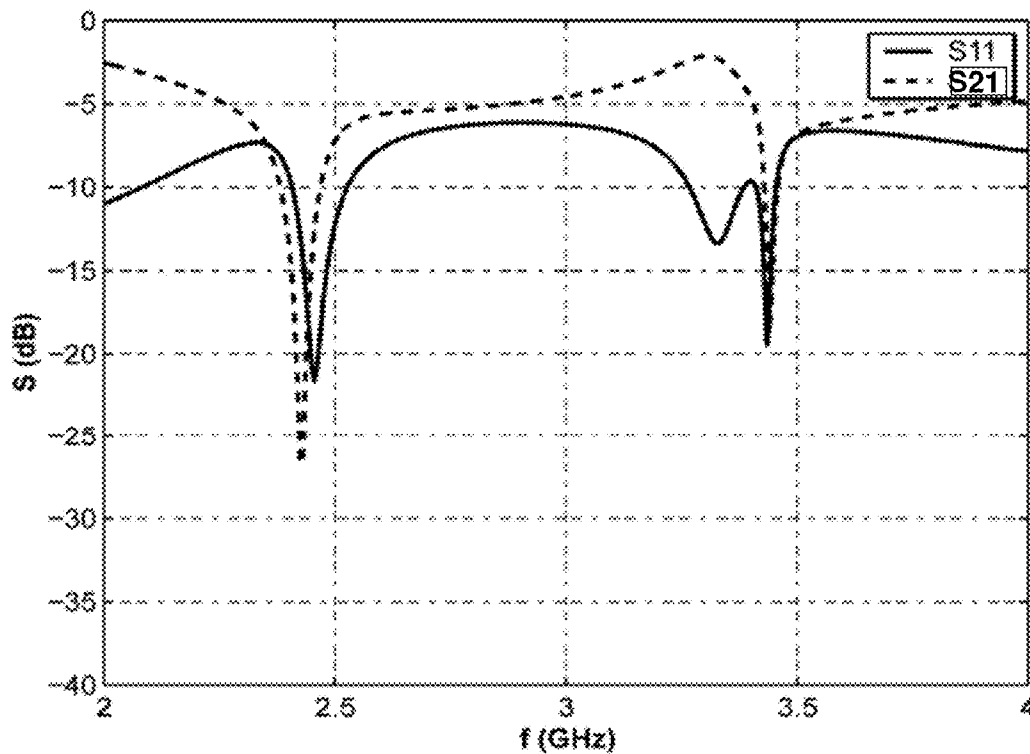


FIG. 8B

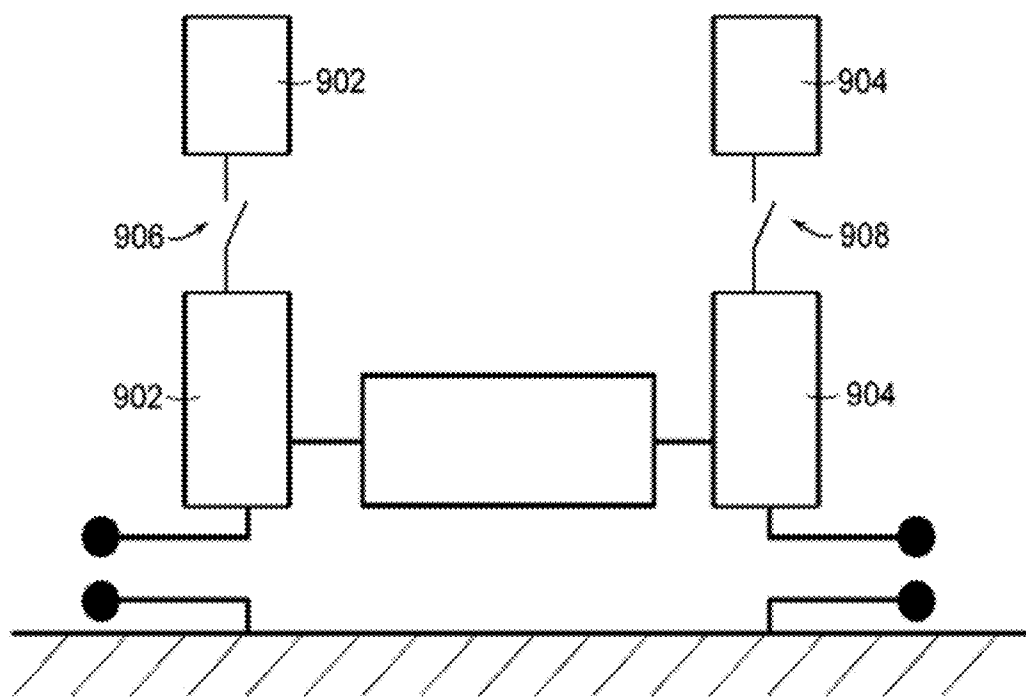


FIG. 9

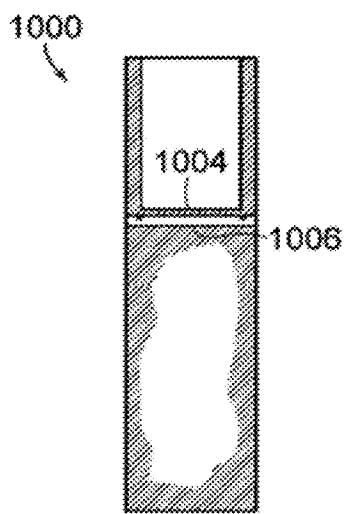


FIG. 10A

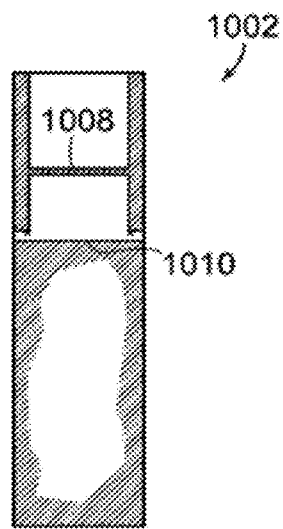


FIG. 10B

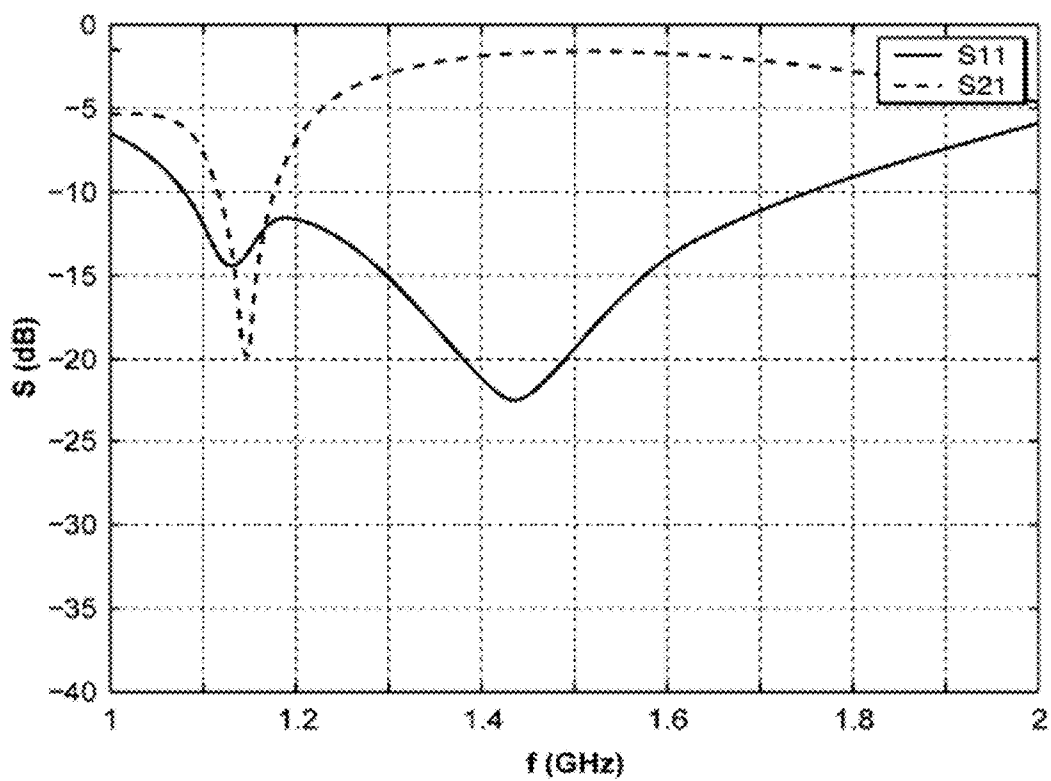


FIG. 10C

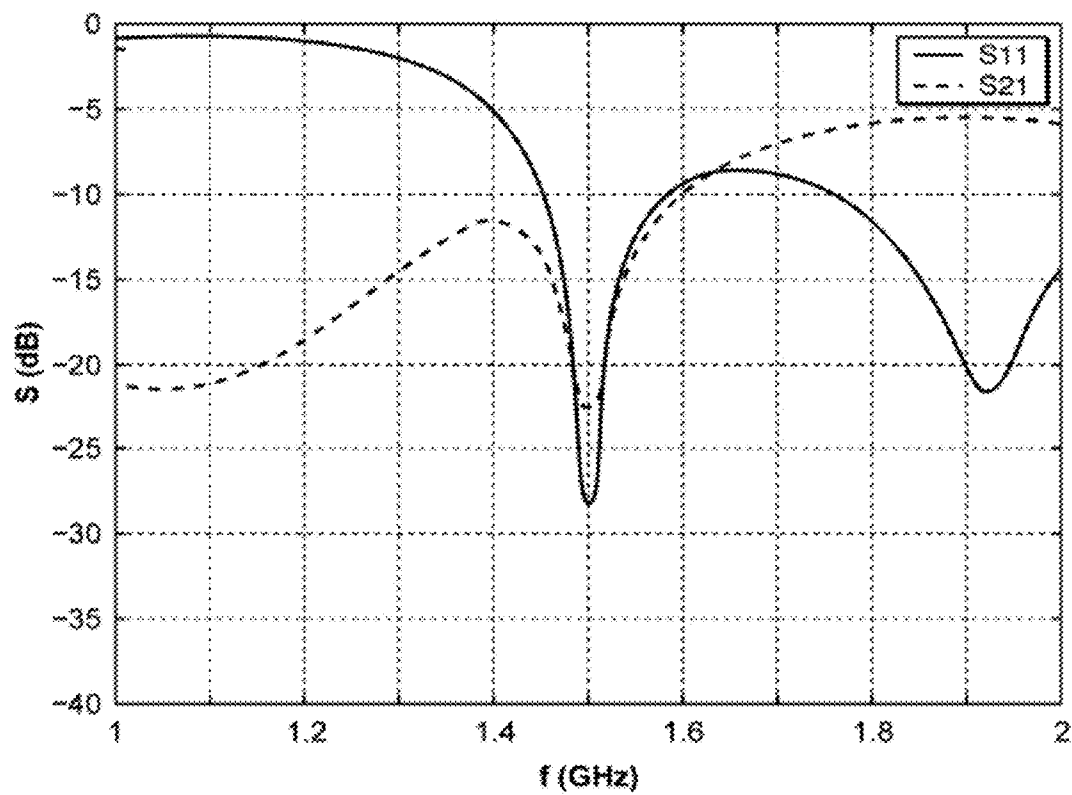


FIG. 10D

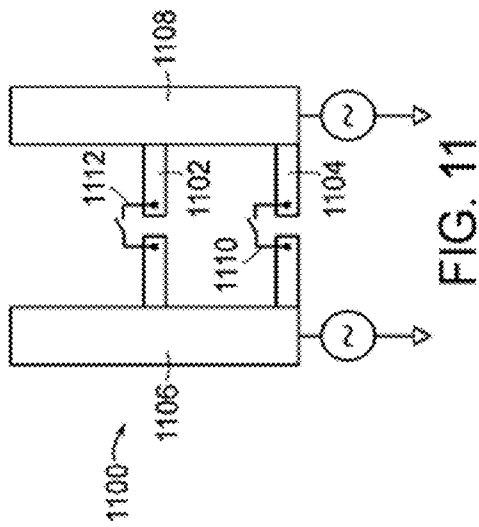


FIG. 11

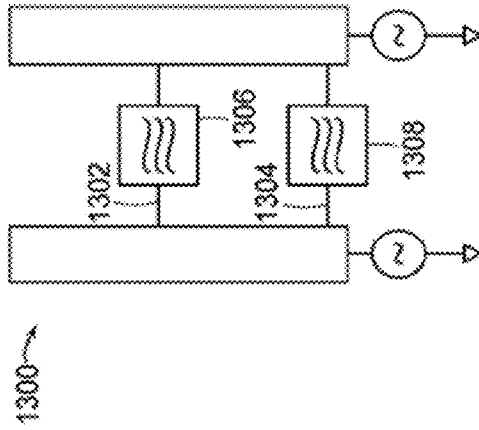


FIG. 13

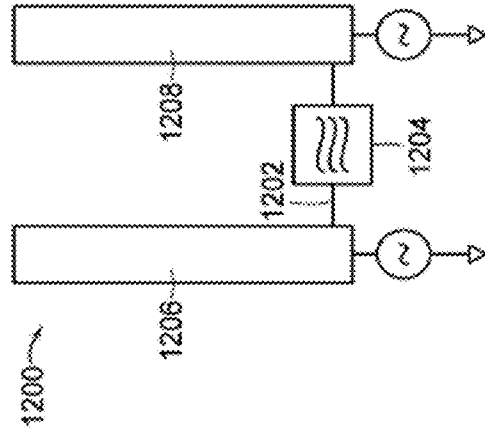


FIG. 12

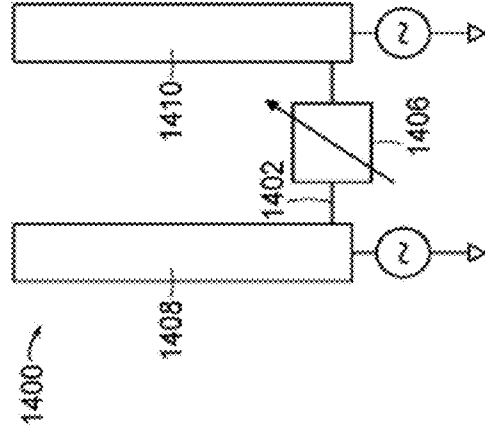


FIG. 14

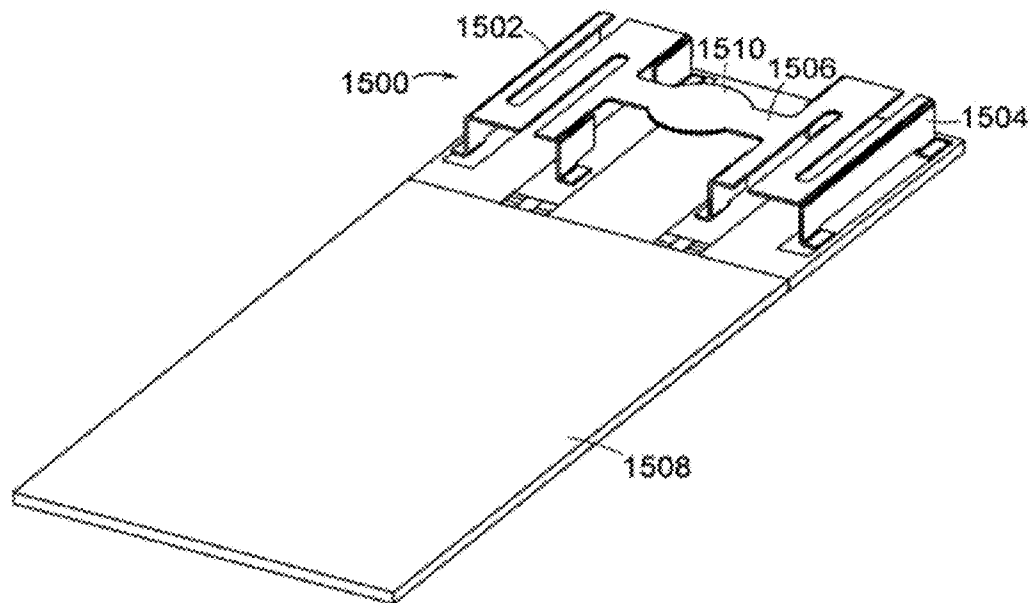


FIG. 15

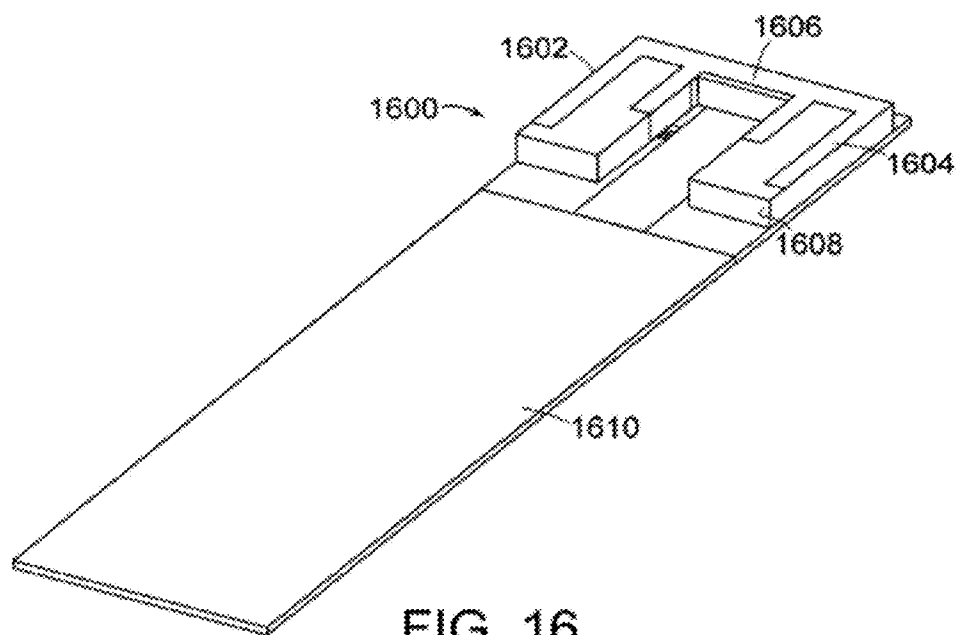


FIG. 16

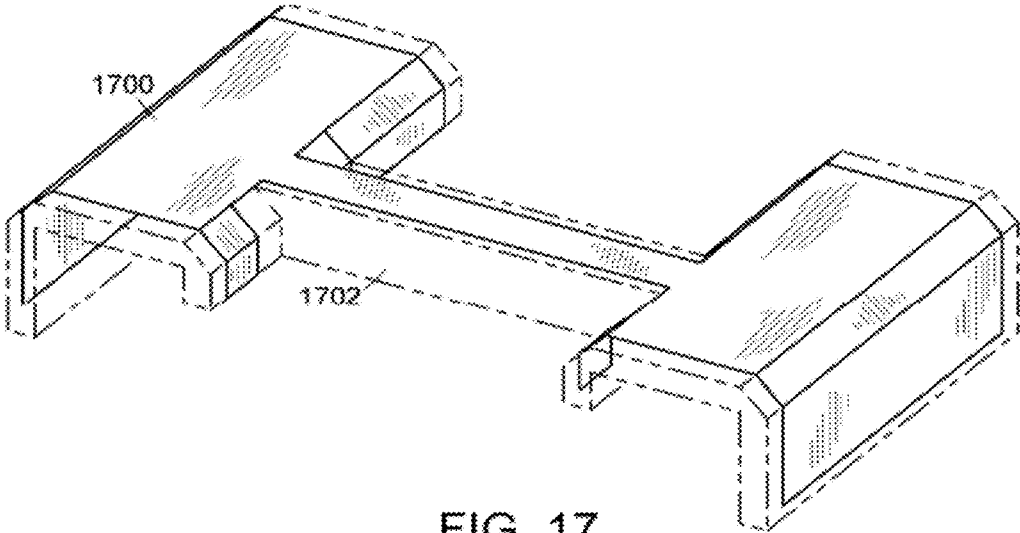


FIG. 17

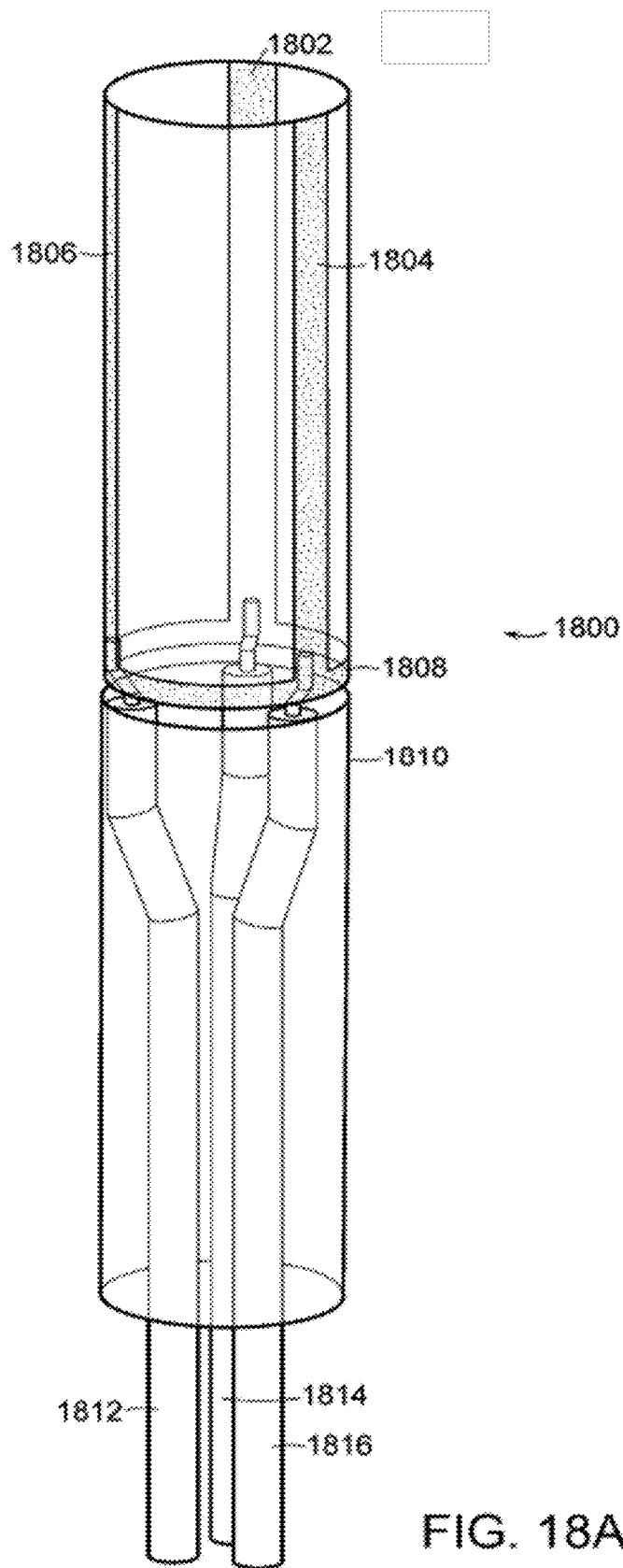


FIG. 18A

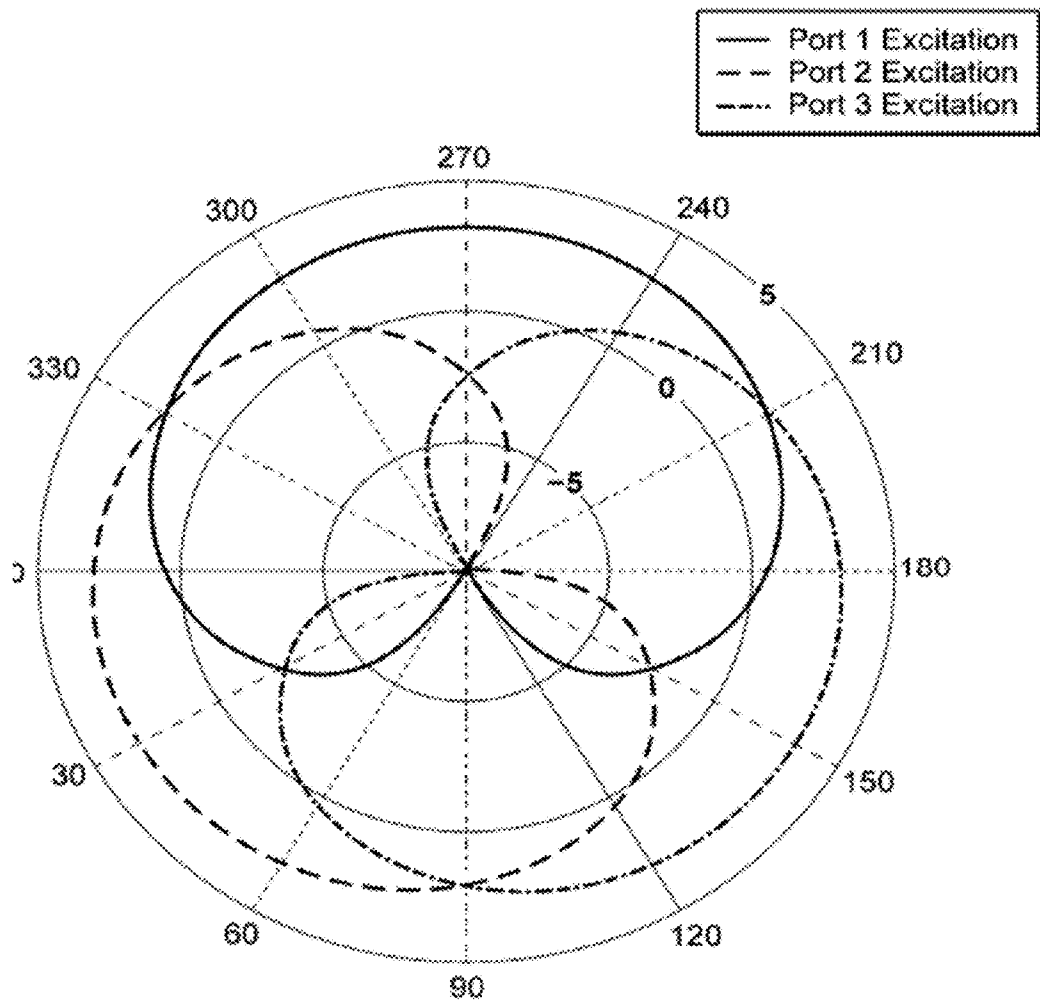


FIG. 18B

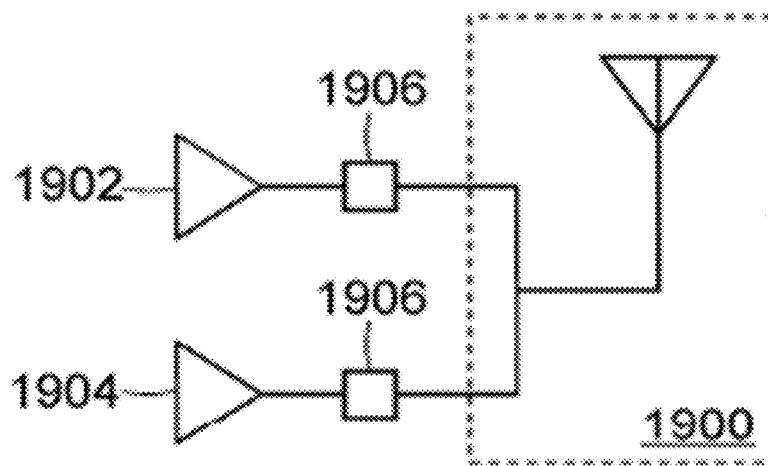


FIG. 19

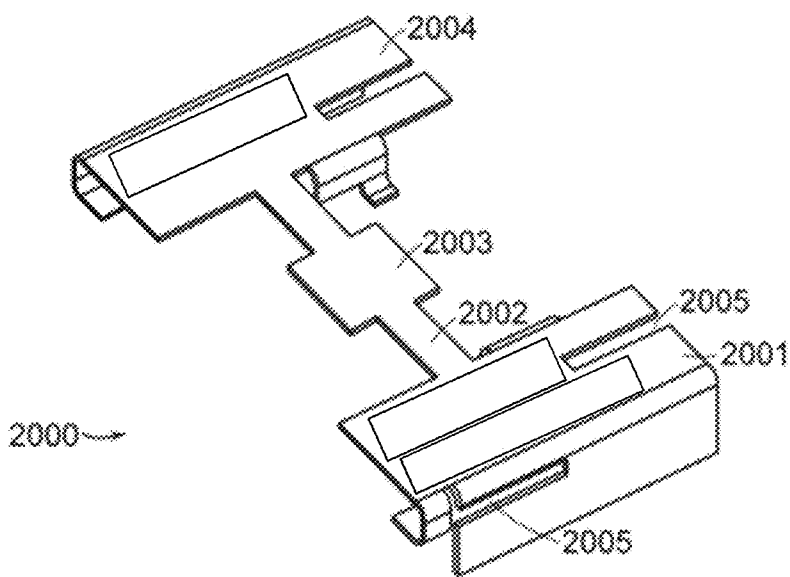


FIG. 20A

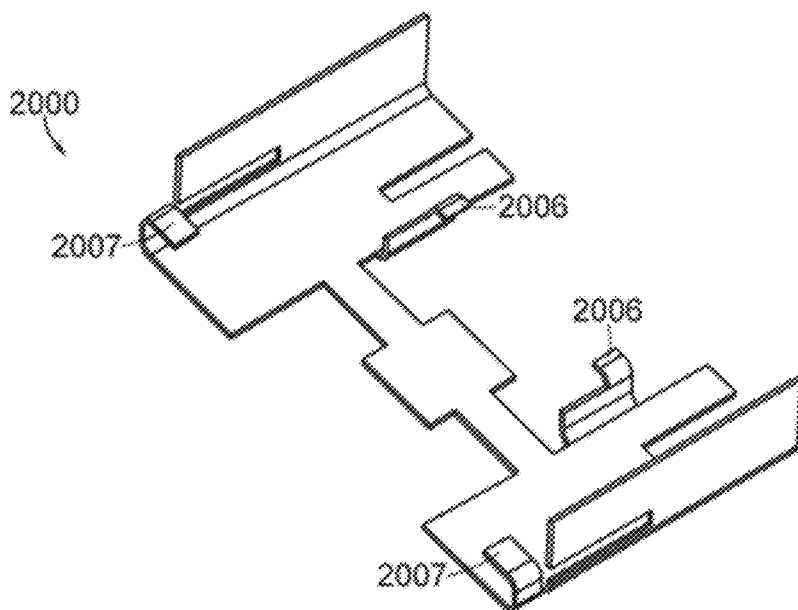


FIG. 20B

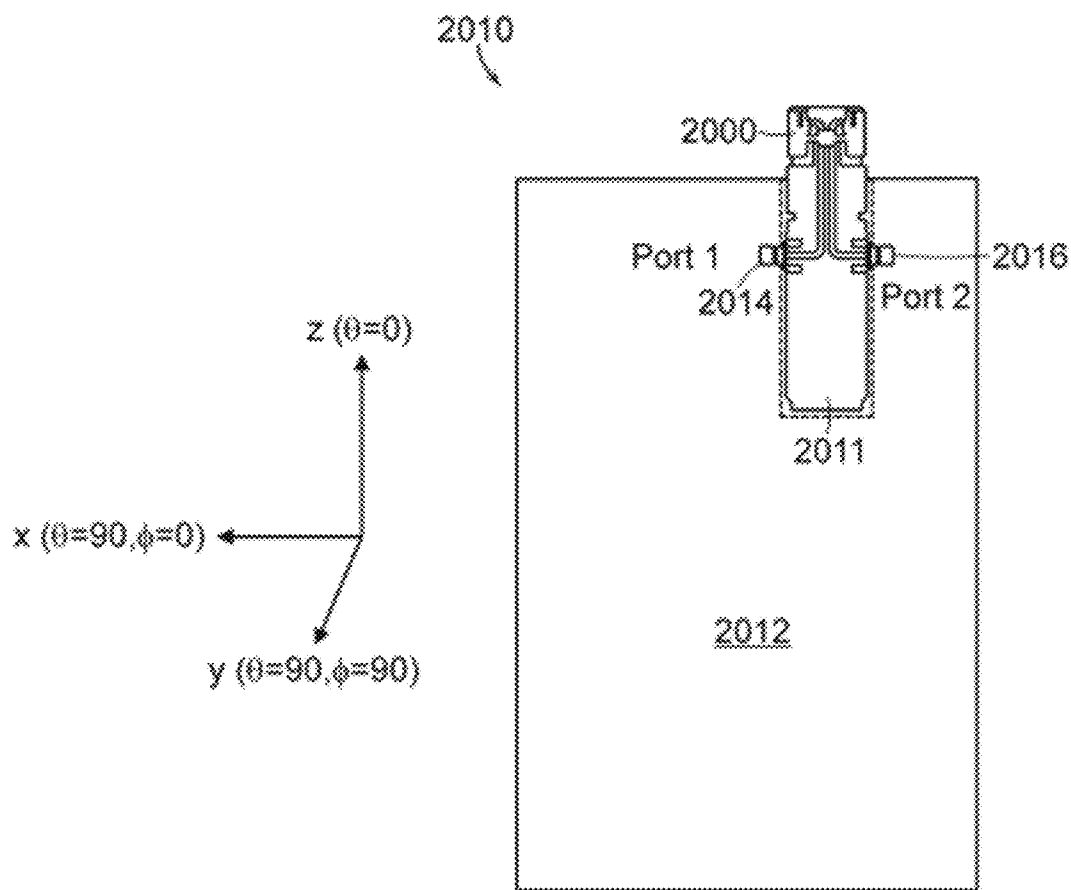


FIG. 20C

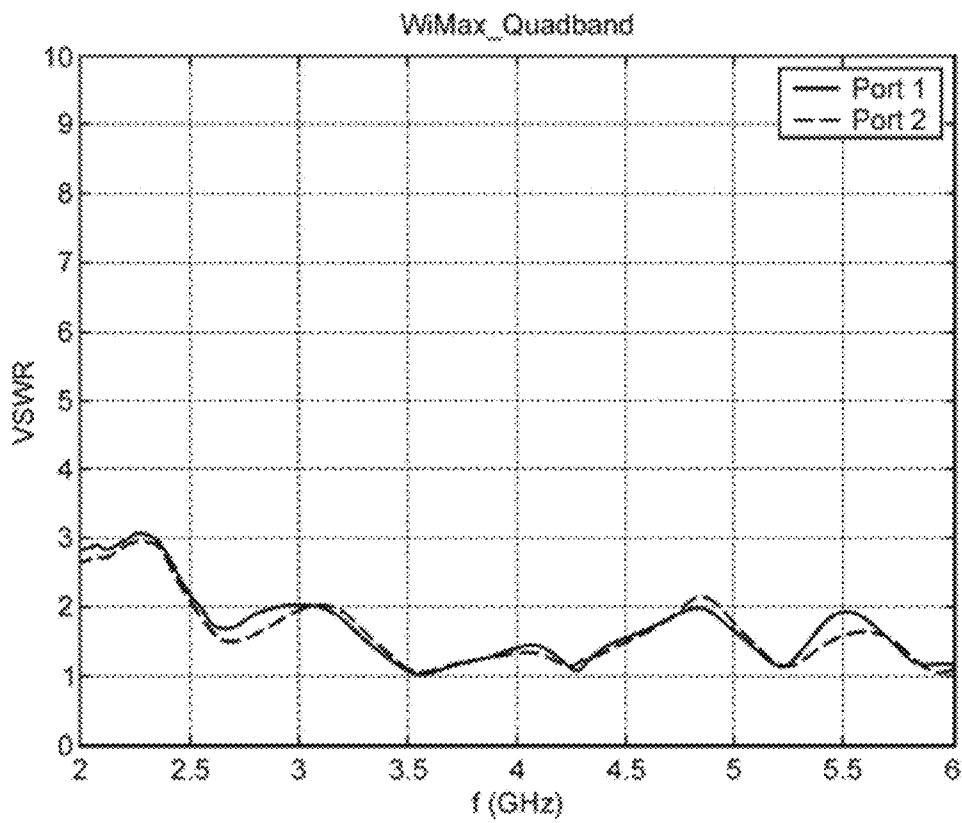


FIG. 20D

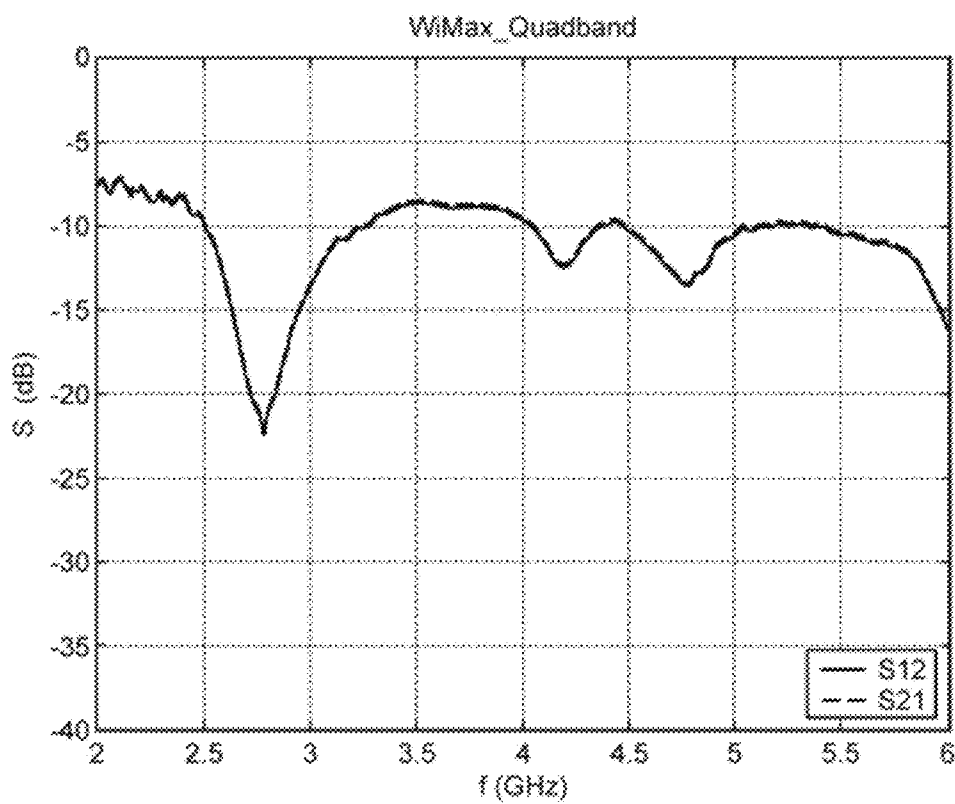


FIG. 20E

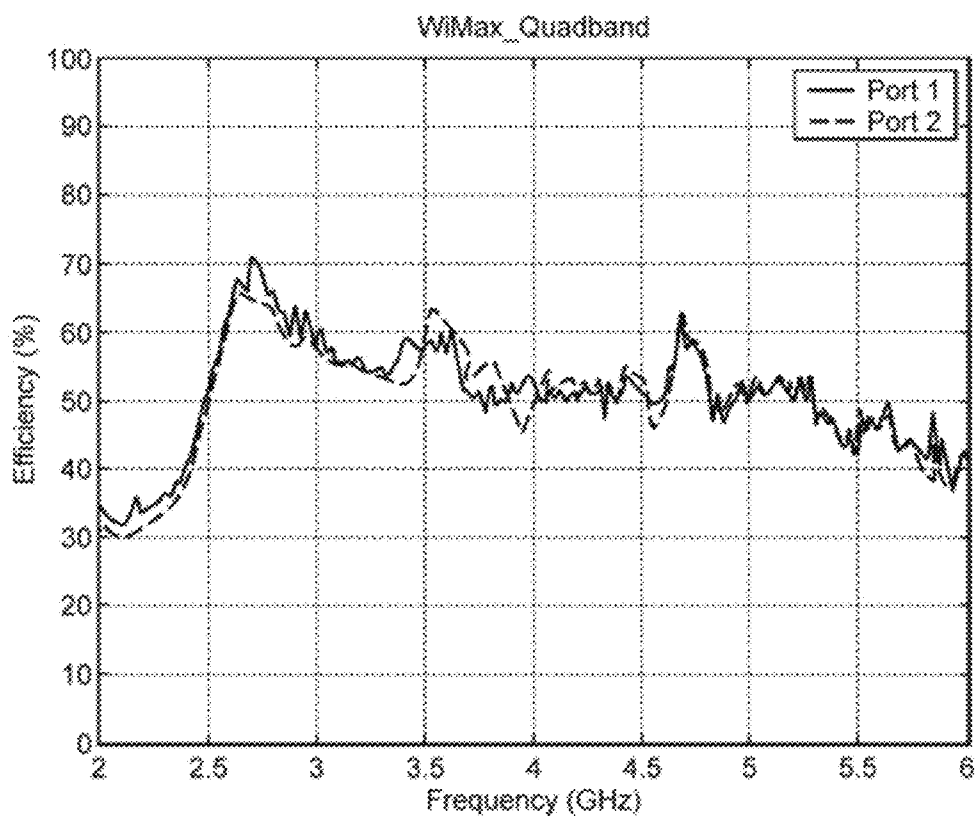


FIG. 20F

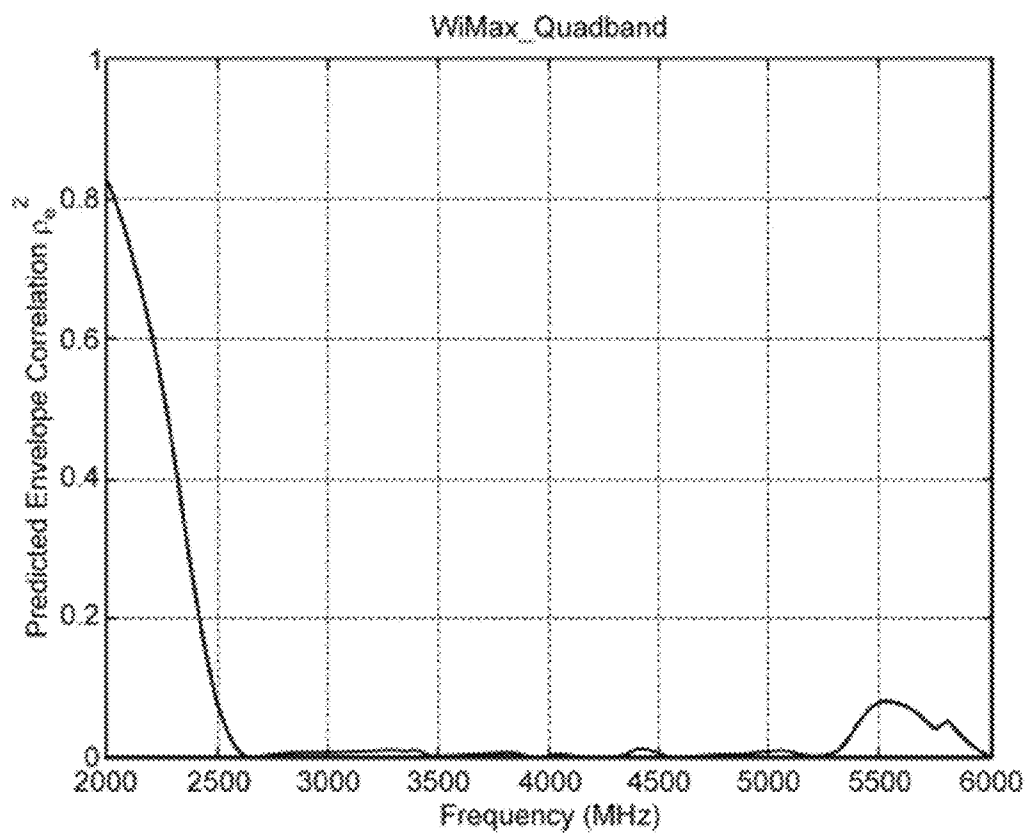


FIG. 20G

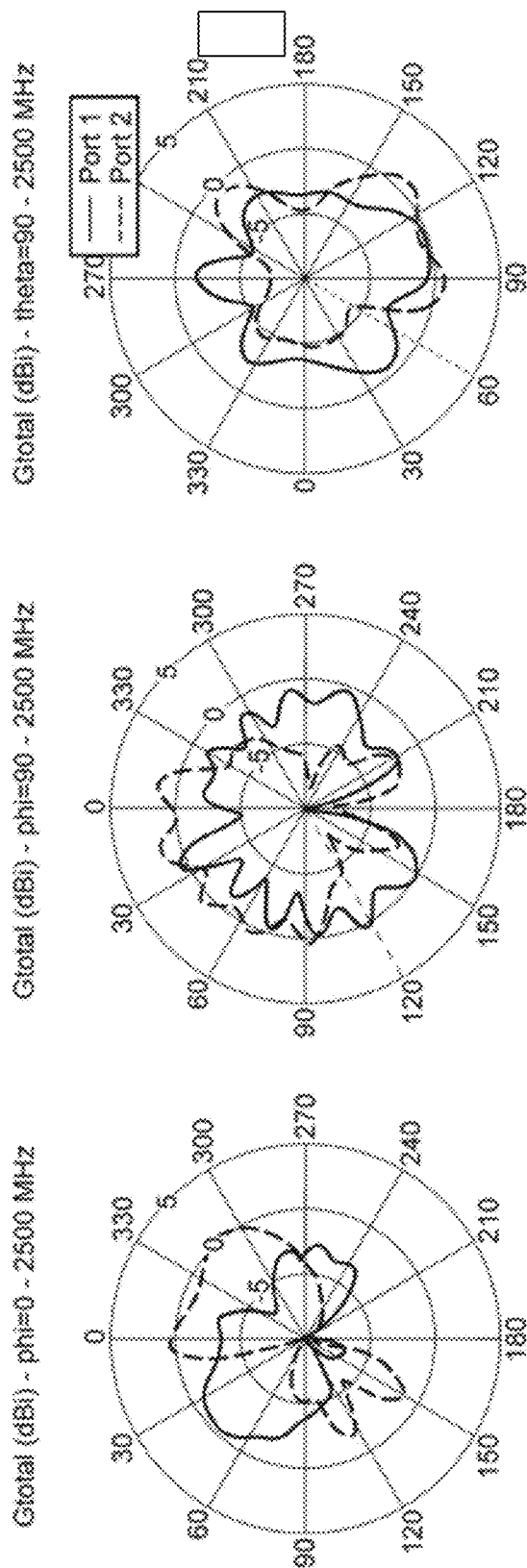


FIG. 20H

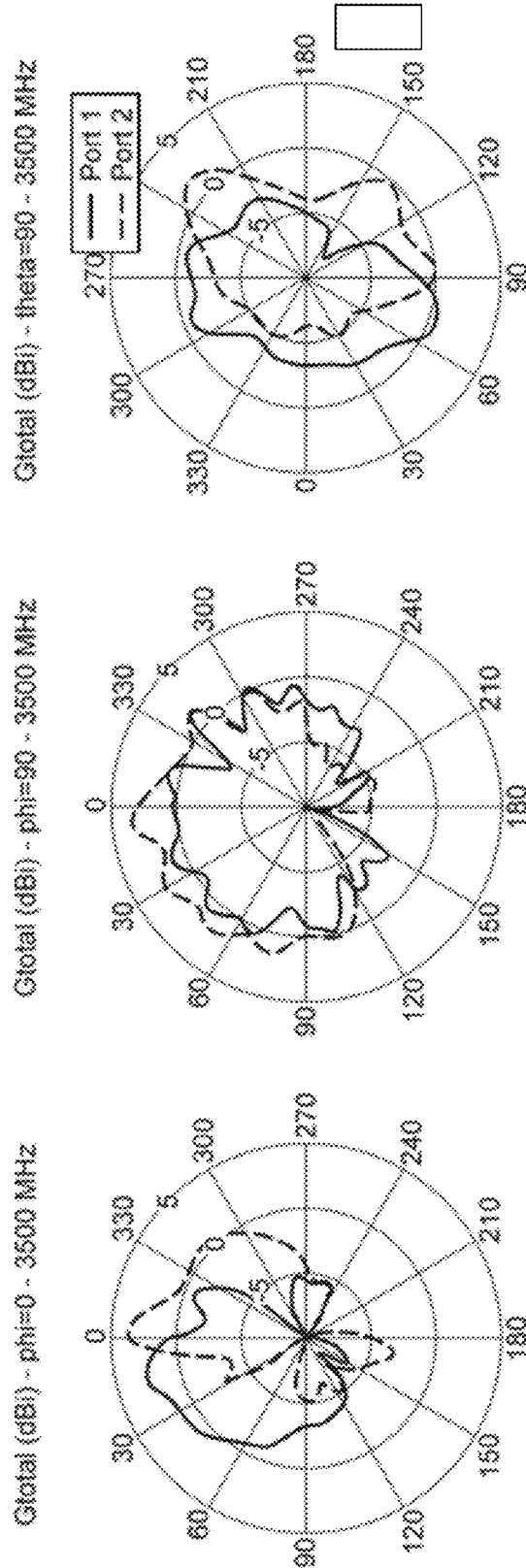


FIG. 20I

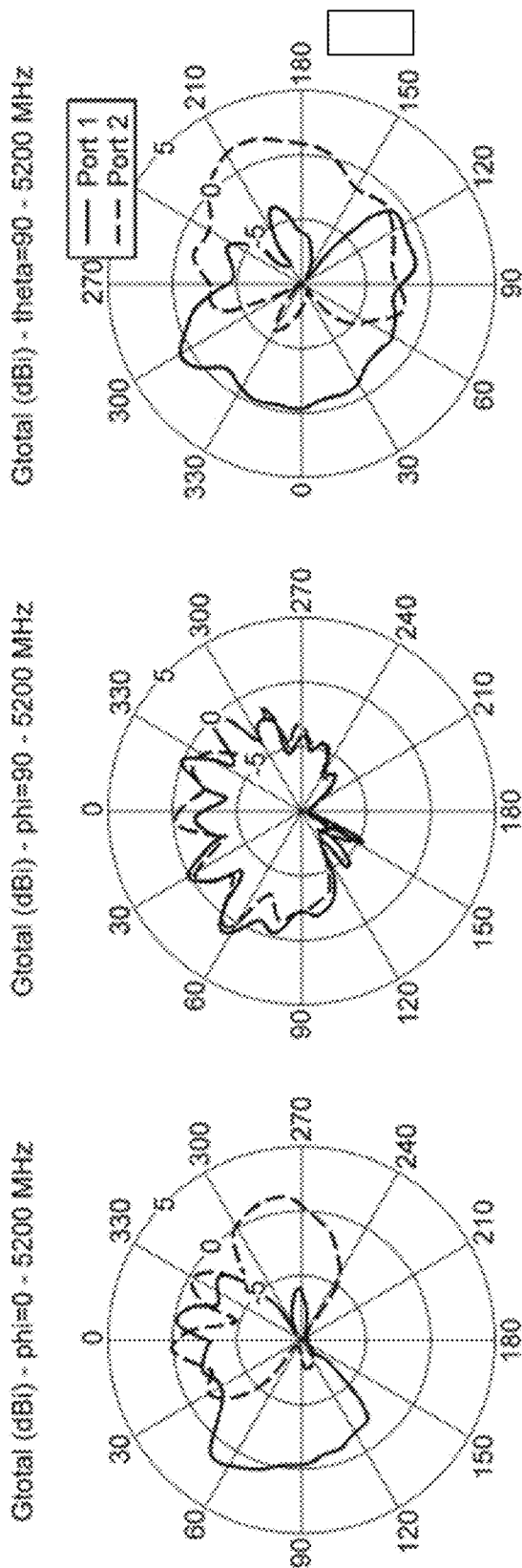


FIG. 20J

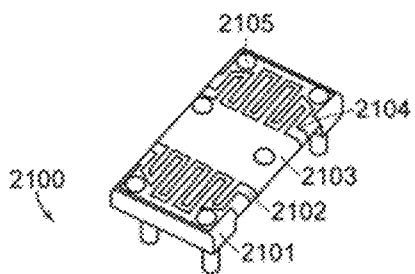


FIG. 21A

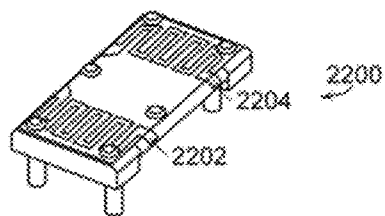


FIG. 22A

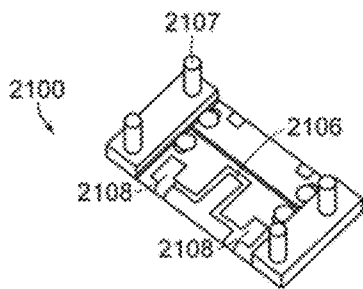


FIG. 21B

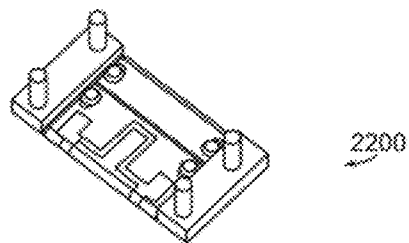


FIG. 22B

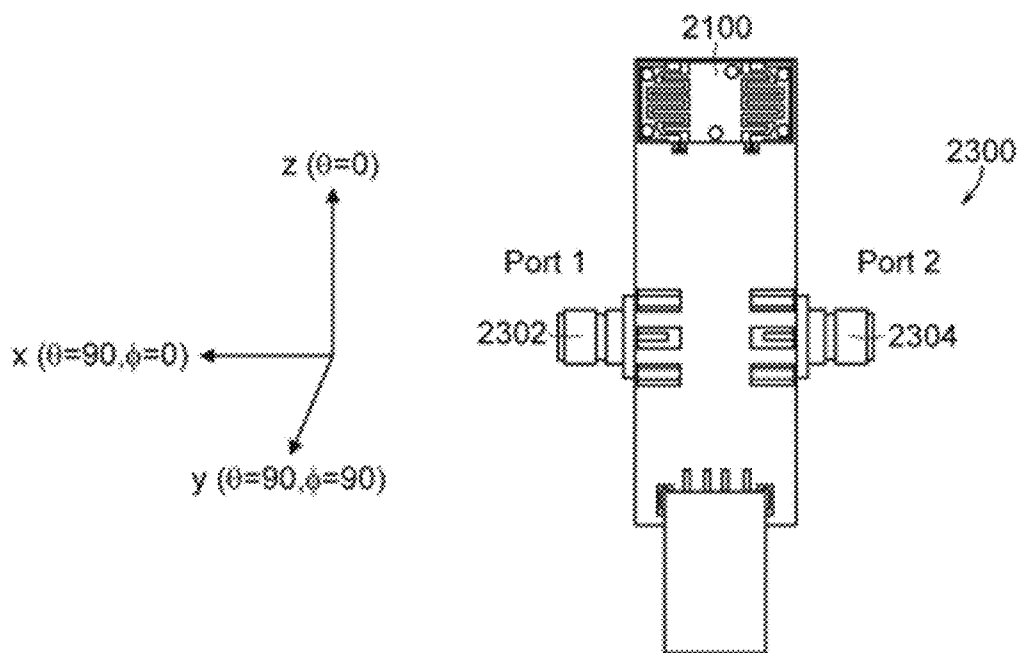


FIG. 23A

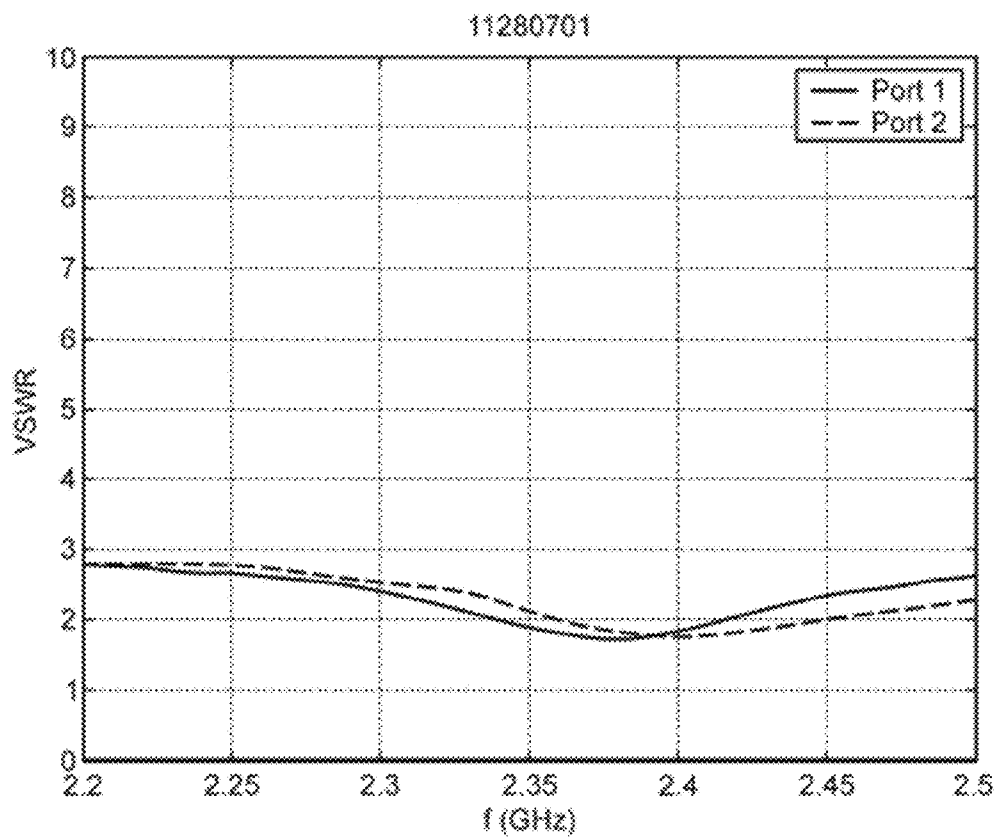


FIG. 23B

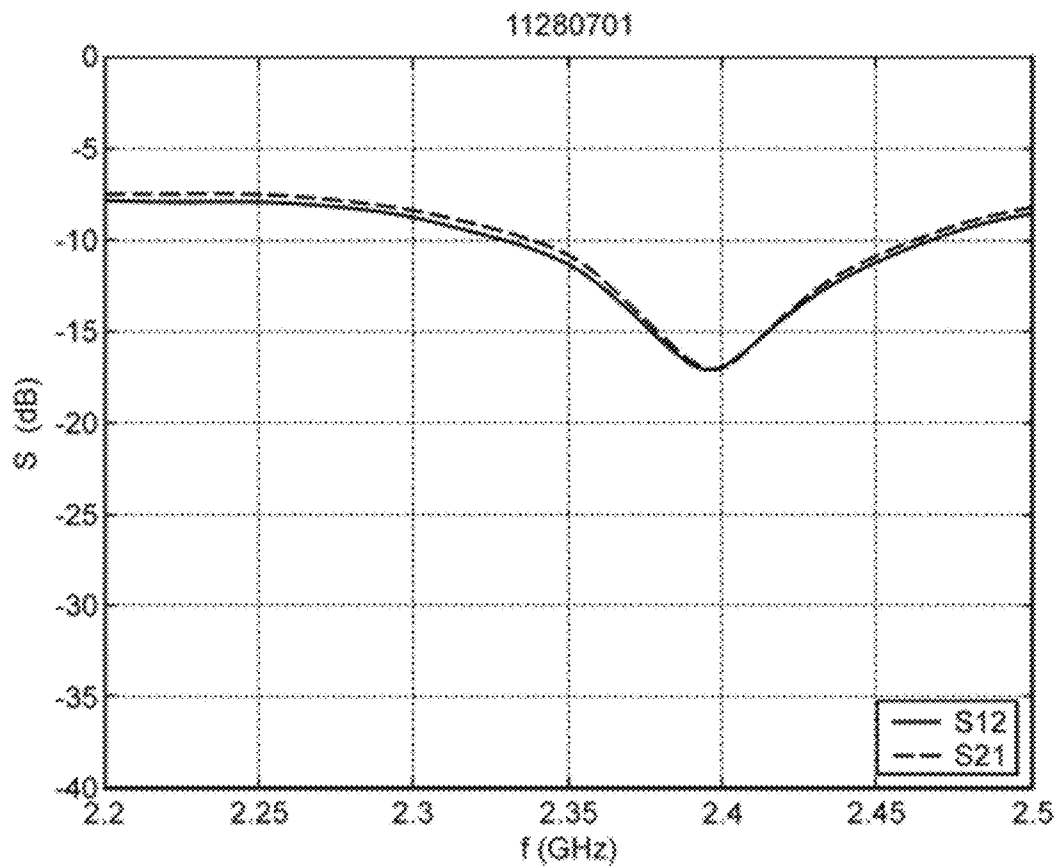


FIG. 23C

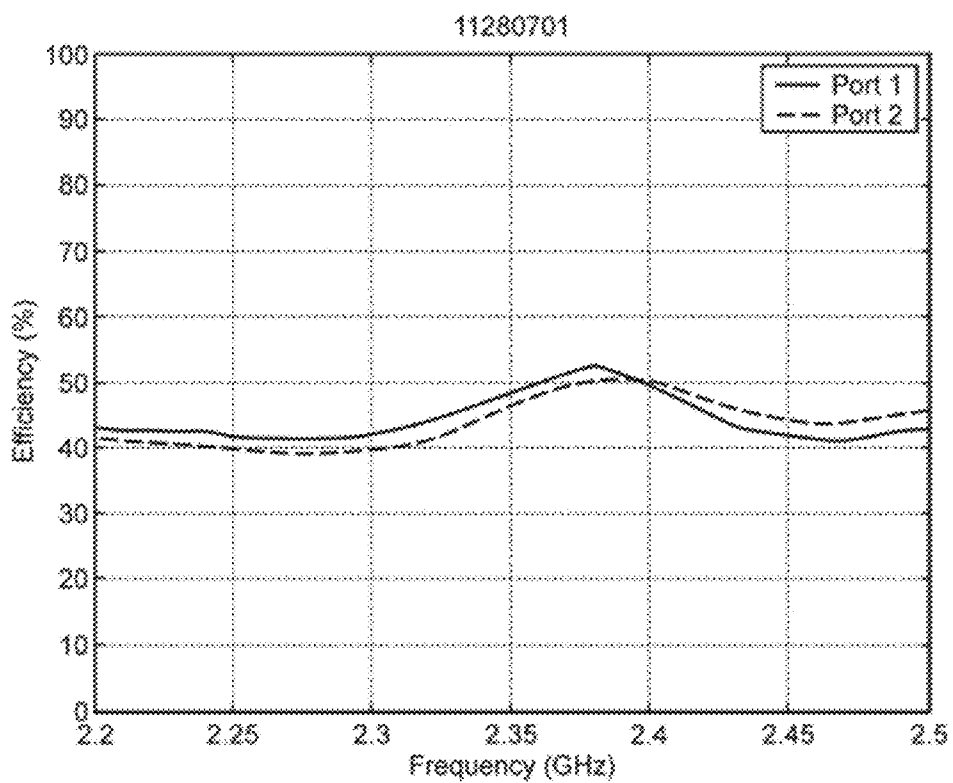


FIG. 23D

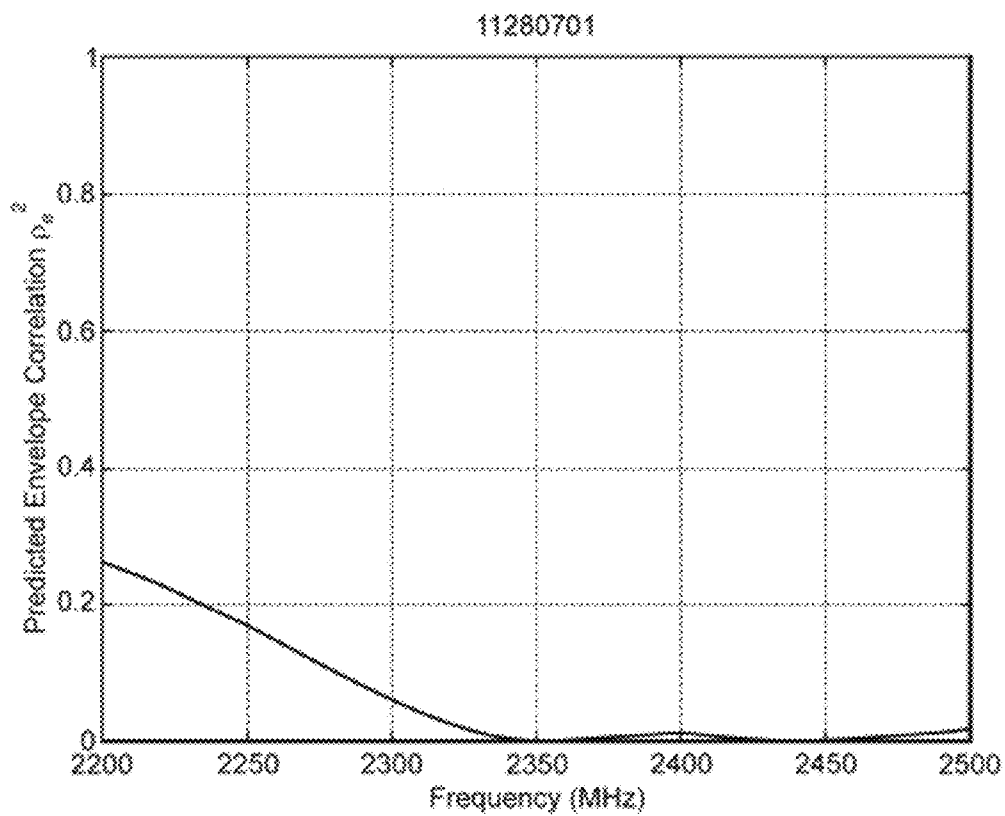


FIG. 23E

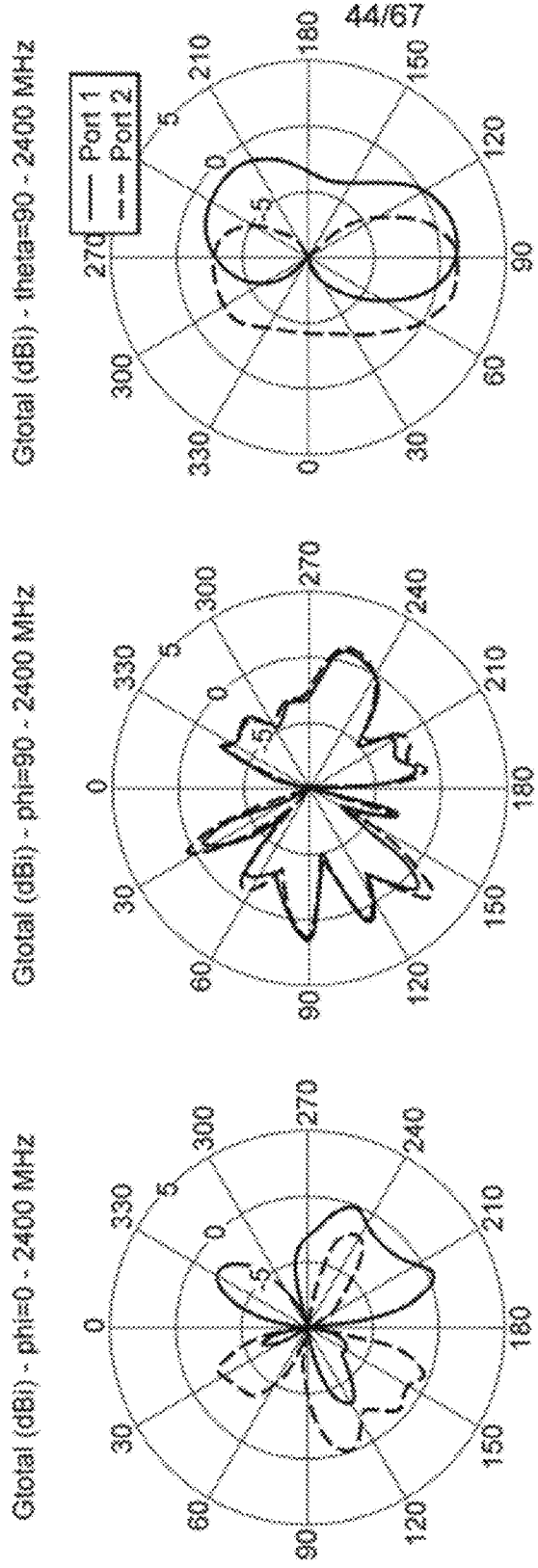


FIG. 23F

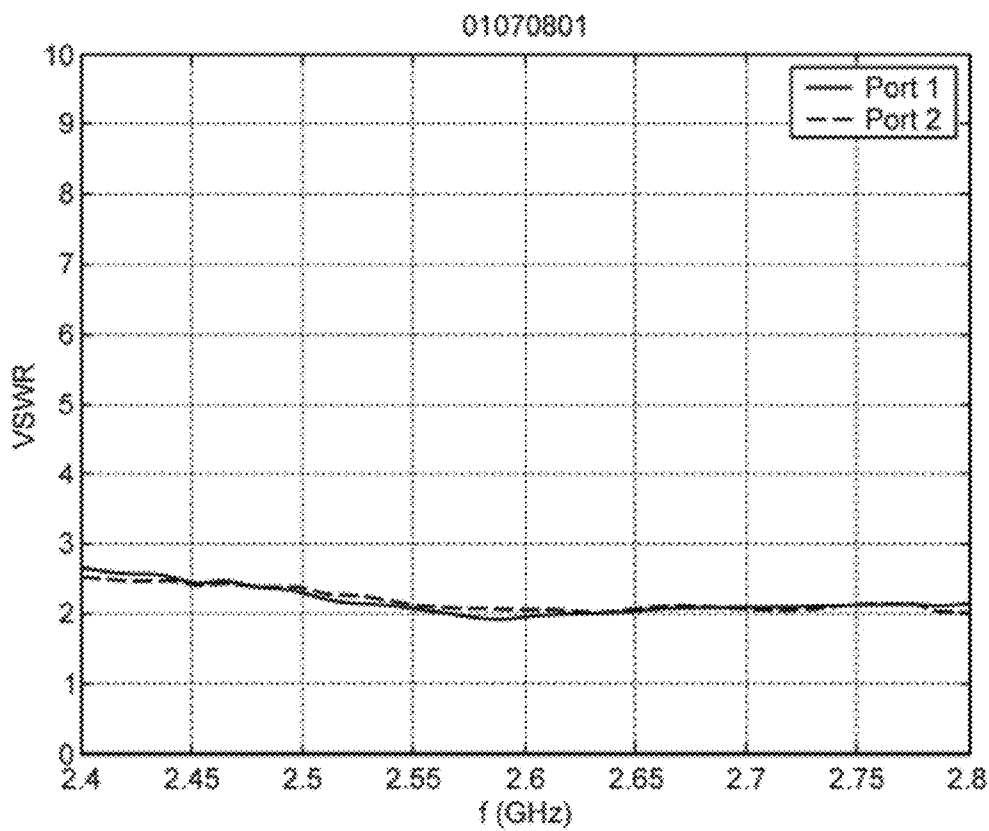


FIG. 23G

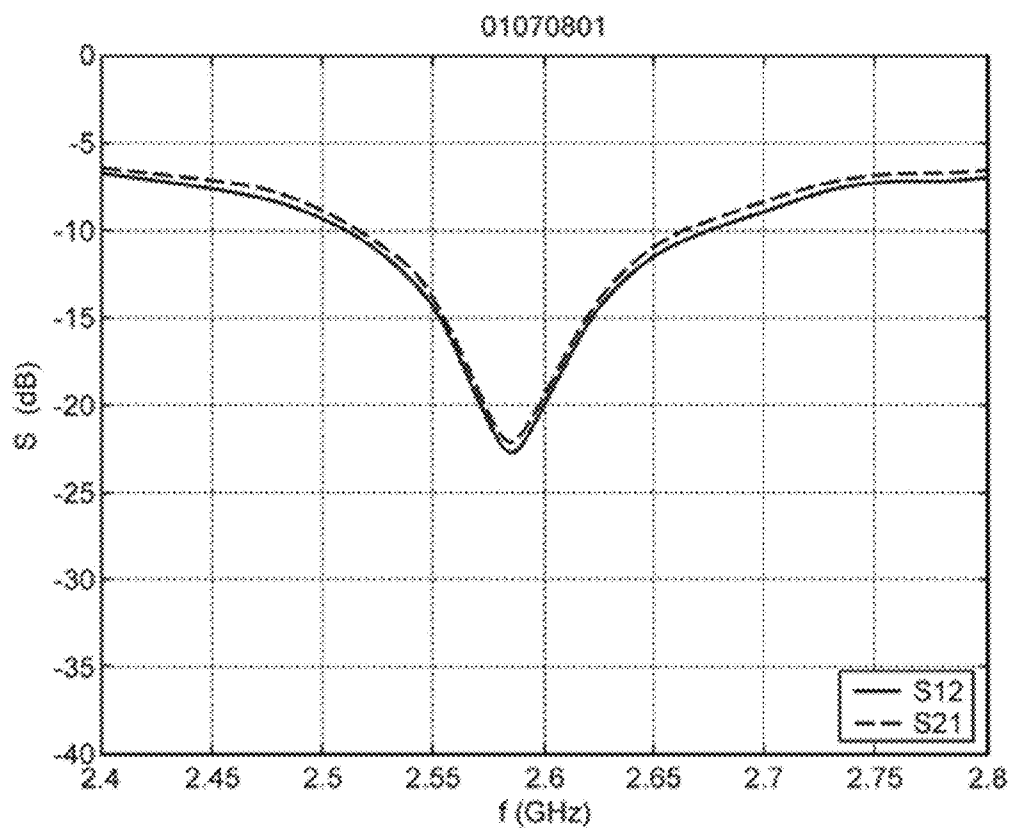


FIG. 23H

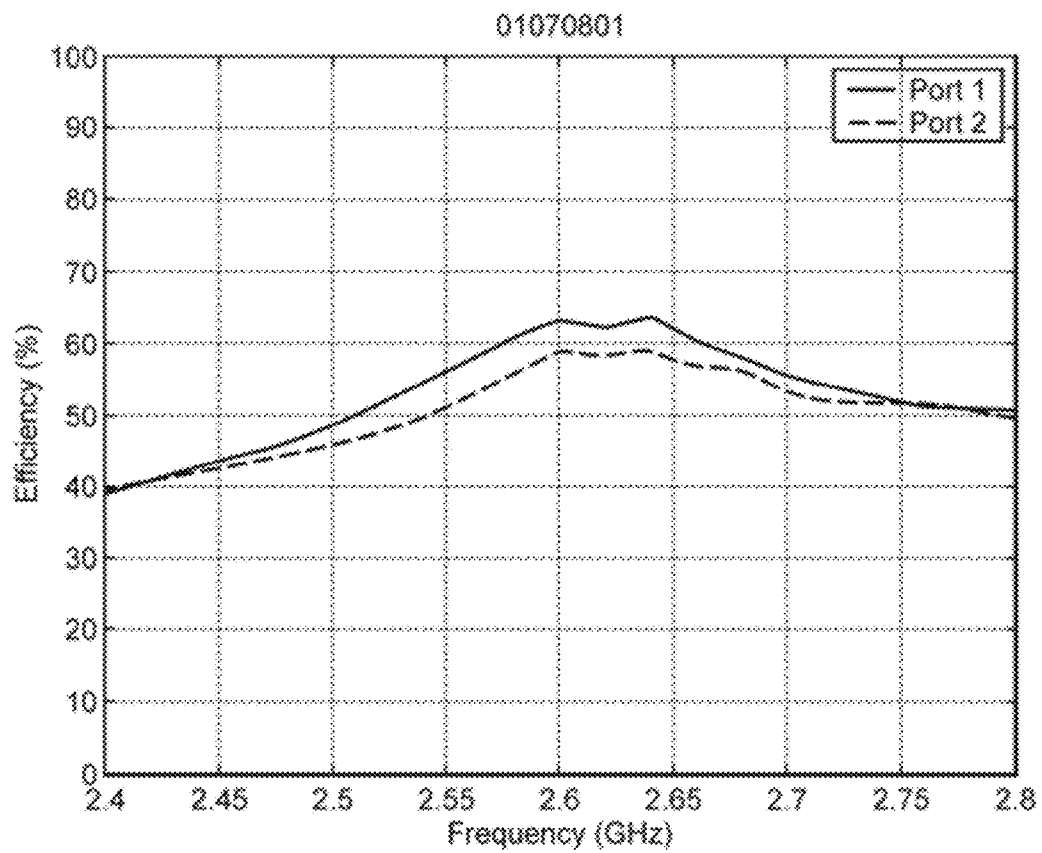


FIG. 23I

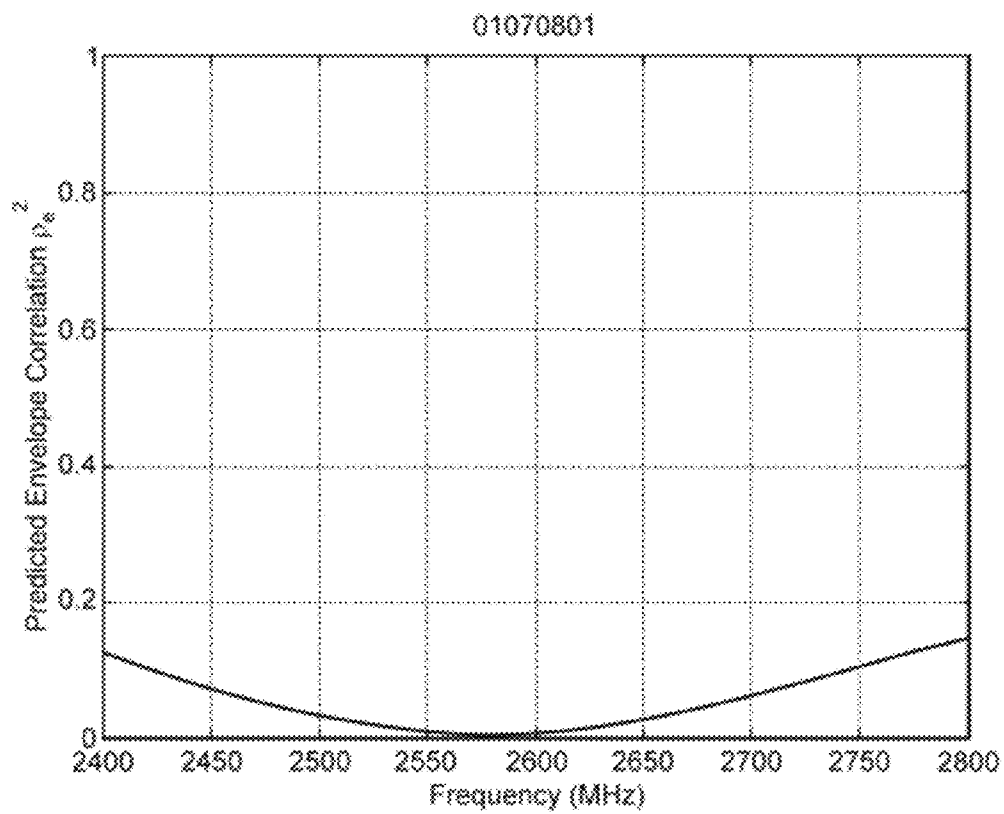


FIG. 23J

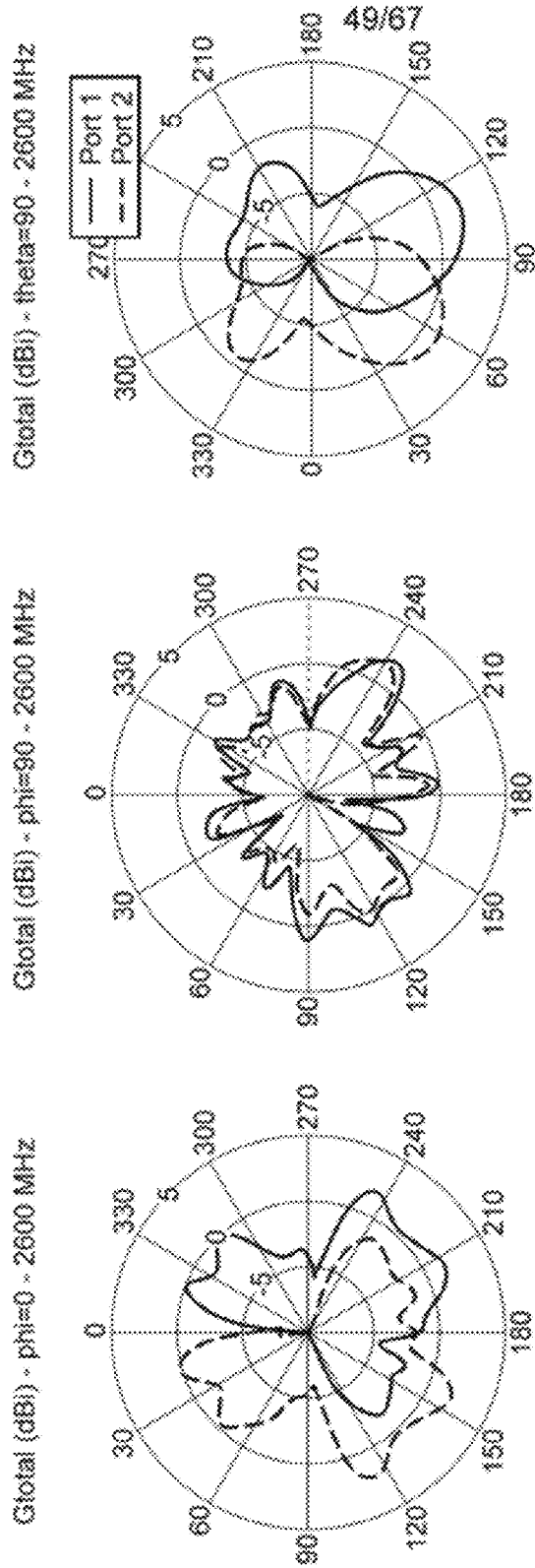


FIG. 23K

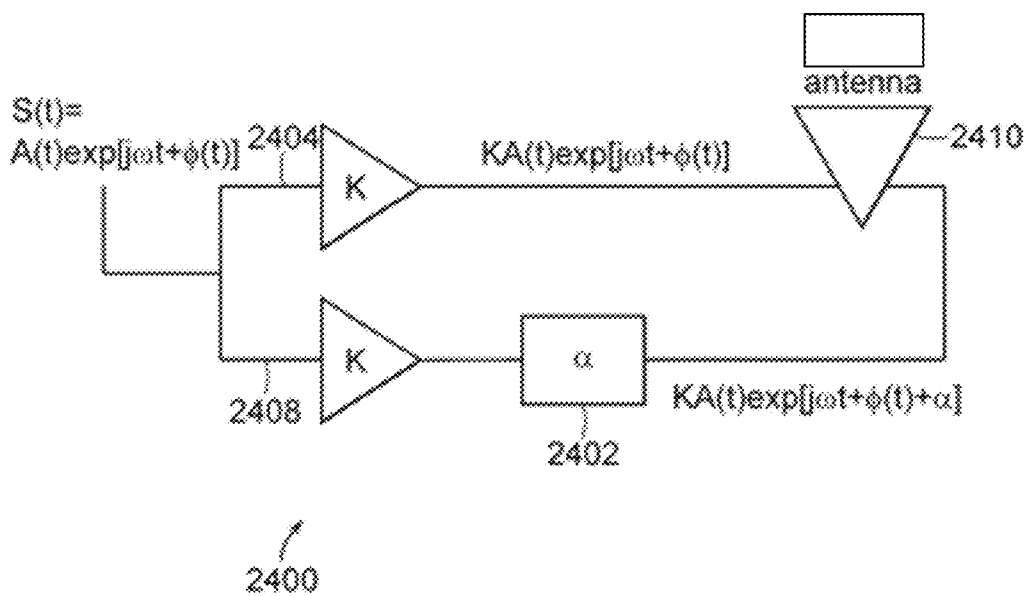


FIG. 24

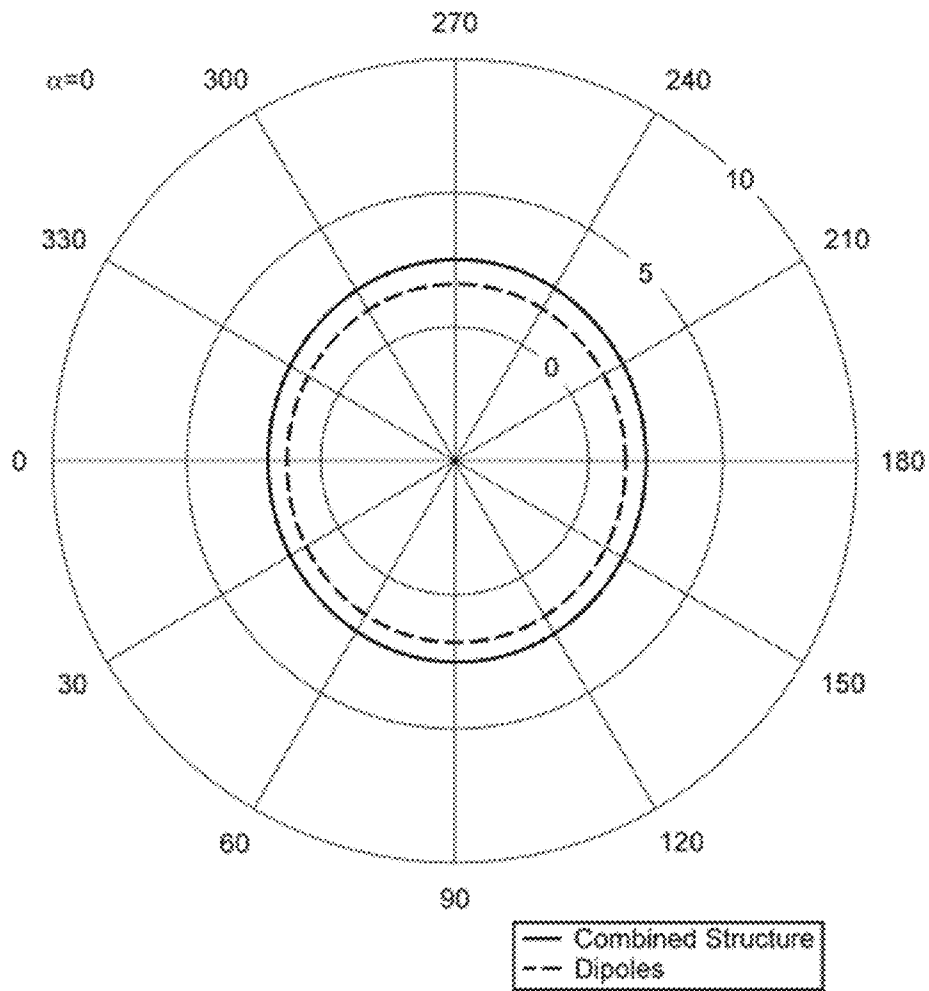


FIG. 25A

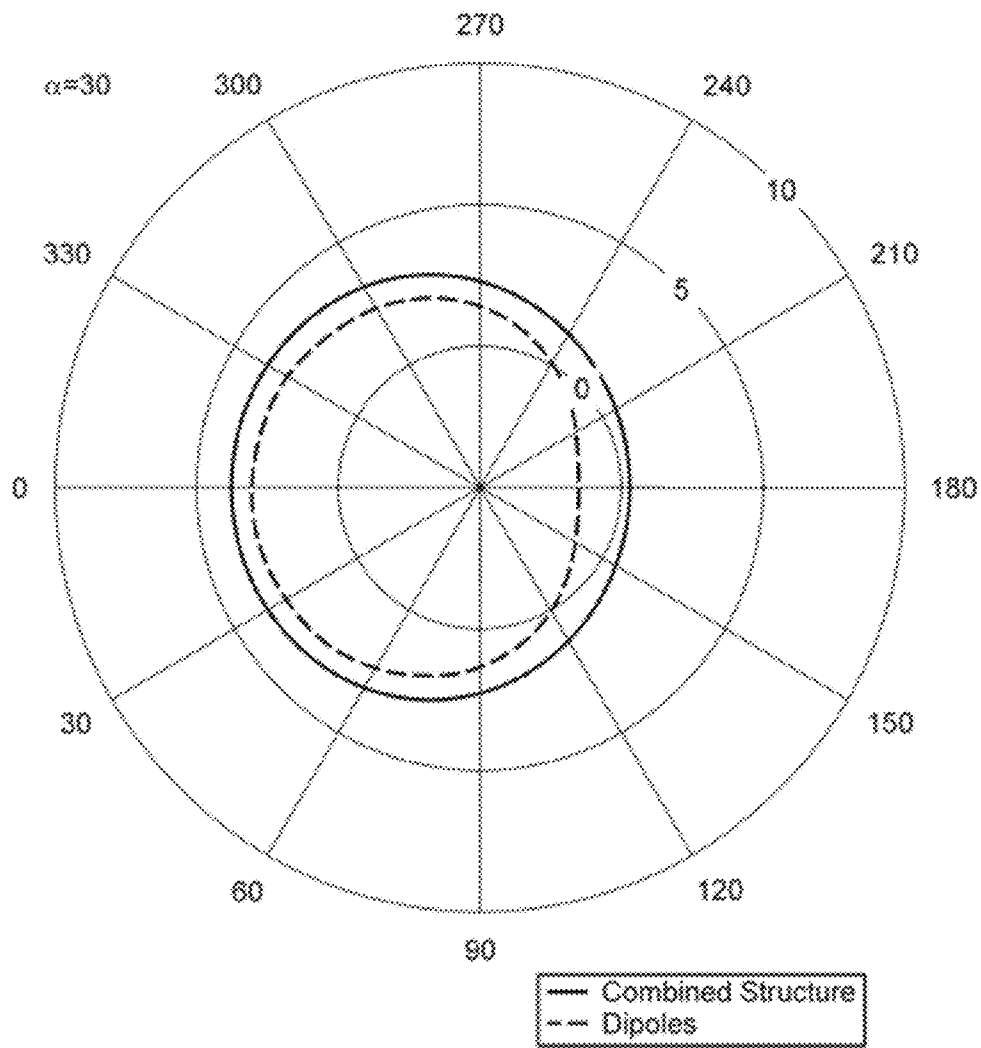


FIG. 25B

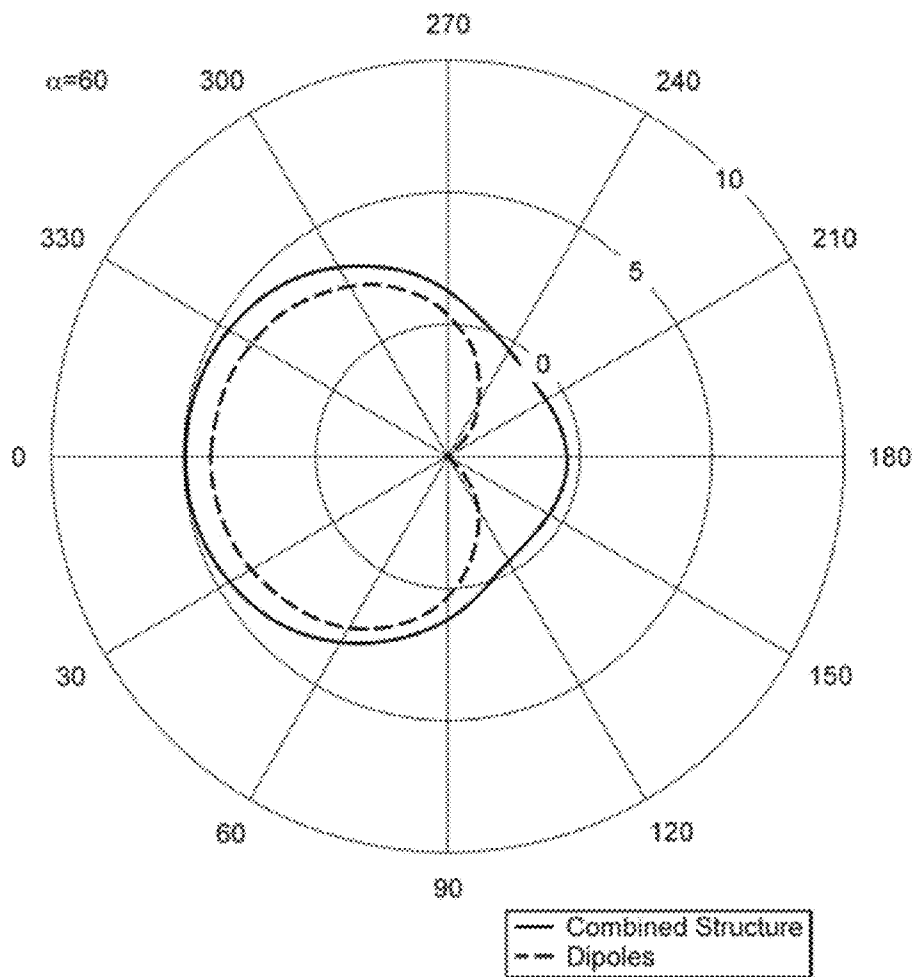


FIG. 25C

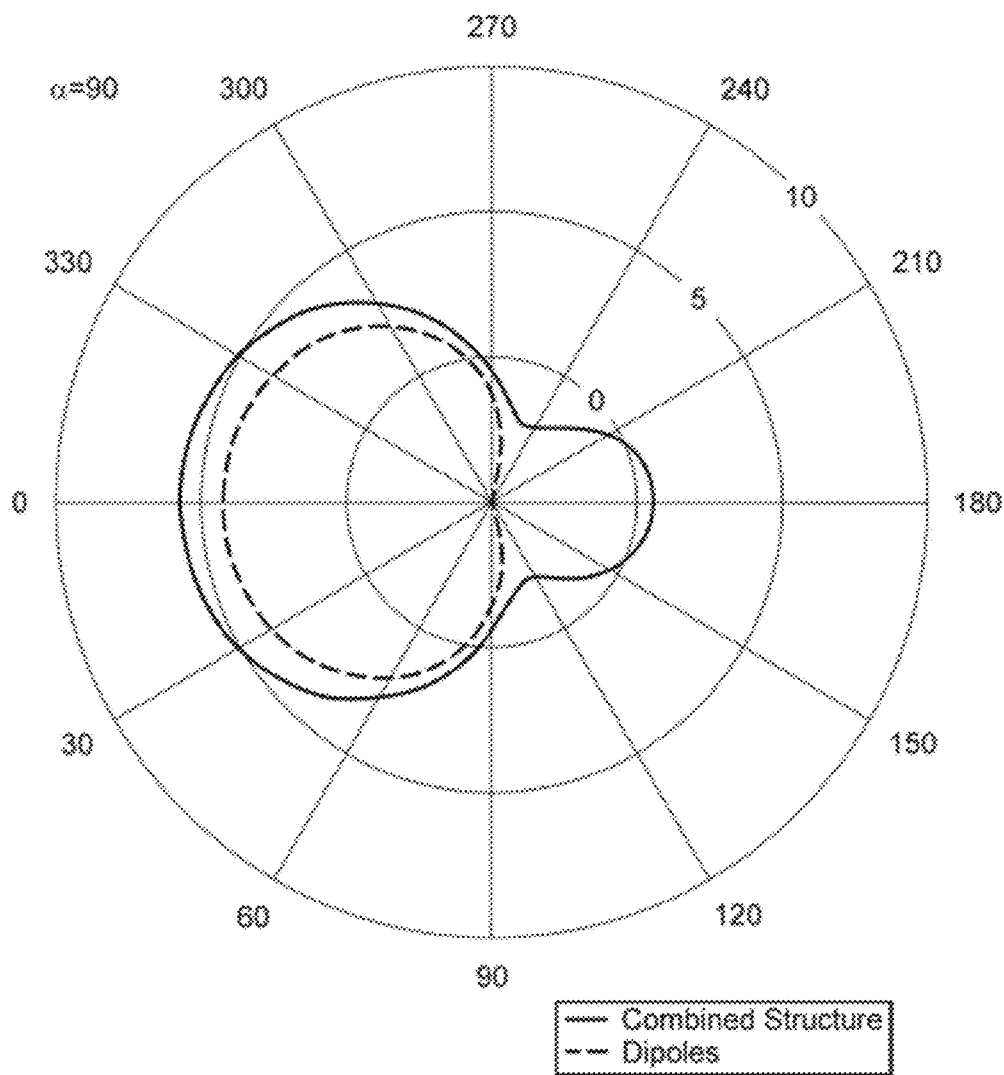


FIG. 25D

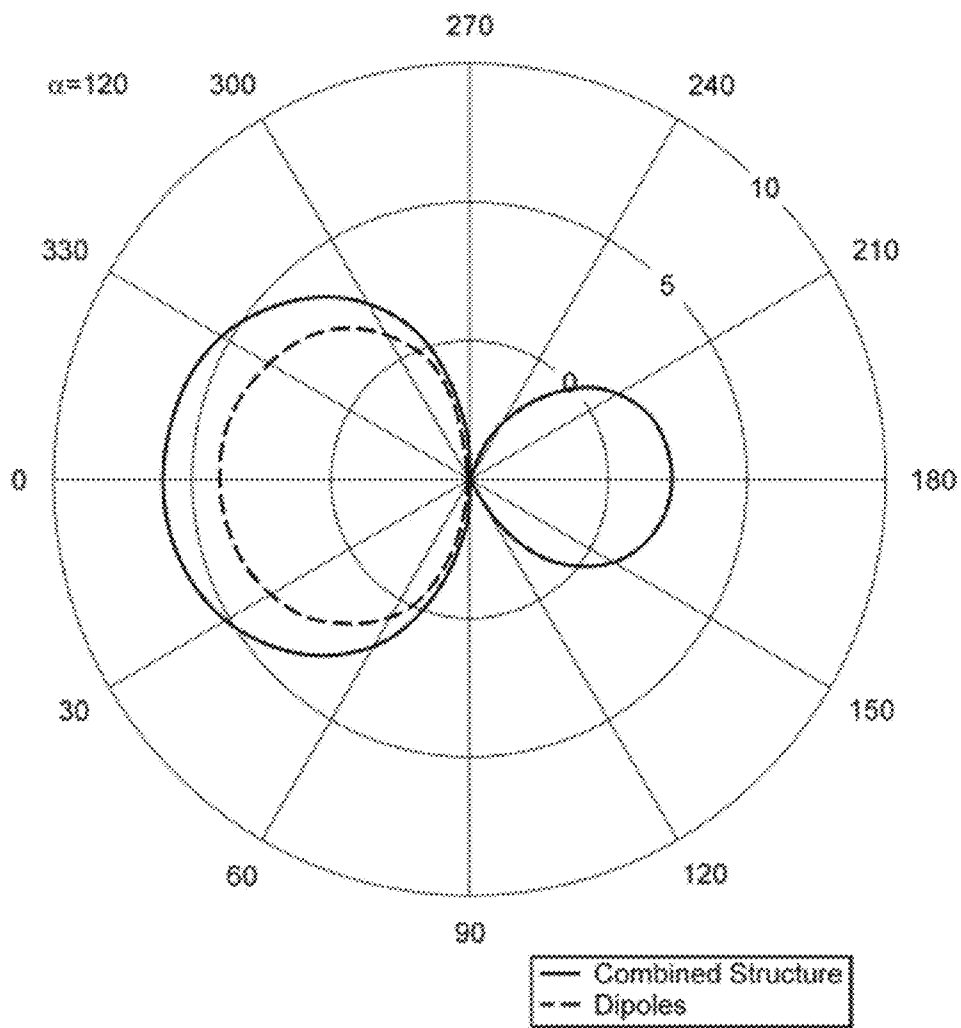


FIG. 25E

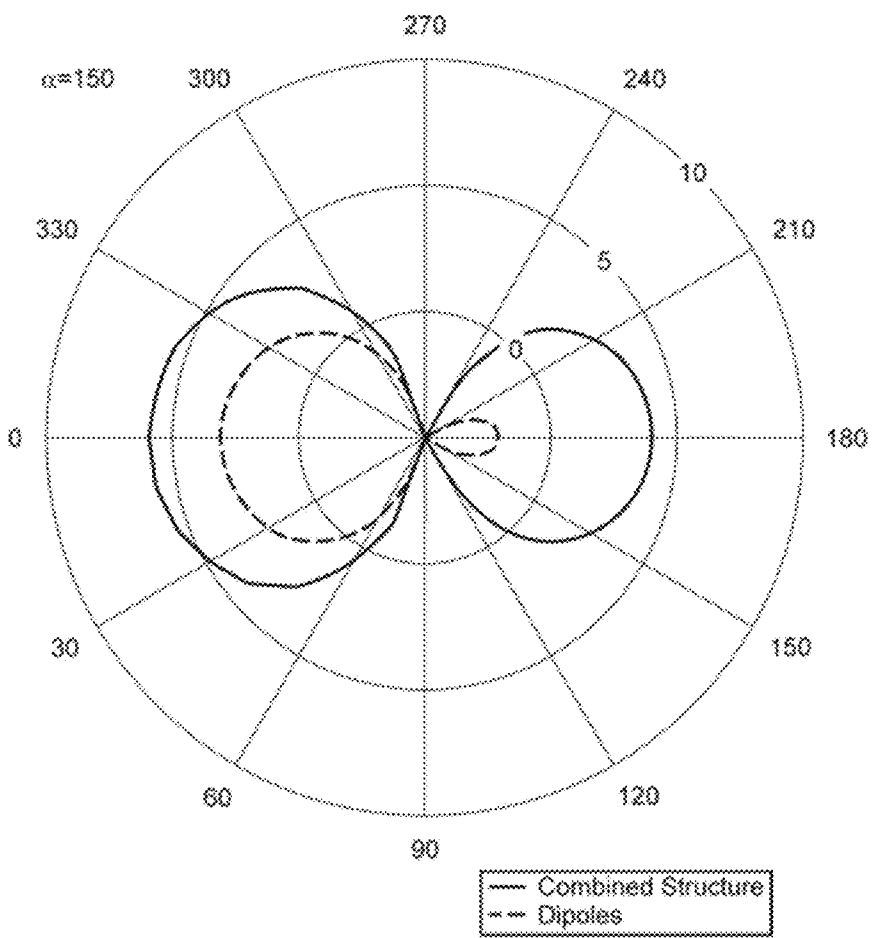


FIG. 25F

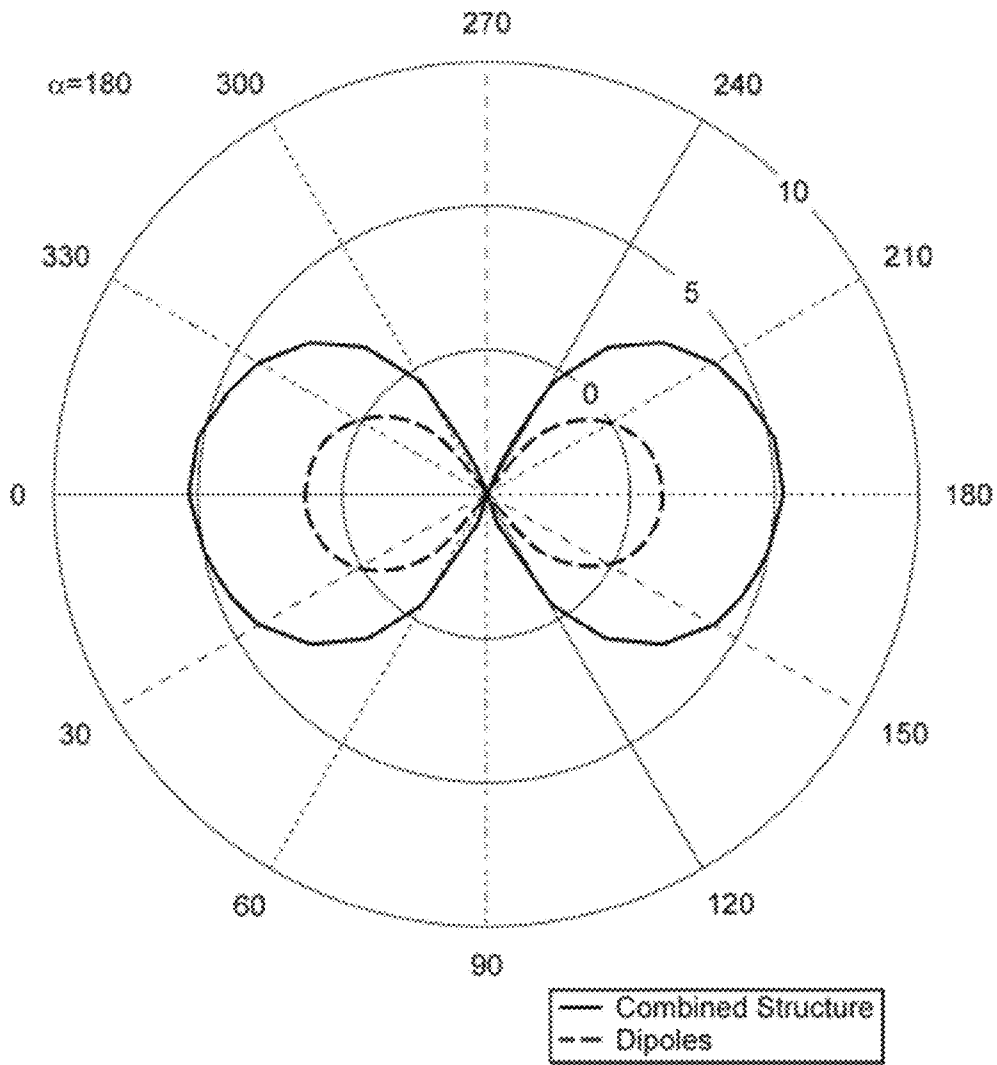


FIG. 25G

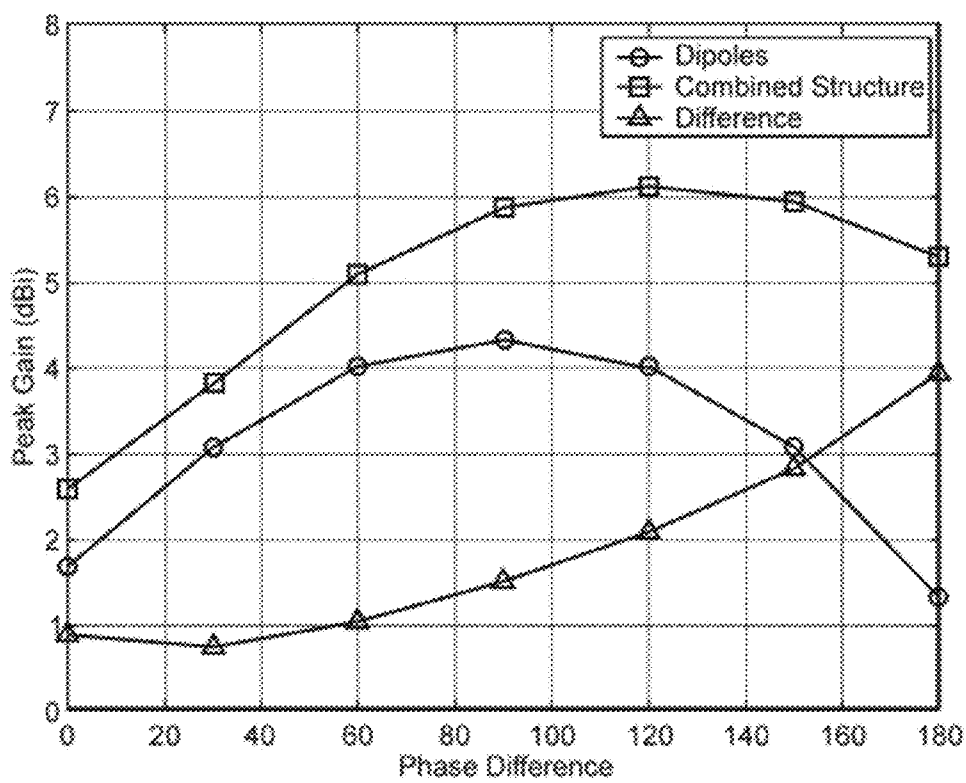


FIG. 26

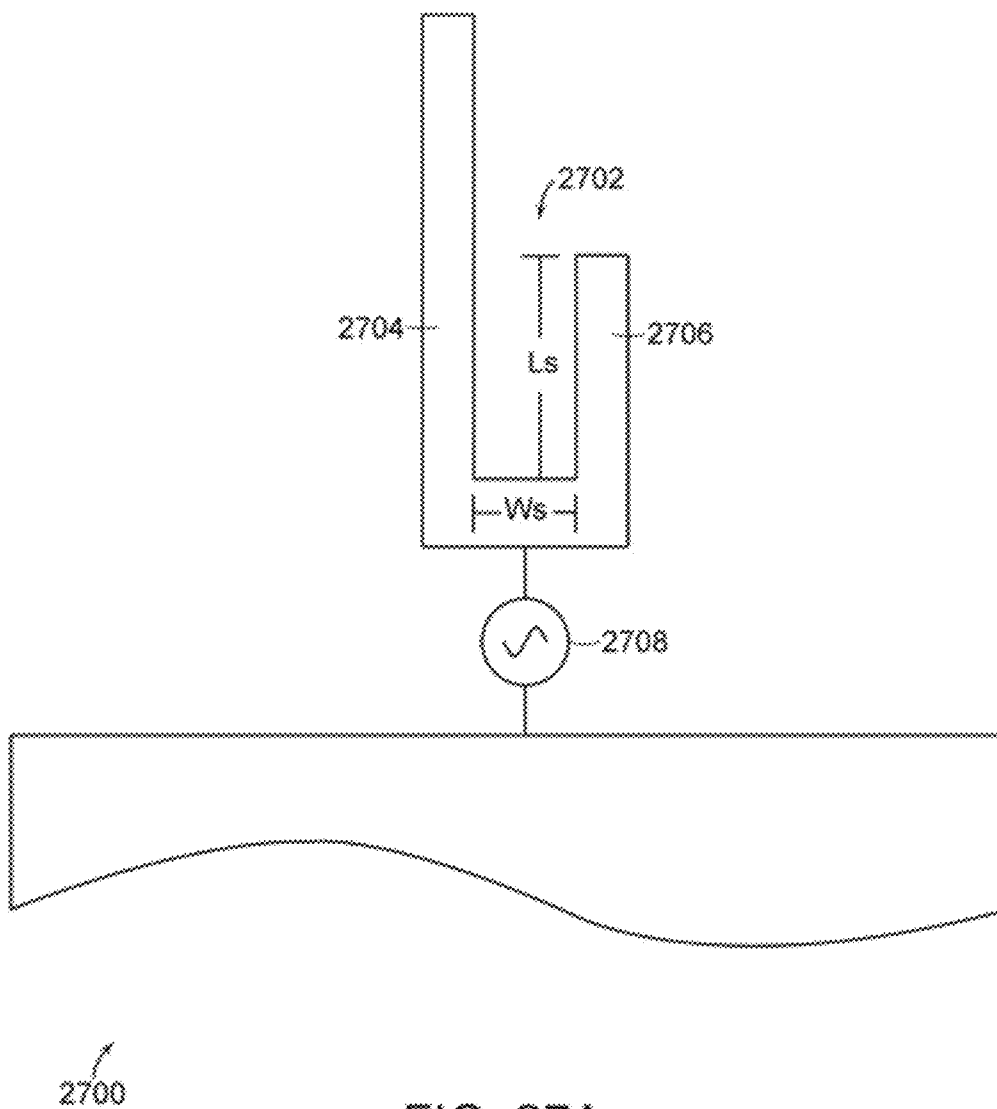


FIG. 27A

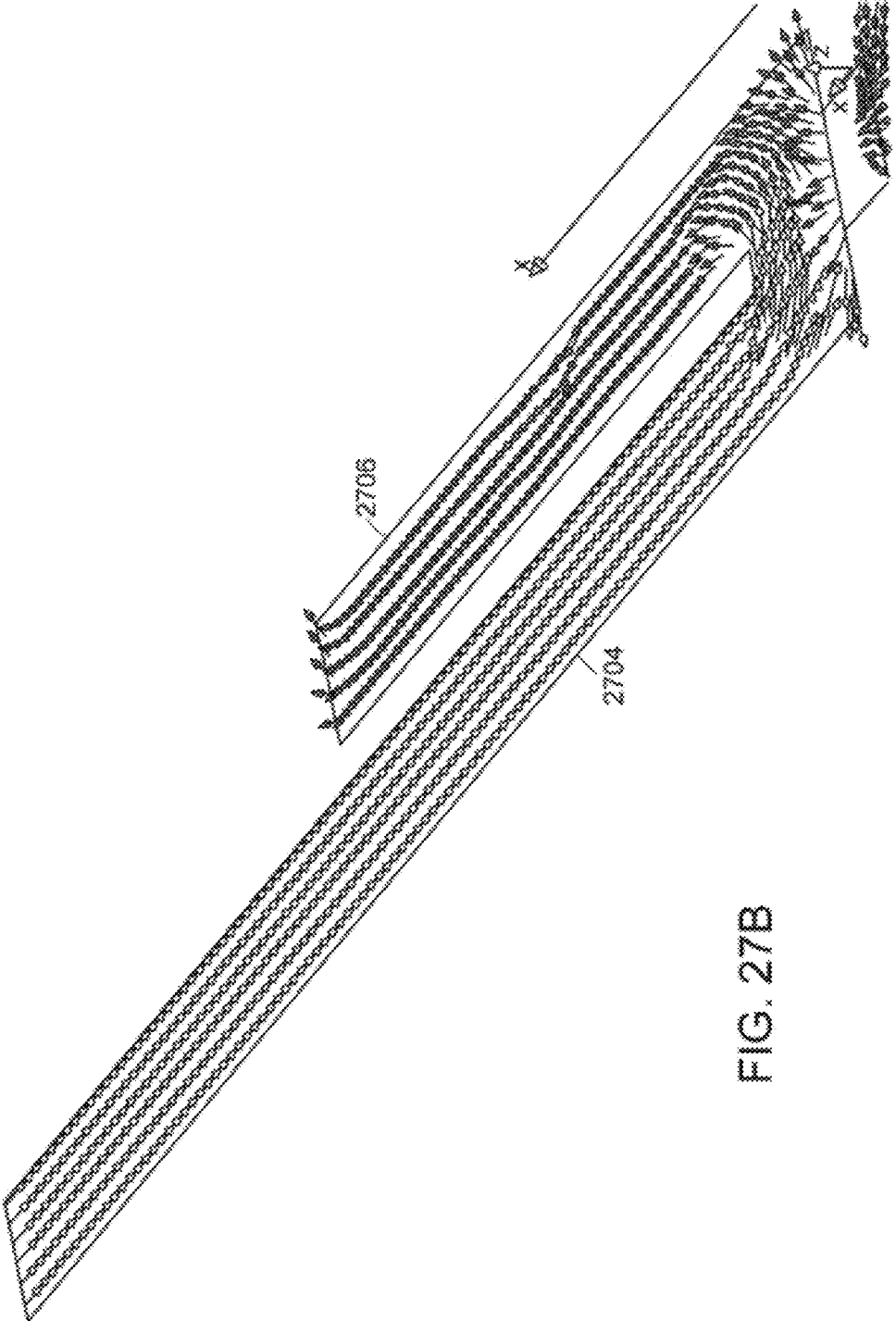


FIG. 27B

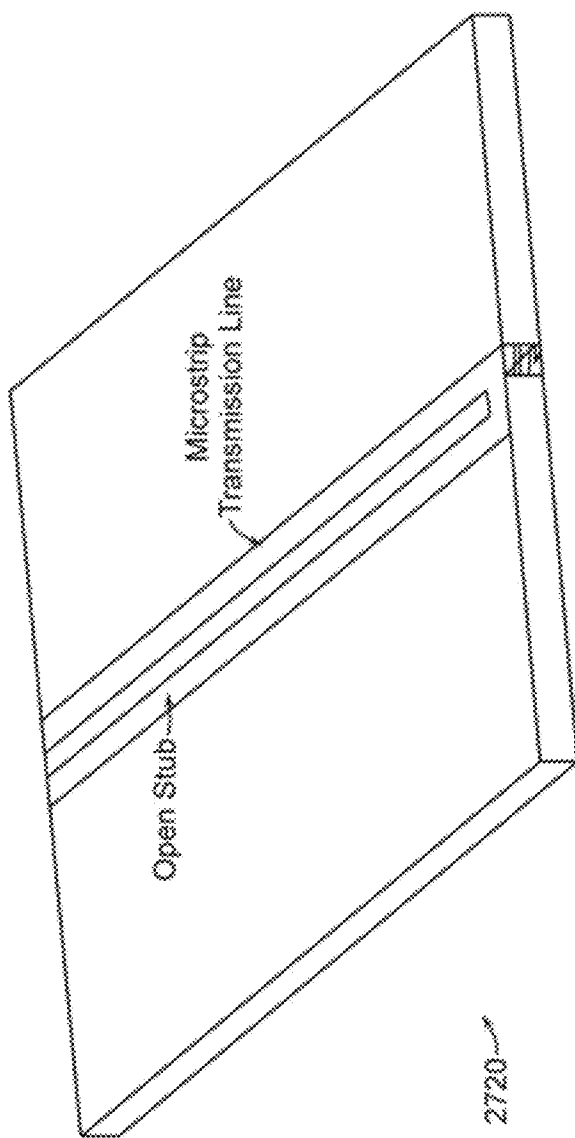


FIG. 27C

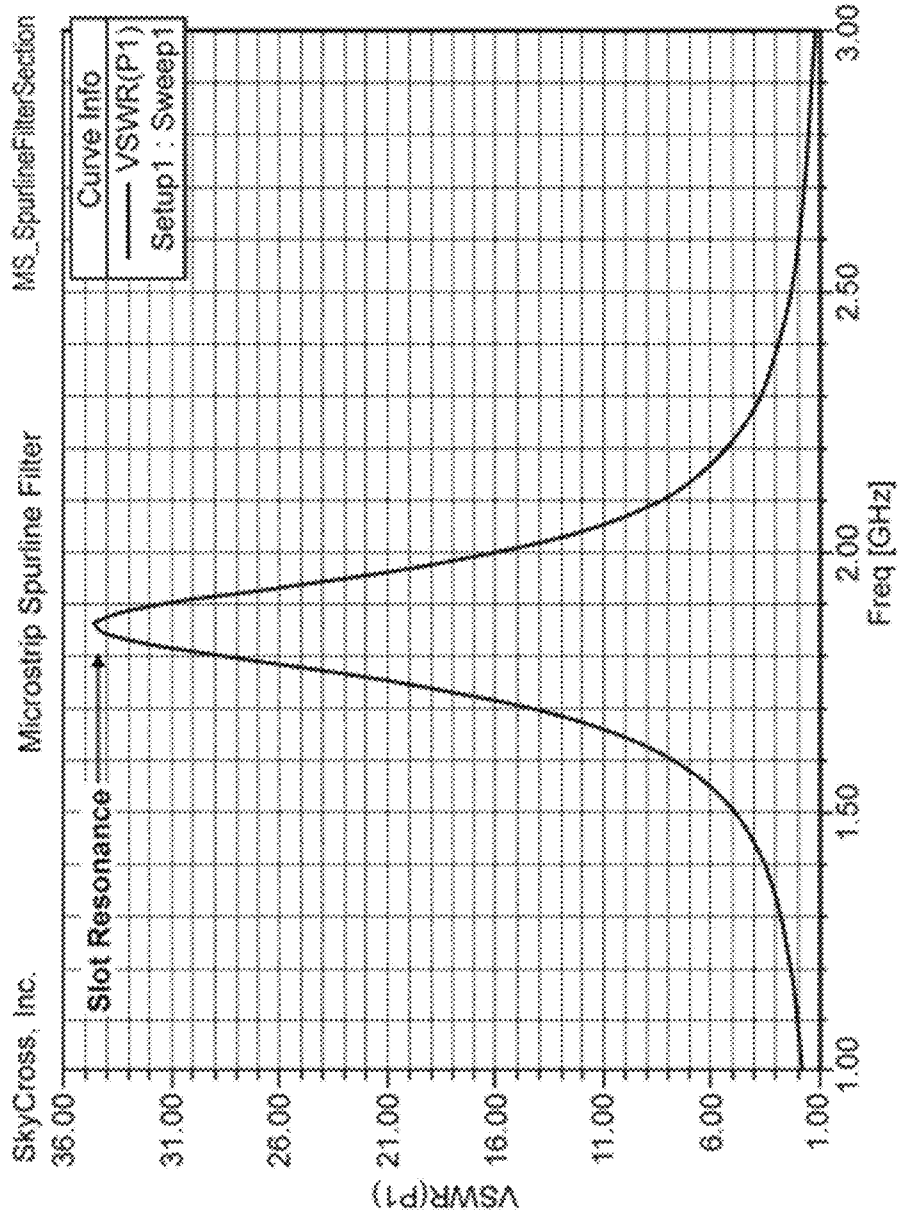


FIG. 27D

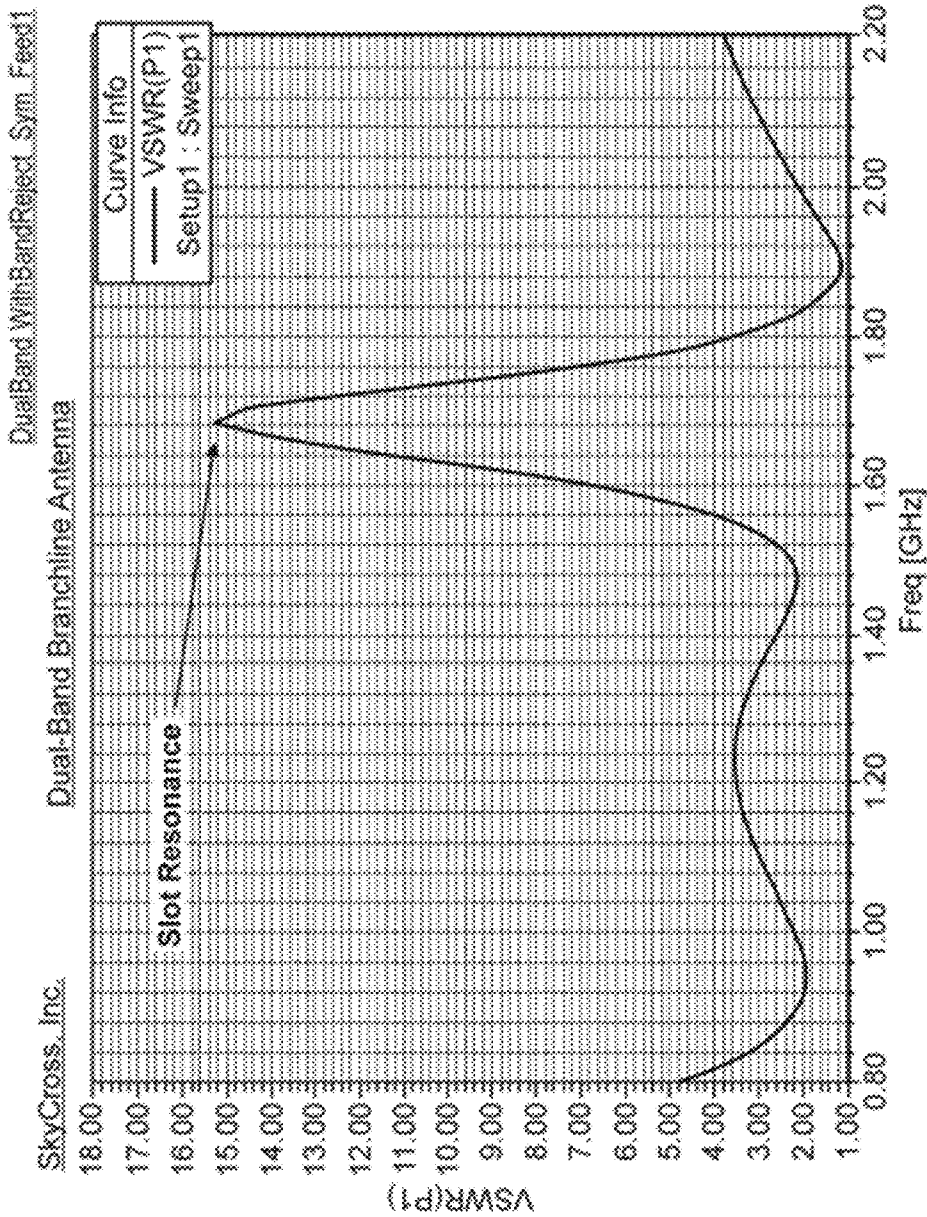


FIG. 27E

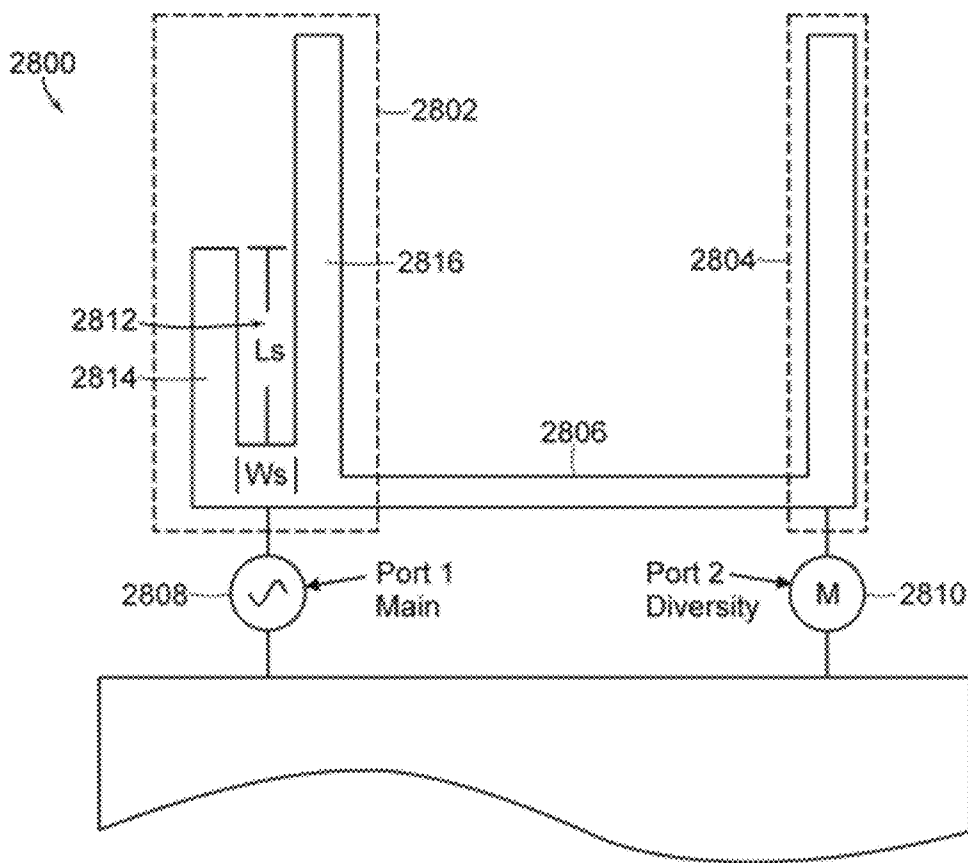


FIG. 28

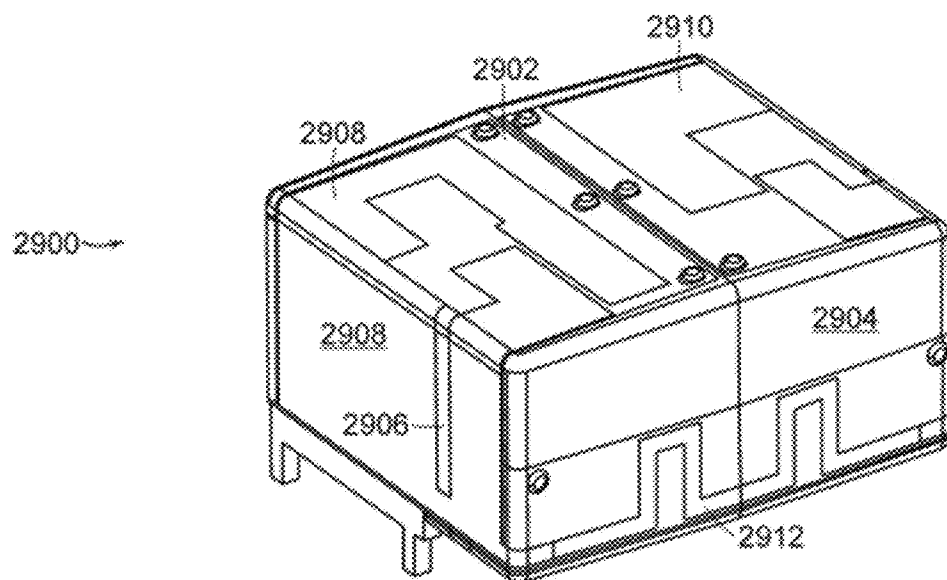


FIG. 29A

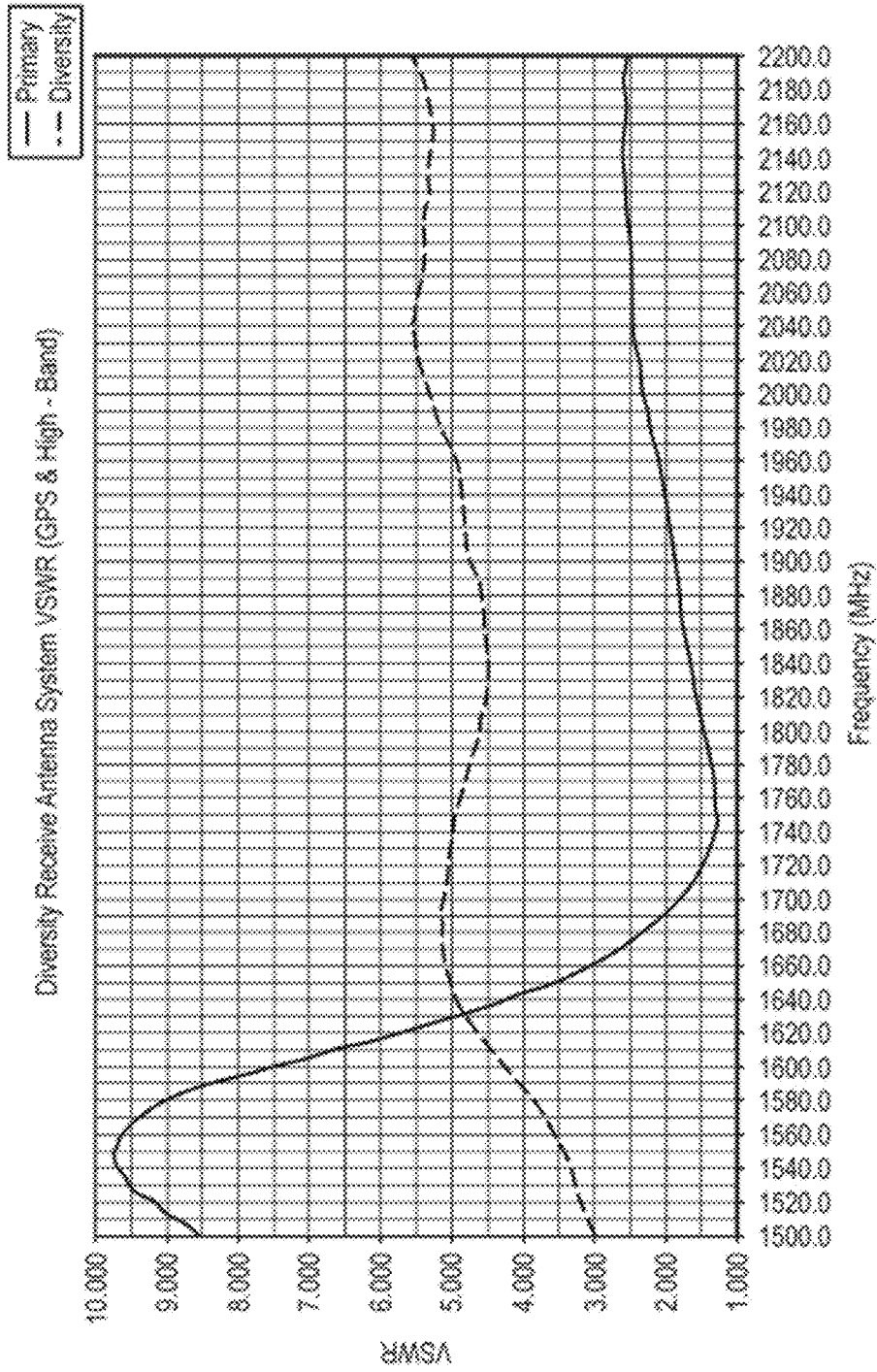


FIG. 29B

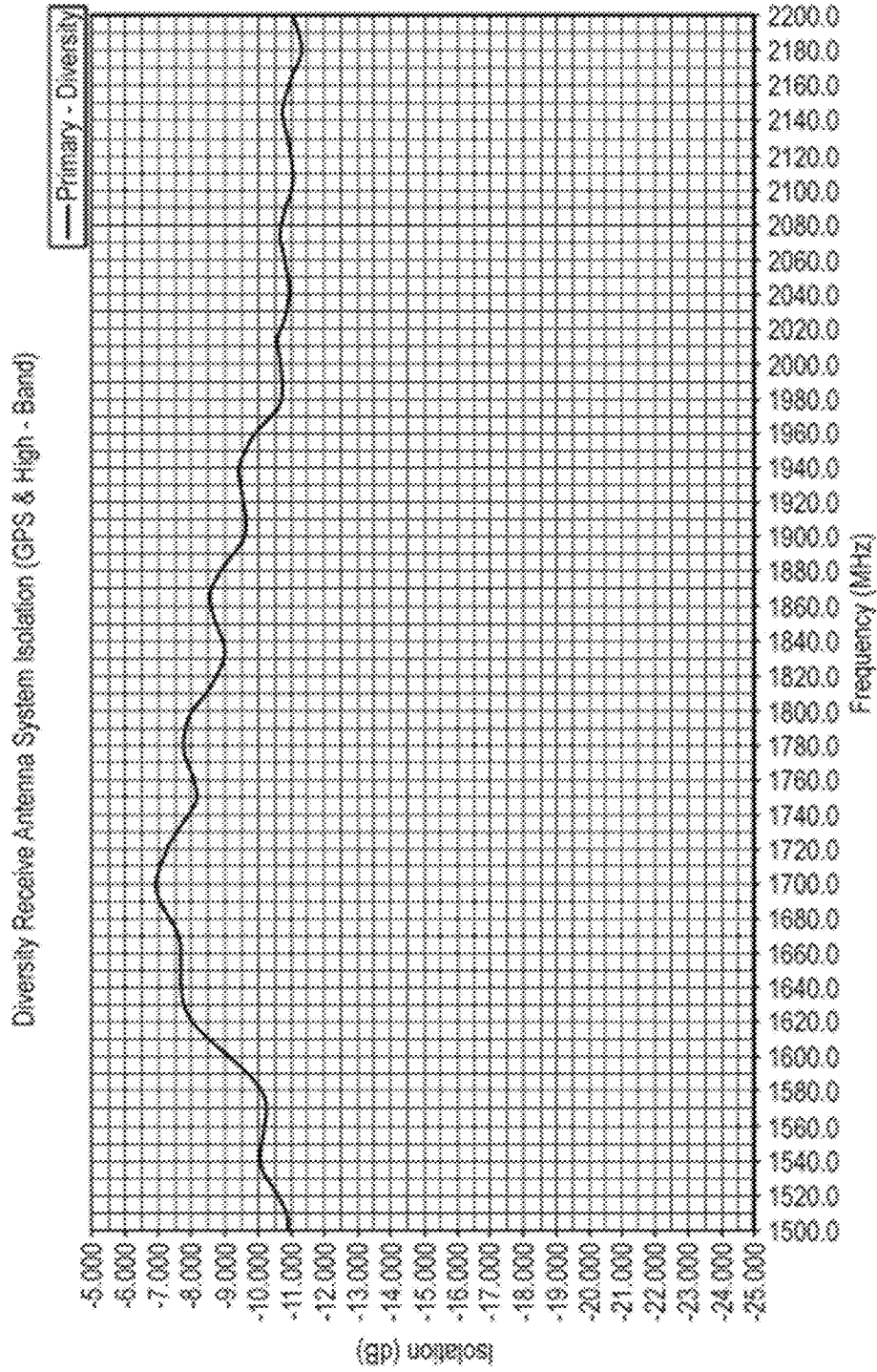


FIG. 29C

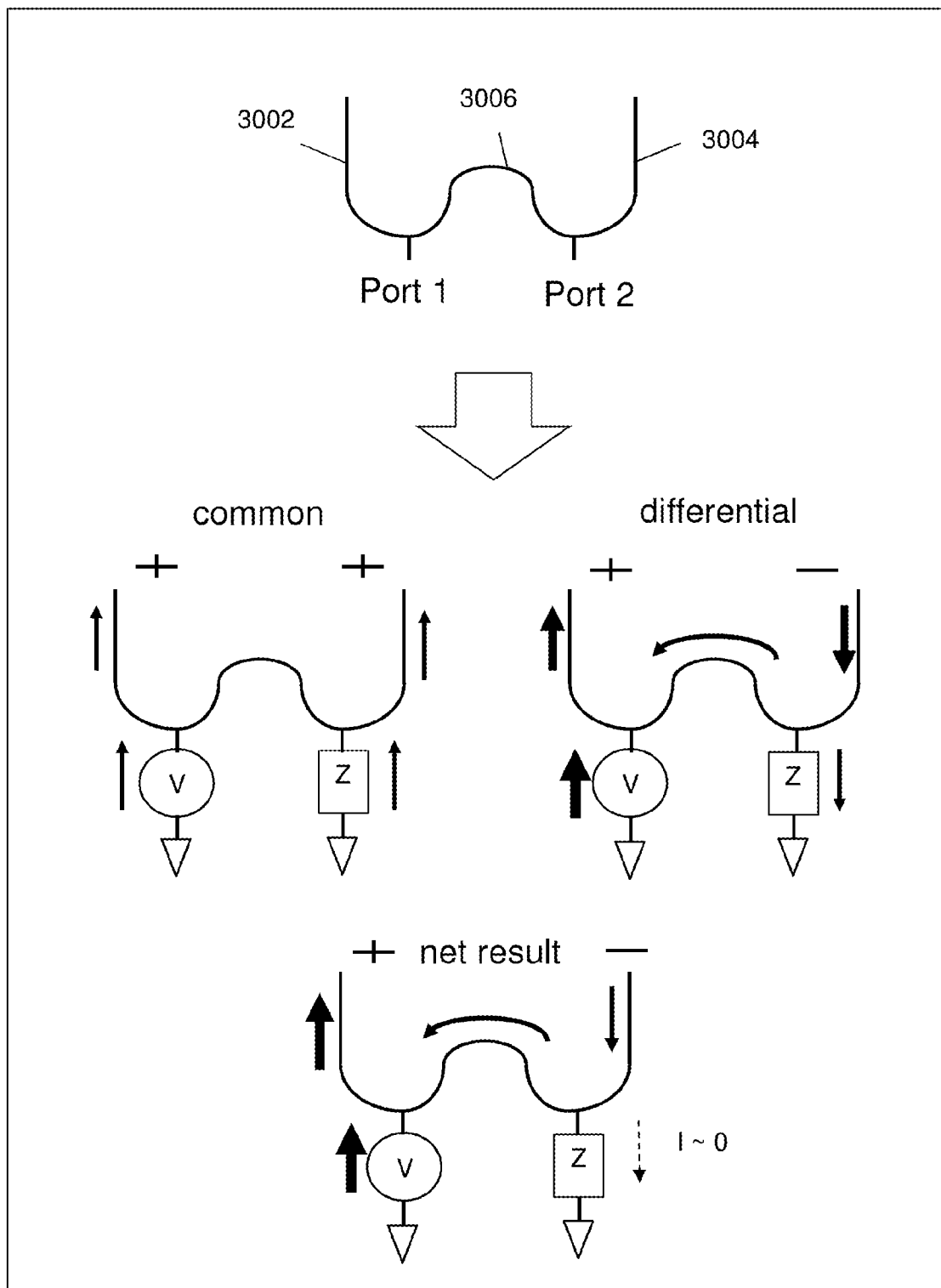


FIG. 30

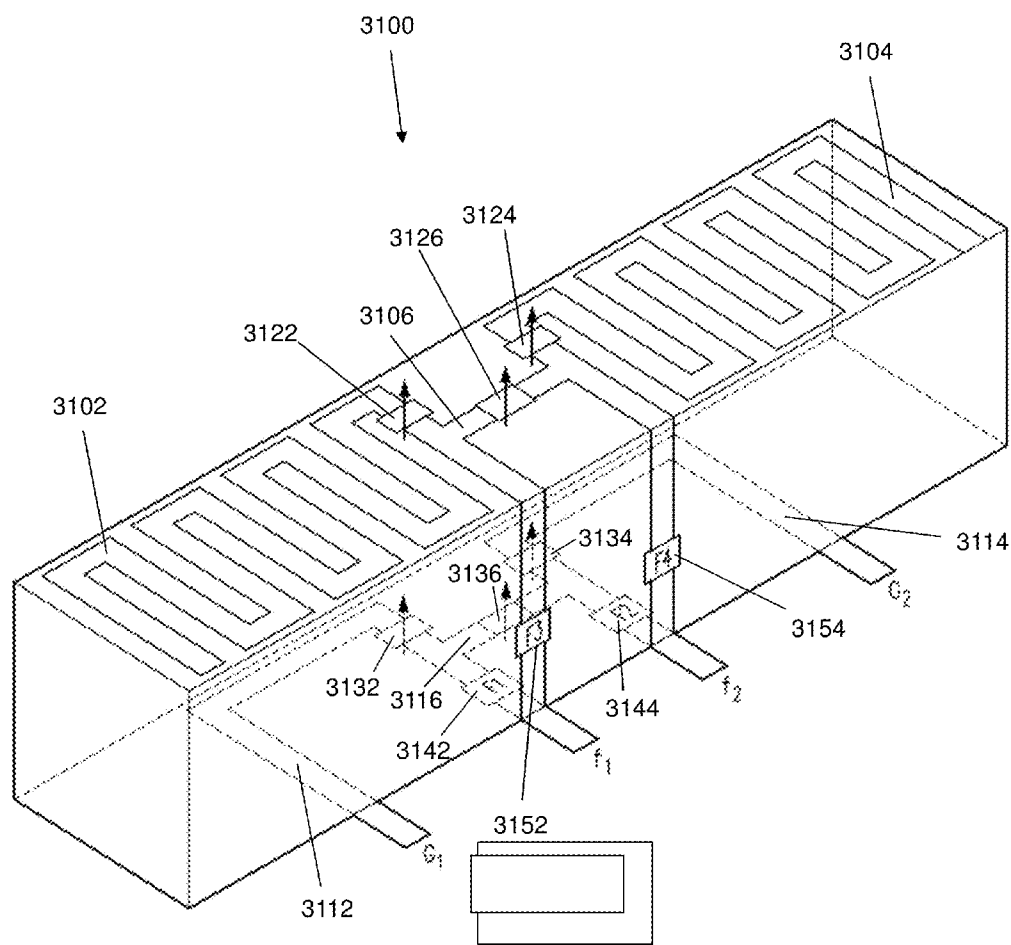


FIG. 31

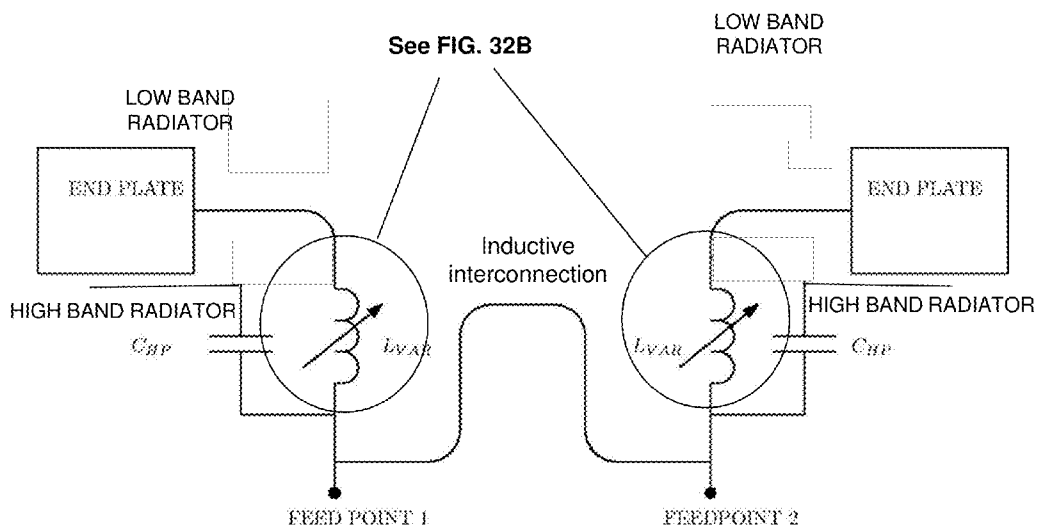


FIG. 32A

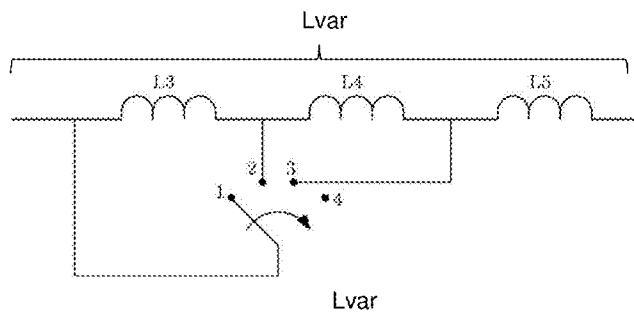


FIG. 32B

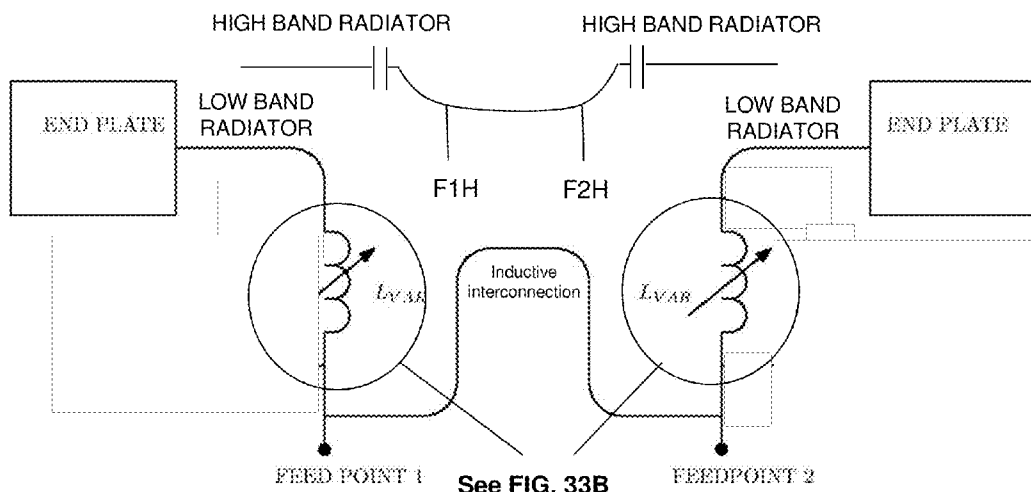


FIG. 33A

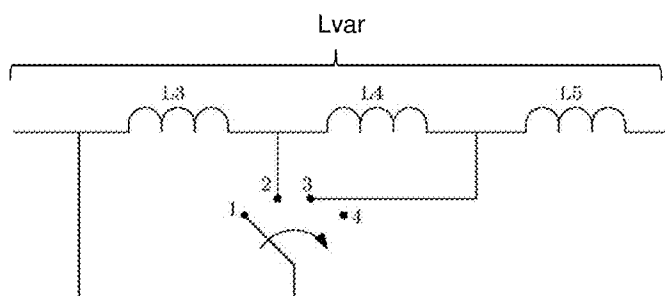


FIG. 33B

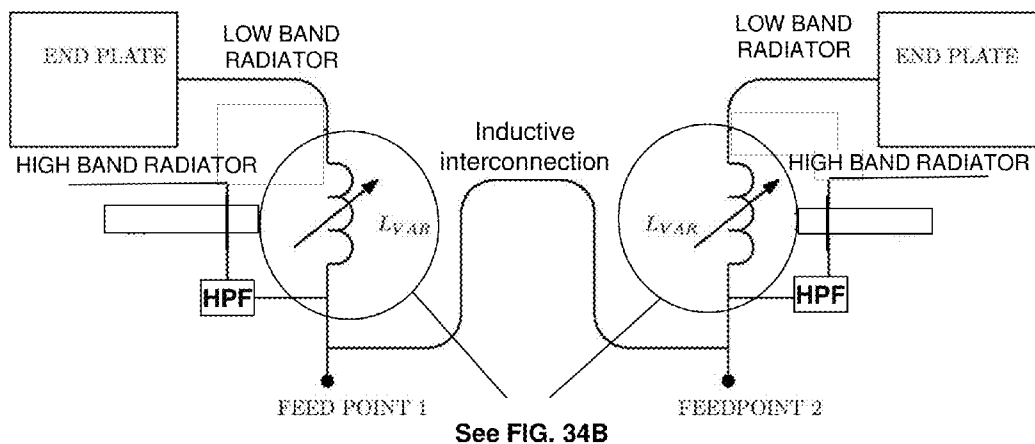


FIG. 34A

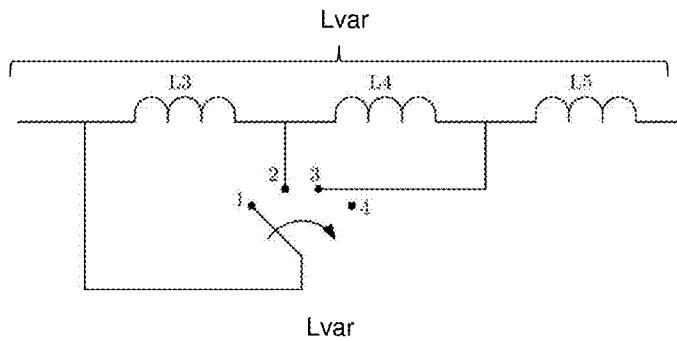


FIG. 34B

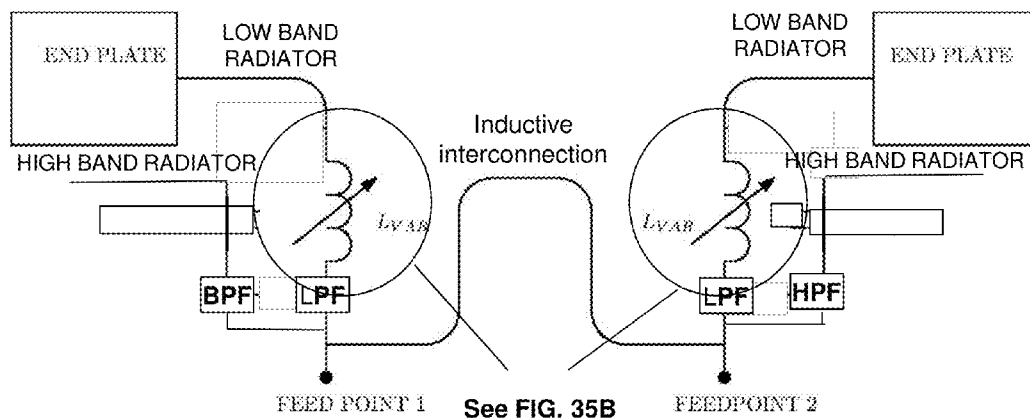


FIG. 35A

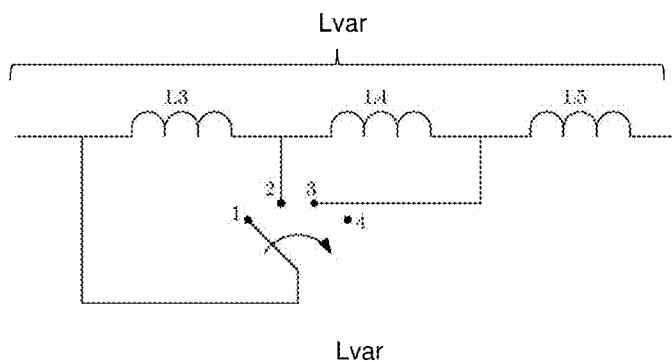
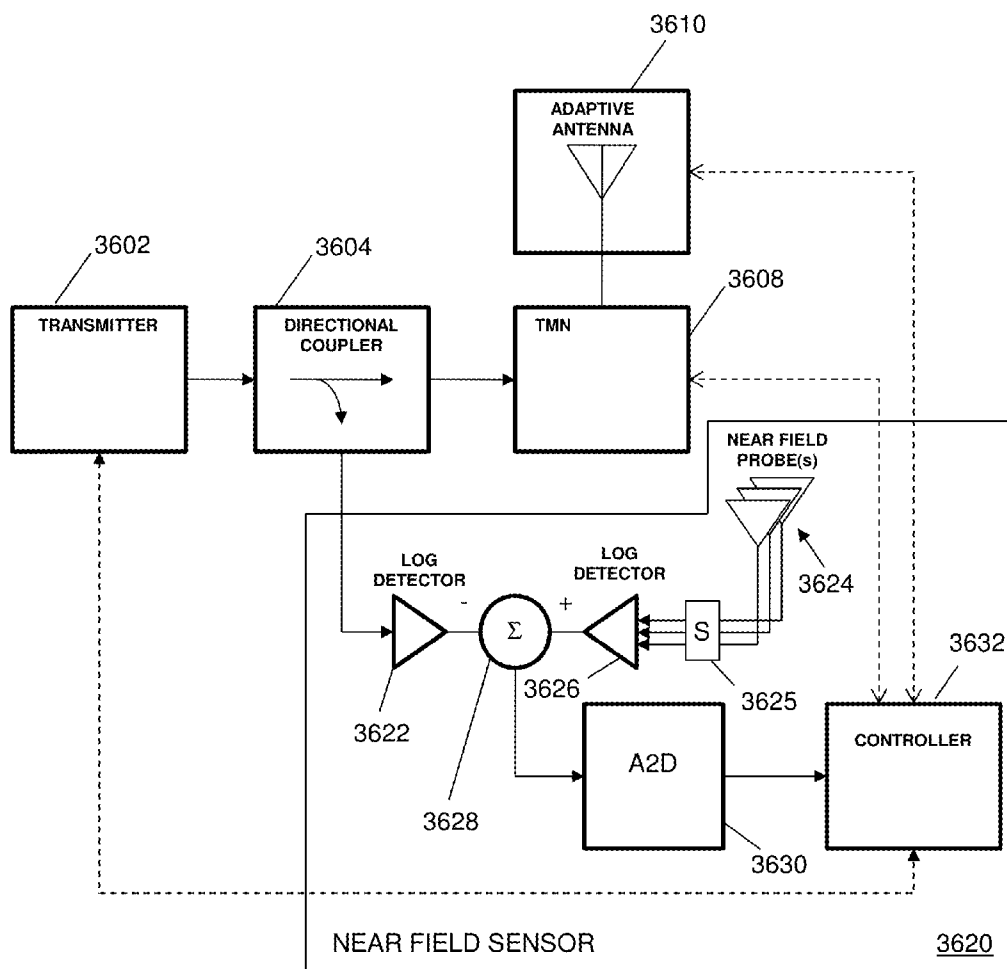
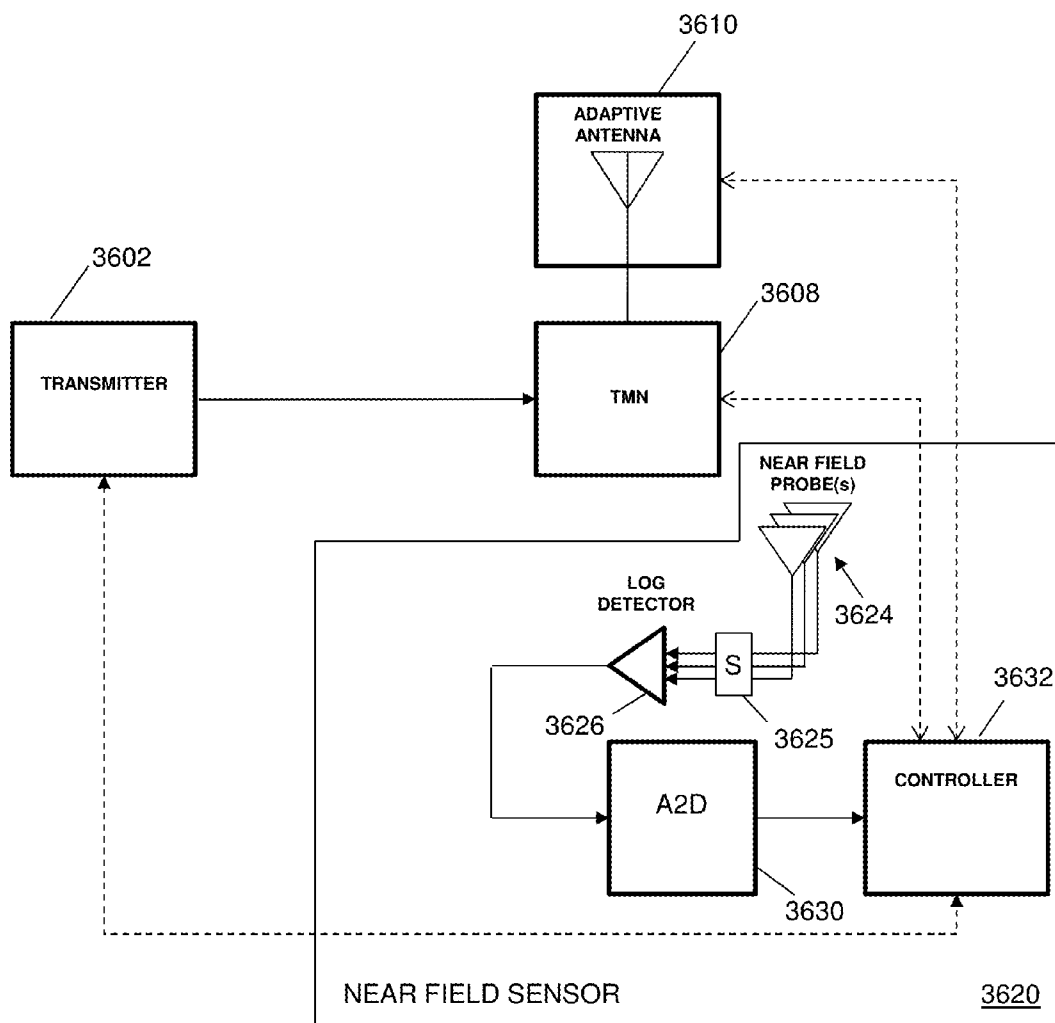


FIG. 35B



3600
FIG. 36A



3600
FIG. 36B

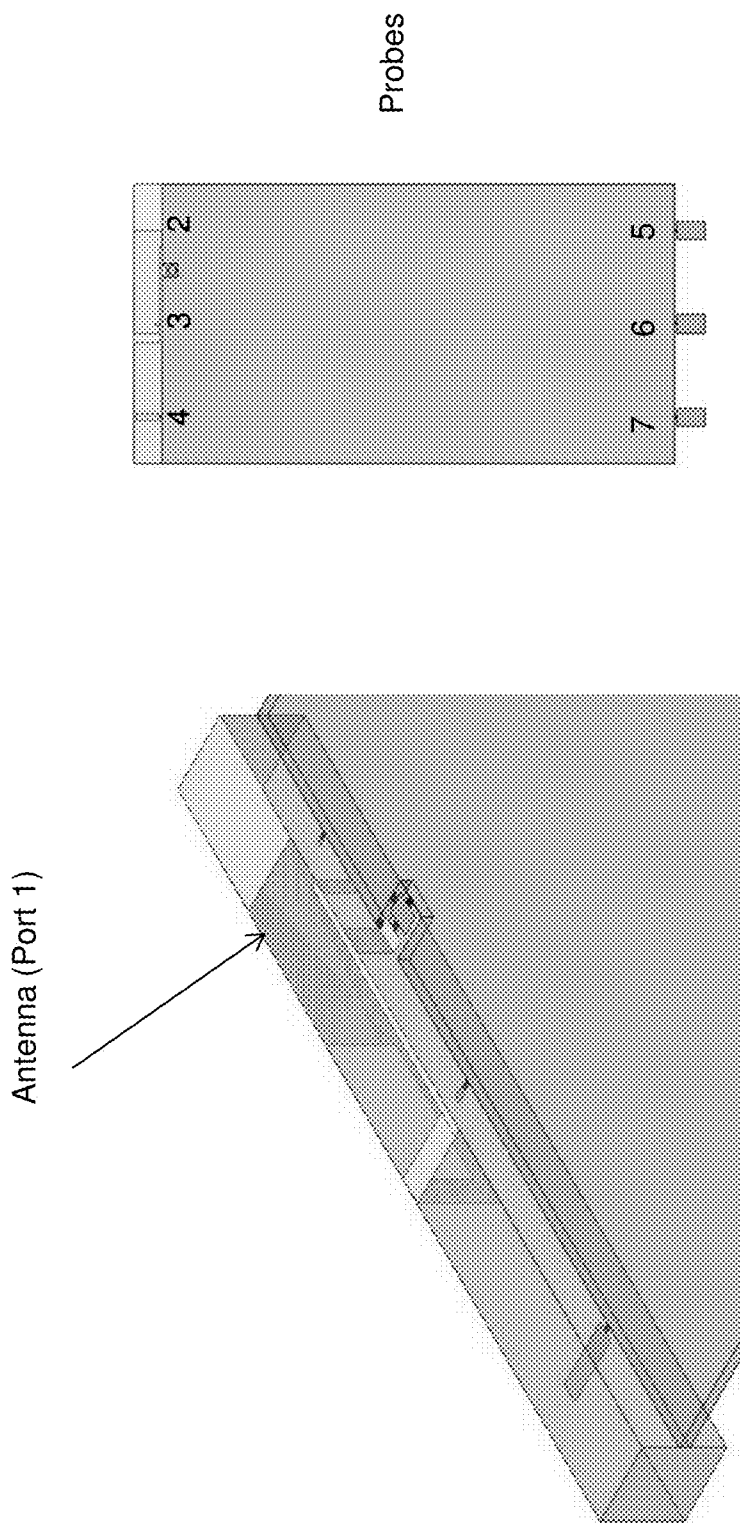


FIG. 37

Material: body tissue or steel (shown as gray)
2mm air gap between furthest model element and load material

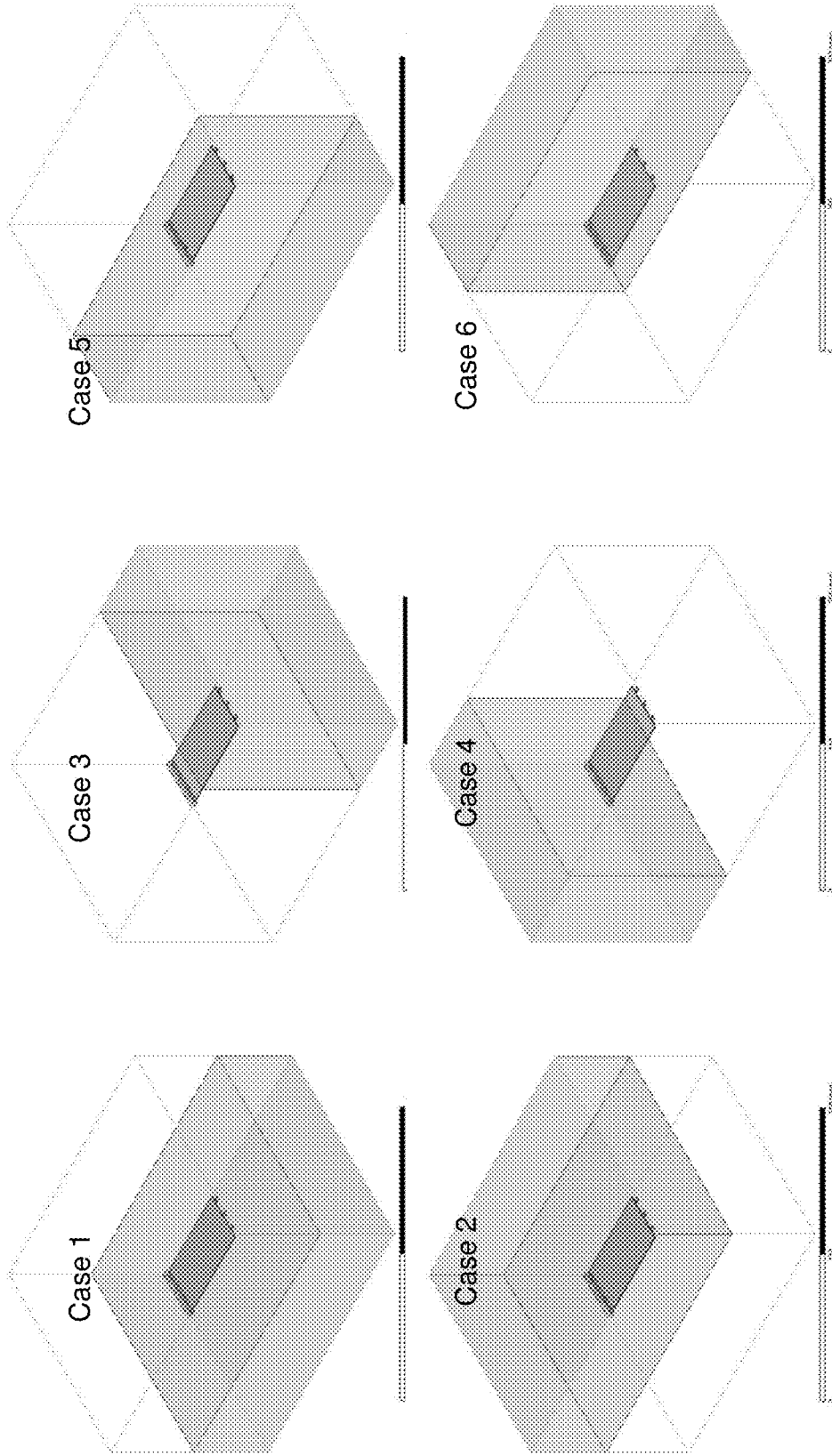


FIG. 38

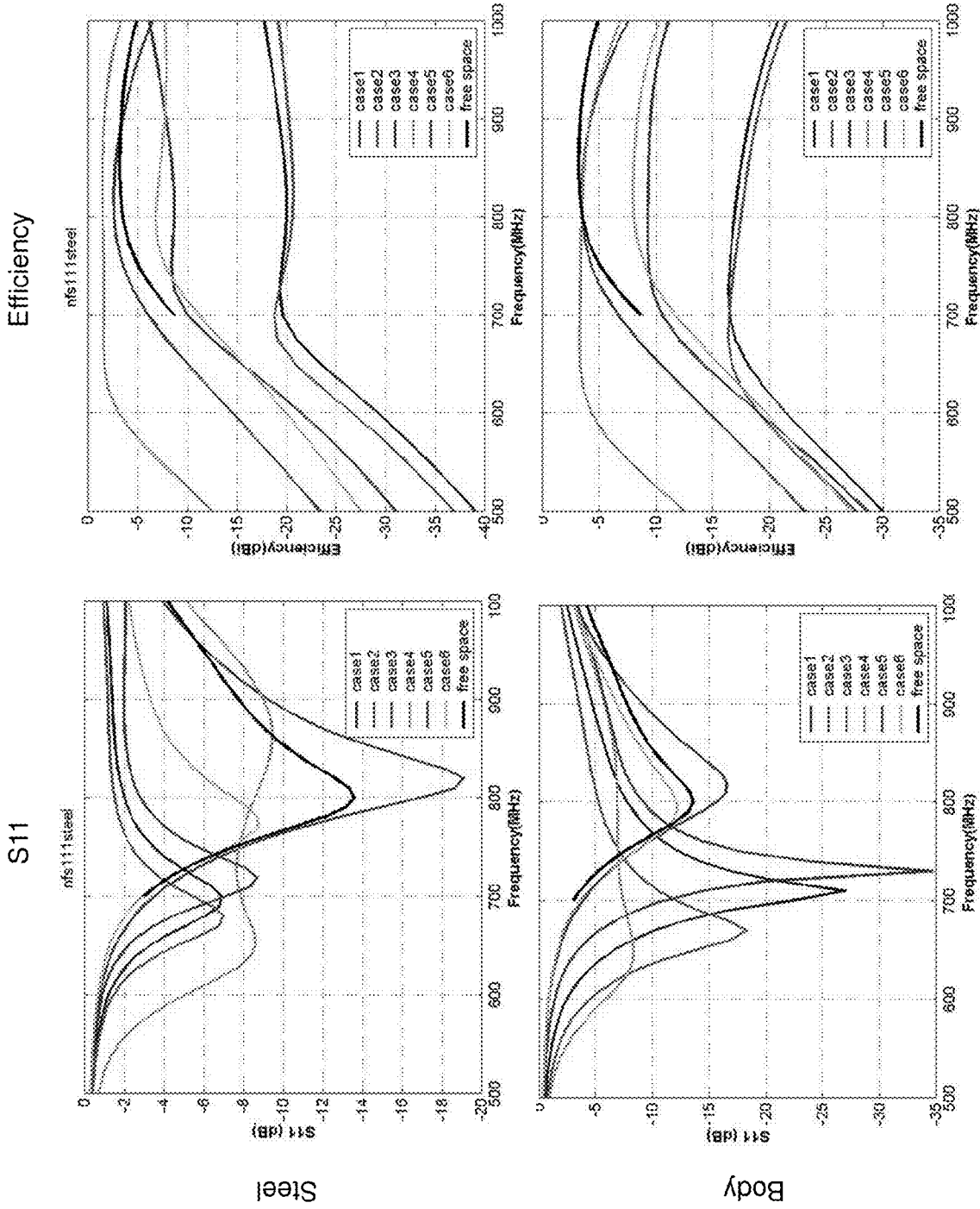


FIG. 39

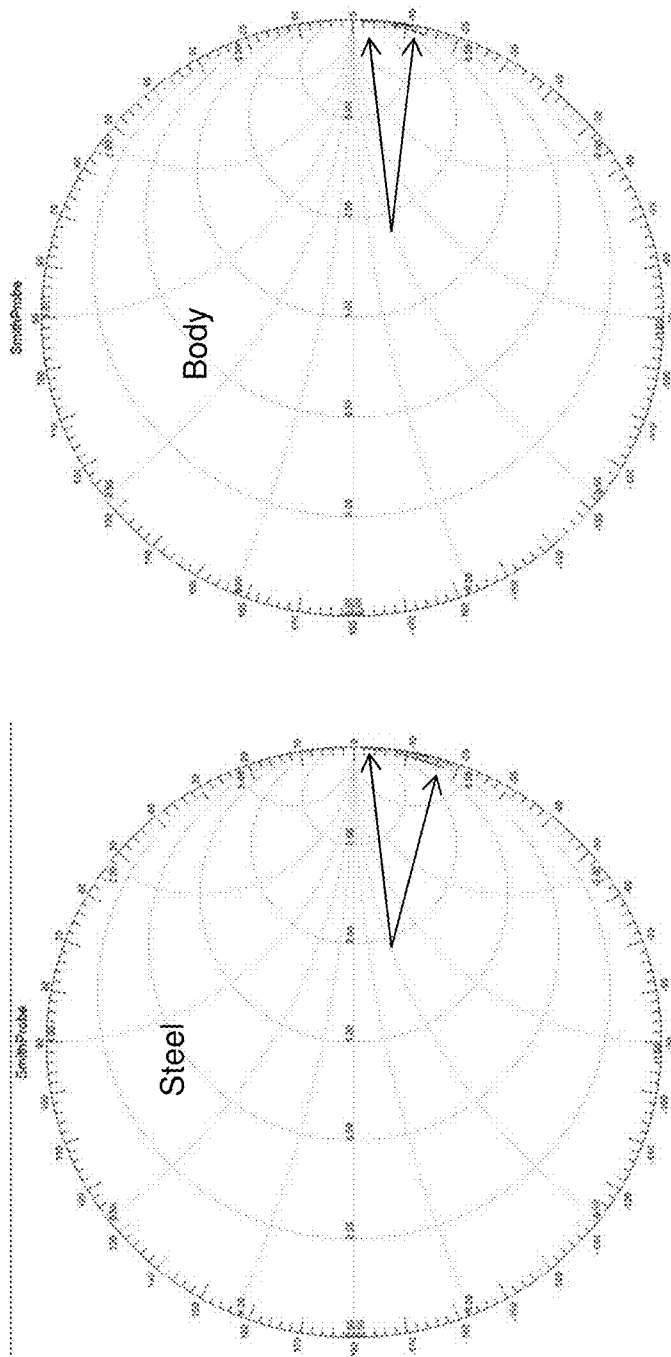


FIG. 40

Probe 2 Response Magnitude and Phase

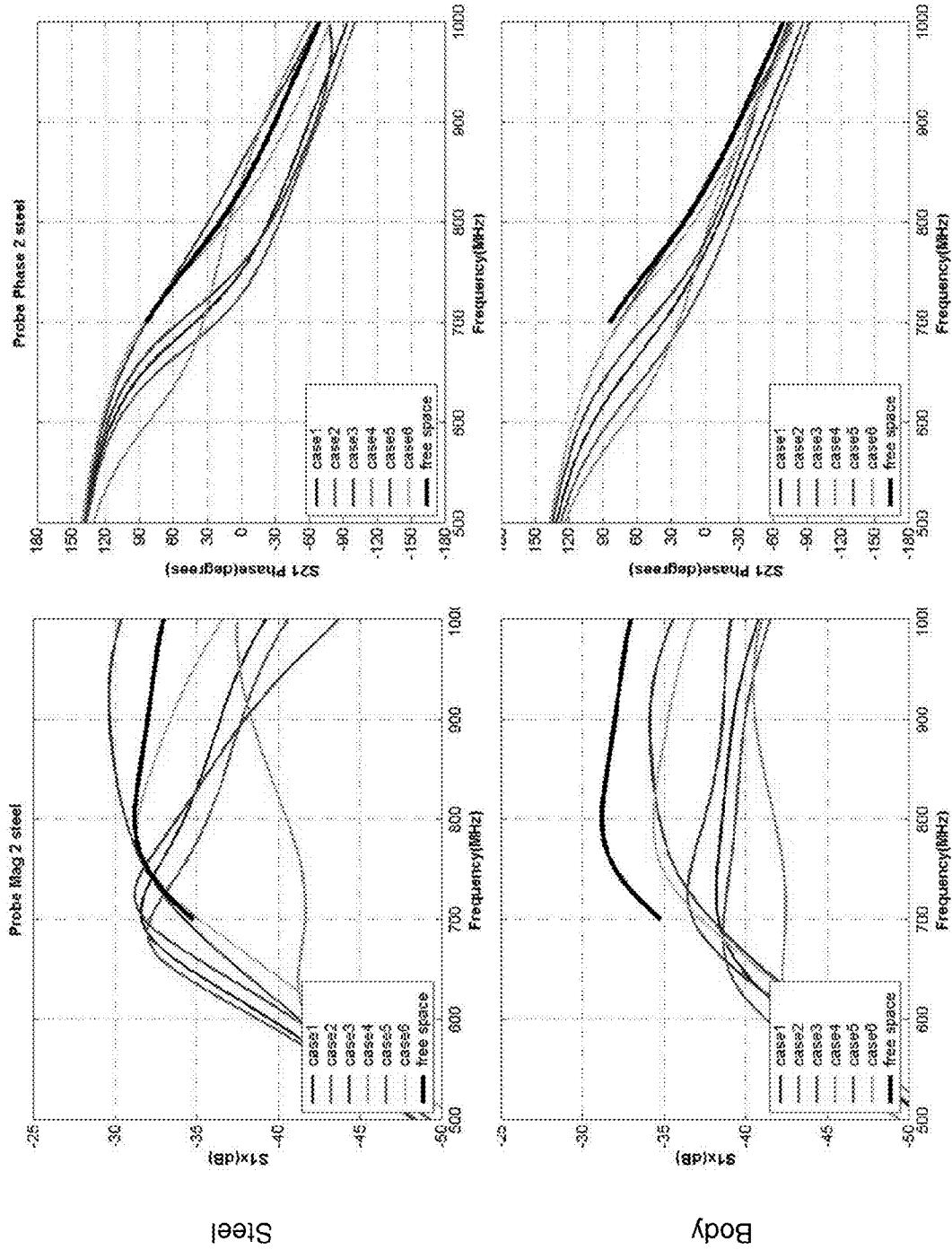


FIG. 41

Probe 4 Response Magnitude and Phase

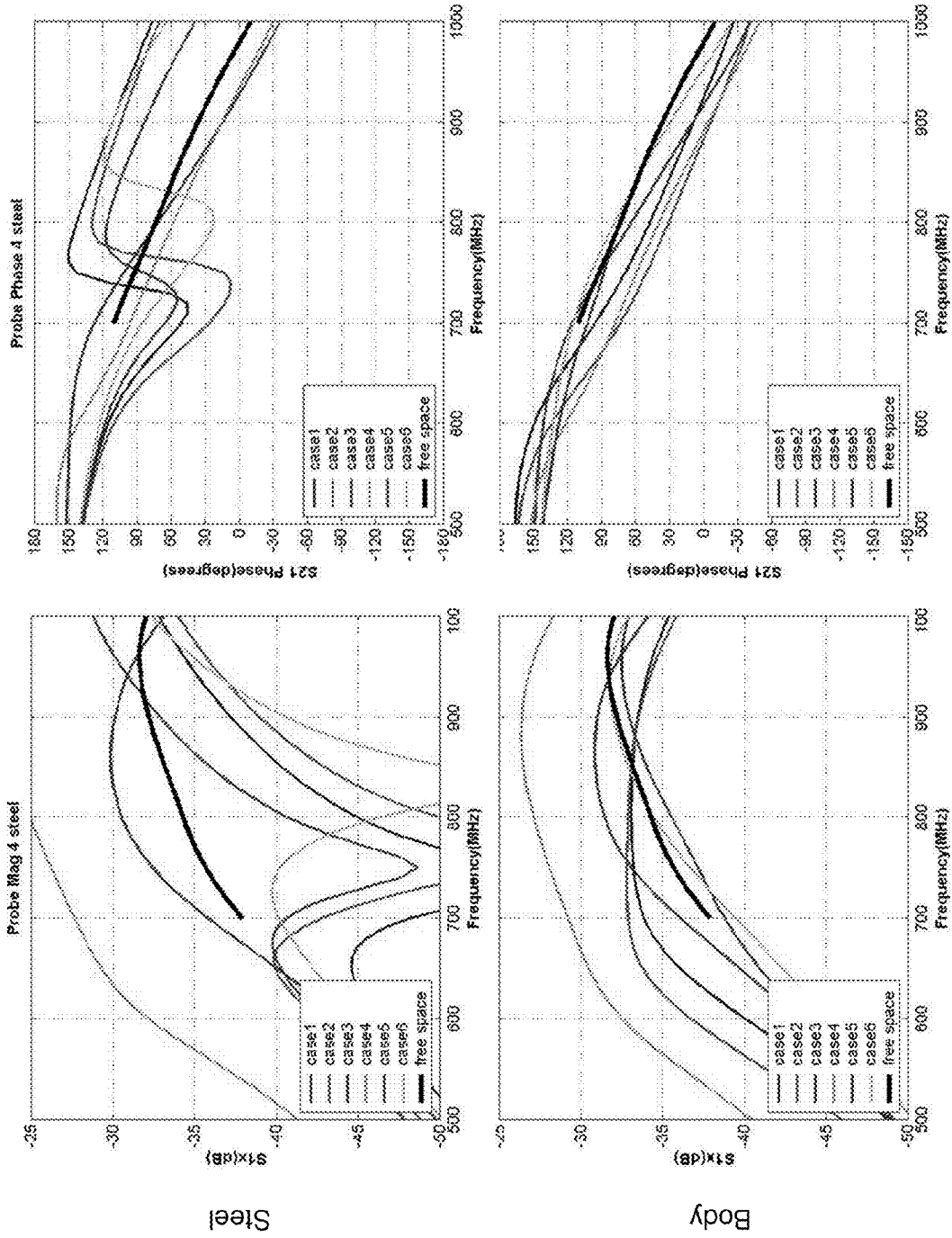
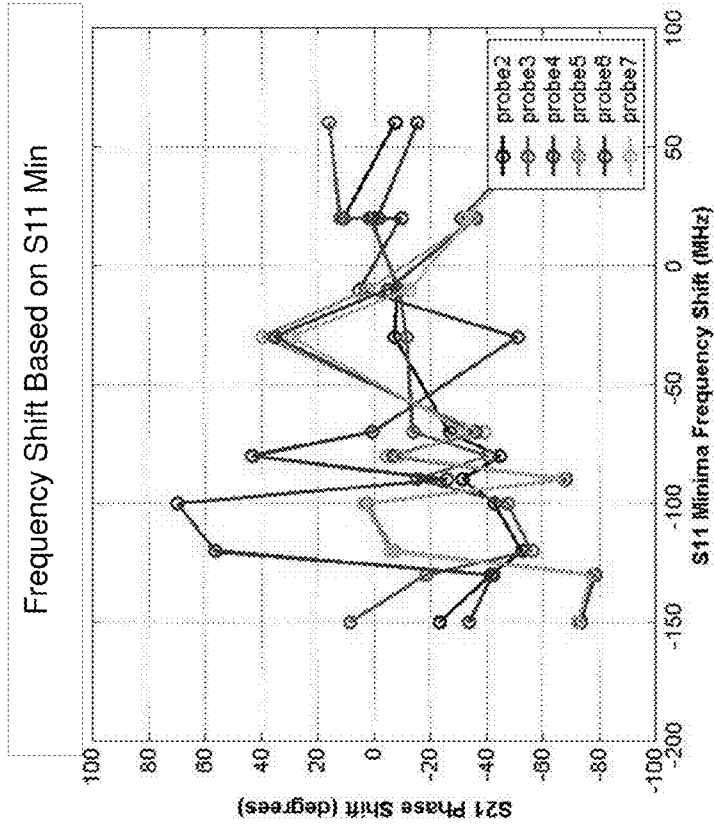
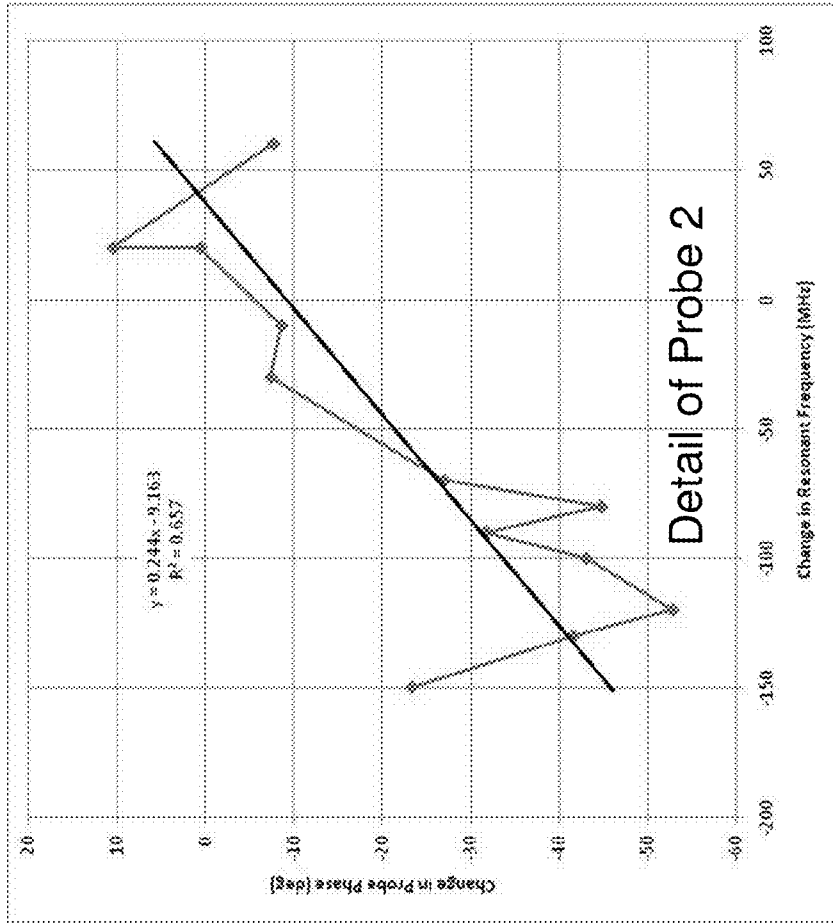


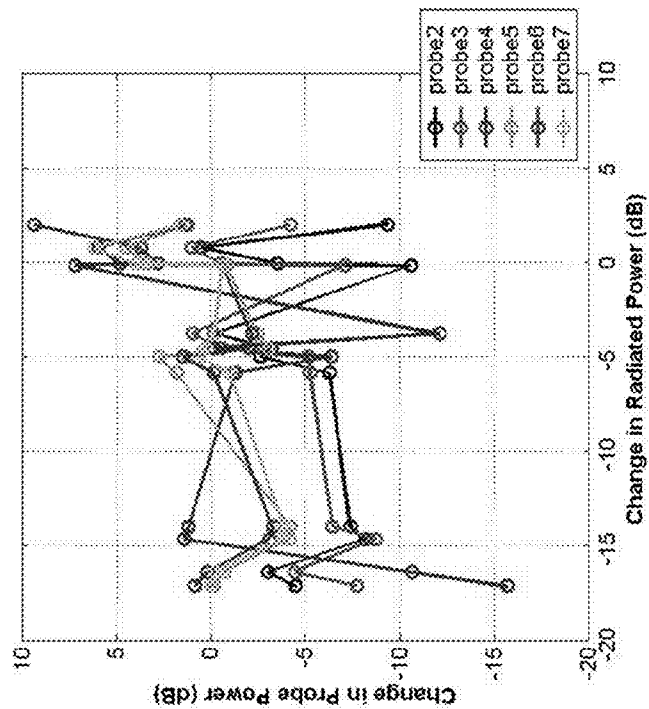
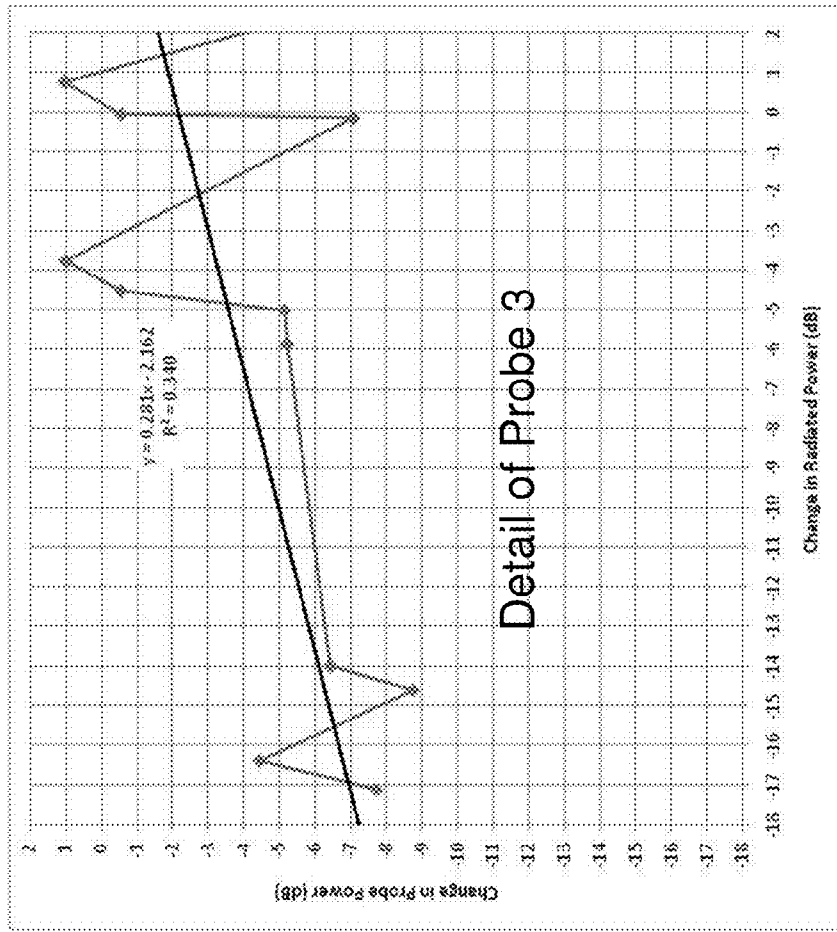
FIG. 42



Probe	r ²
2	0.6572
3	0.3314
4	0.0218
5	0.0235
6	0.0221
7	0.0176

- Probe 2 phase shift correlates best with observed frequency shift
- Sensitivity is about 0.24 deg per MHz

FIG. 43



Probe	r ²
2	0.003
3	0.341
4	0.380
5	0.298
6	0.352
7	0.428

- Probe 2 mag shift correlates worst with observed radiated power shift
- Probe 7 (opposite end of ground) correlates best
- Sensitivity of about 0.28 dB per dB of radiated power shift

FIG. 44

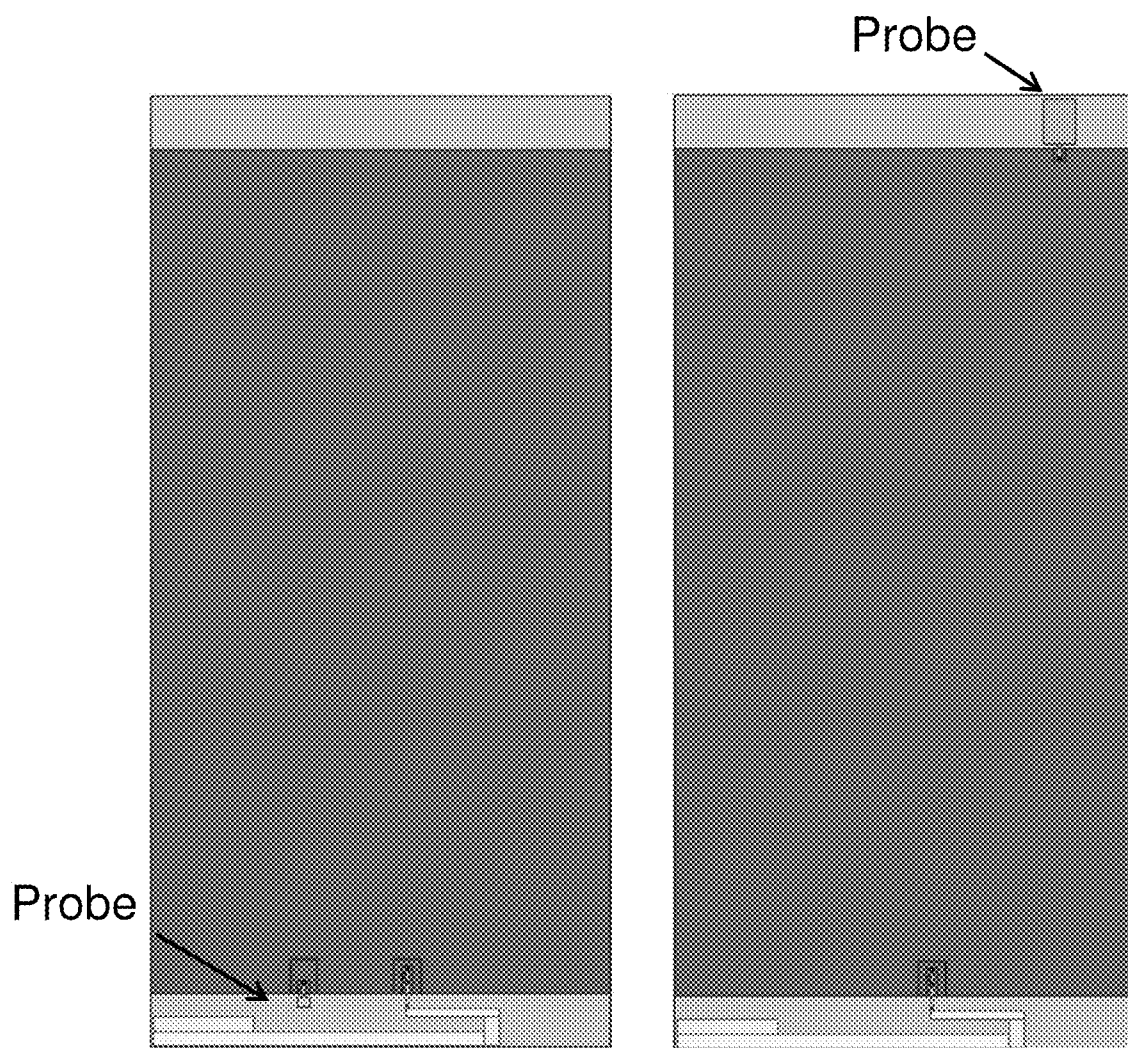


FIG. 45

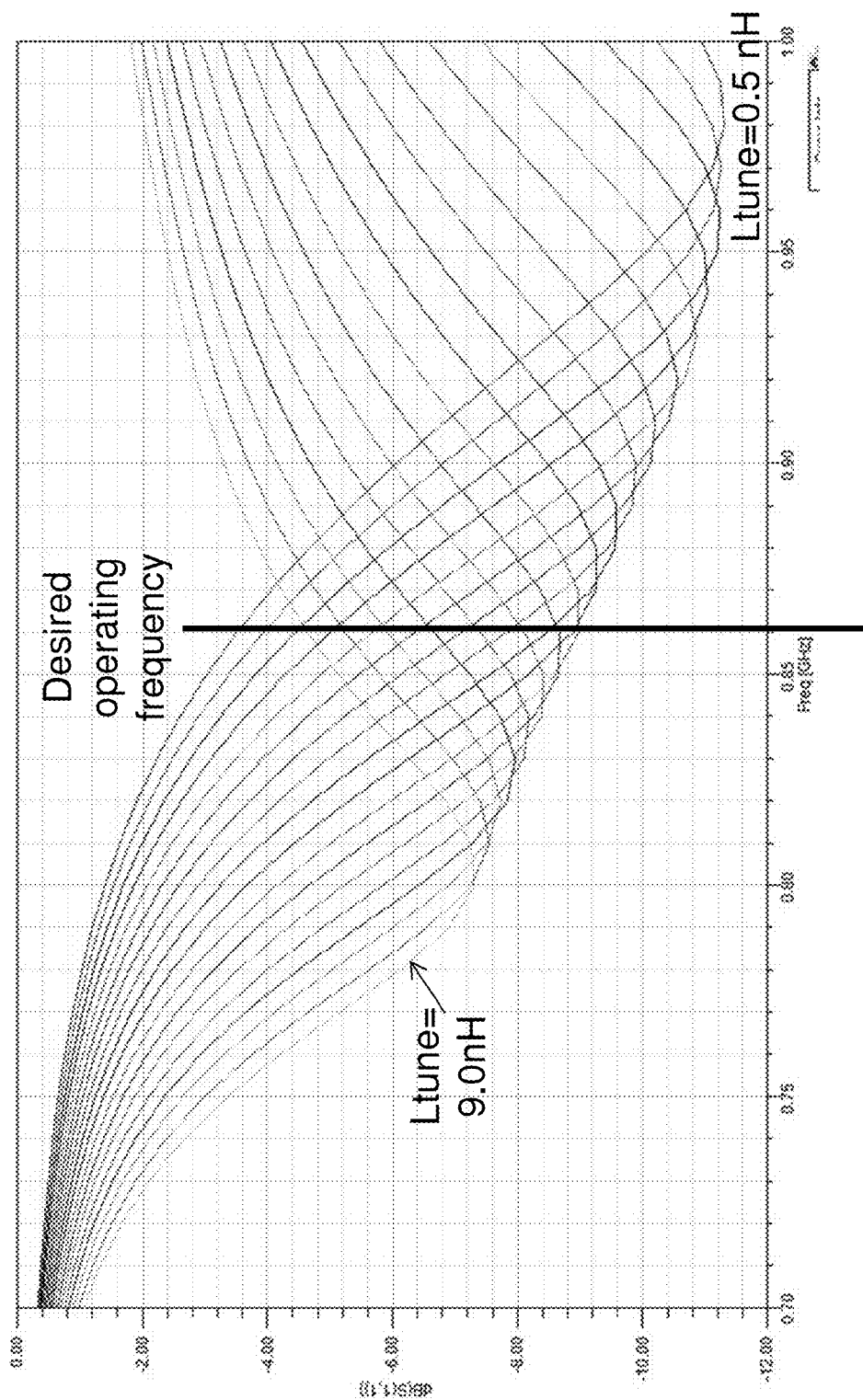


FIG. 46

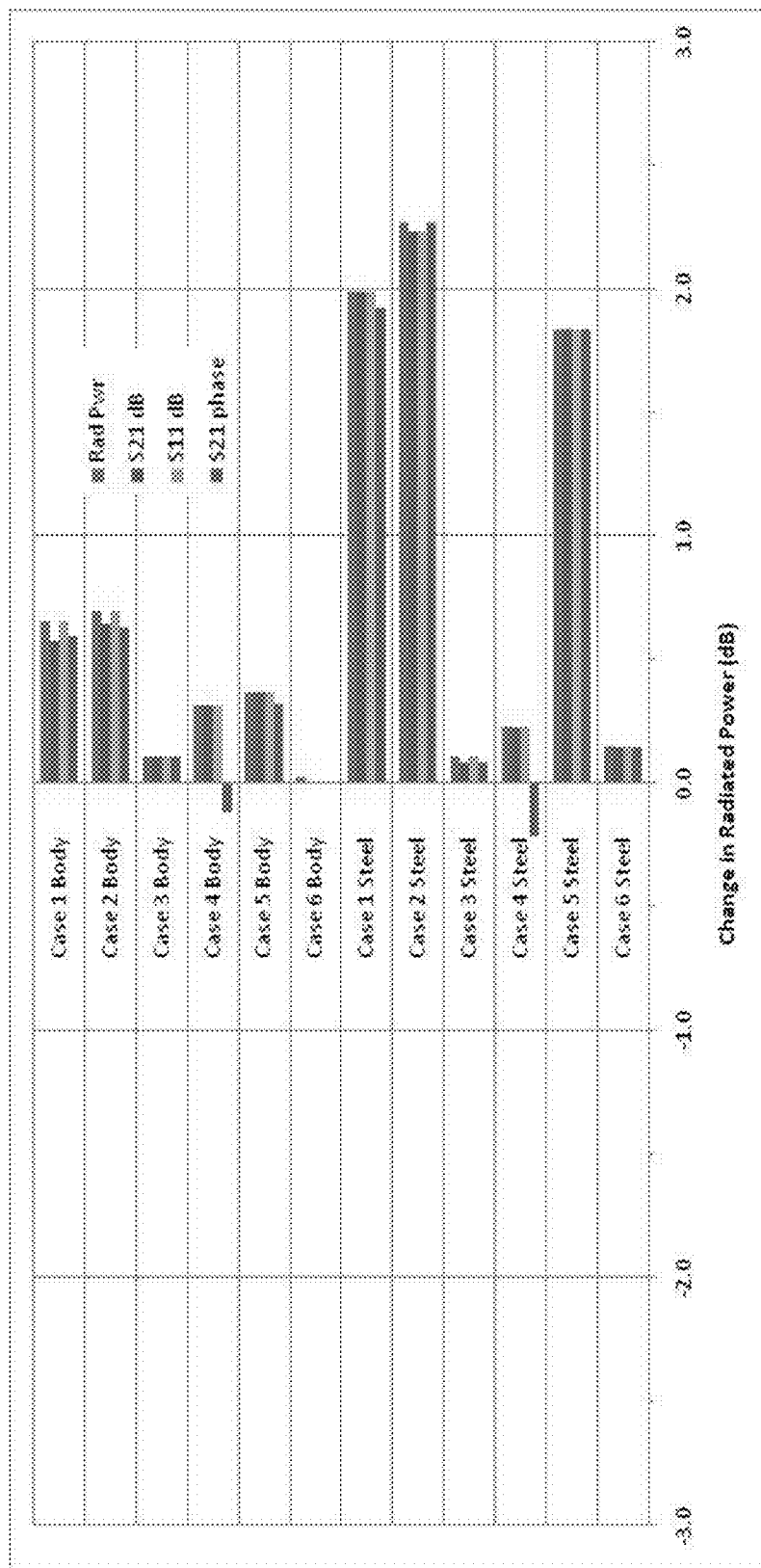


FIG. 47

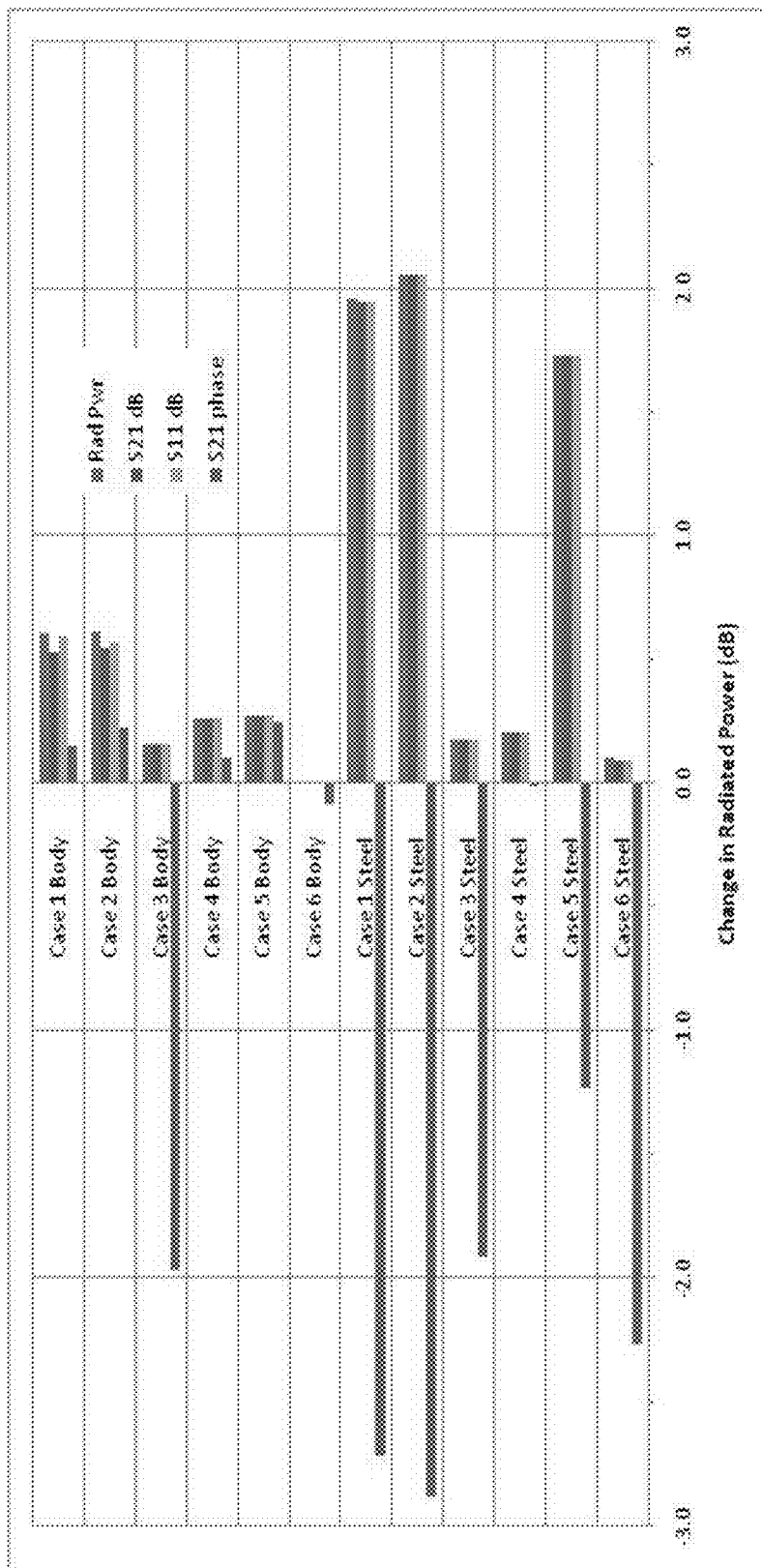


FIG. 48

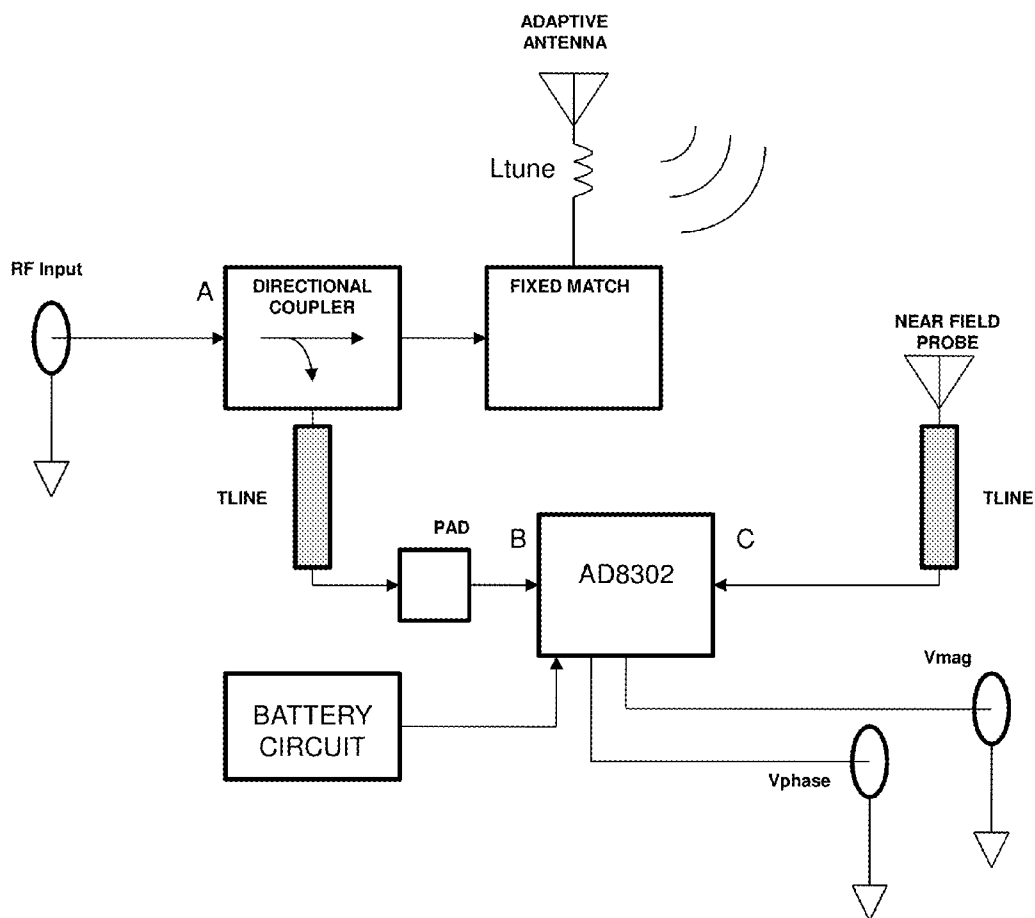


FIG. 49

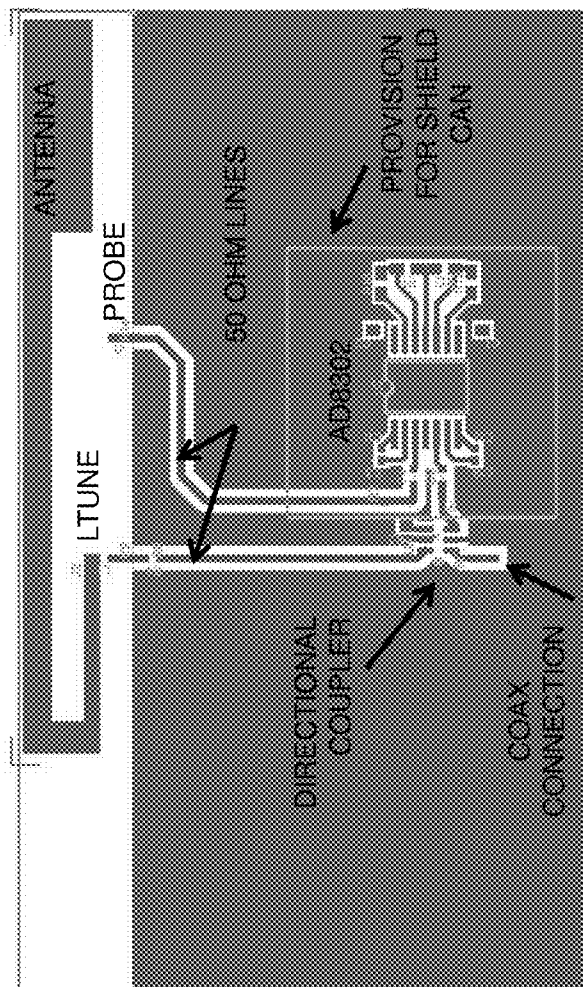
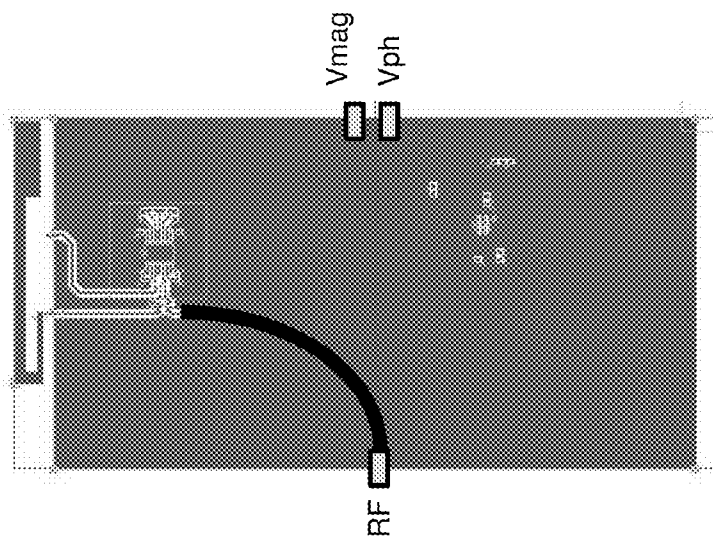
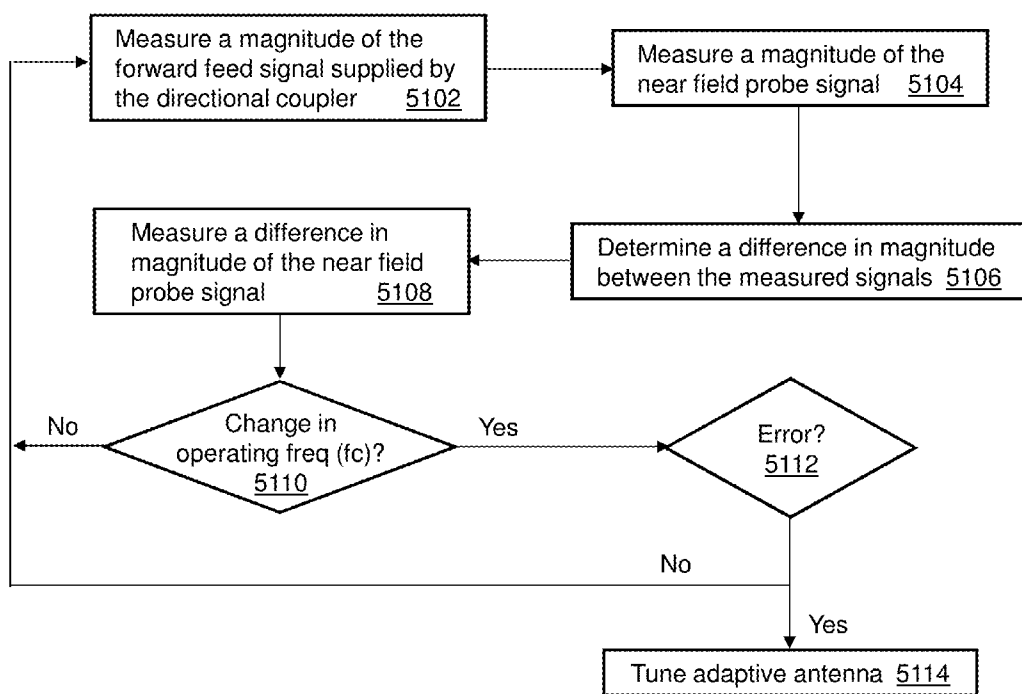


FIG. 50



5100
FIG. 51

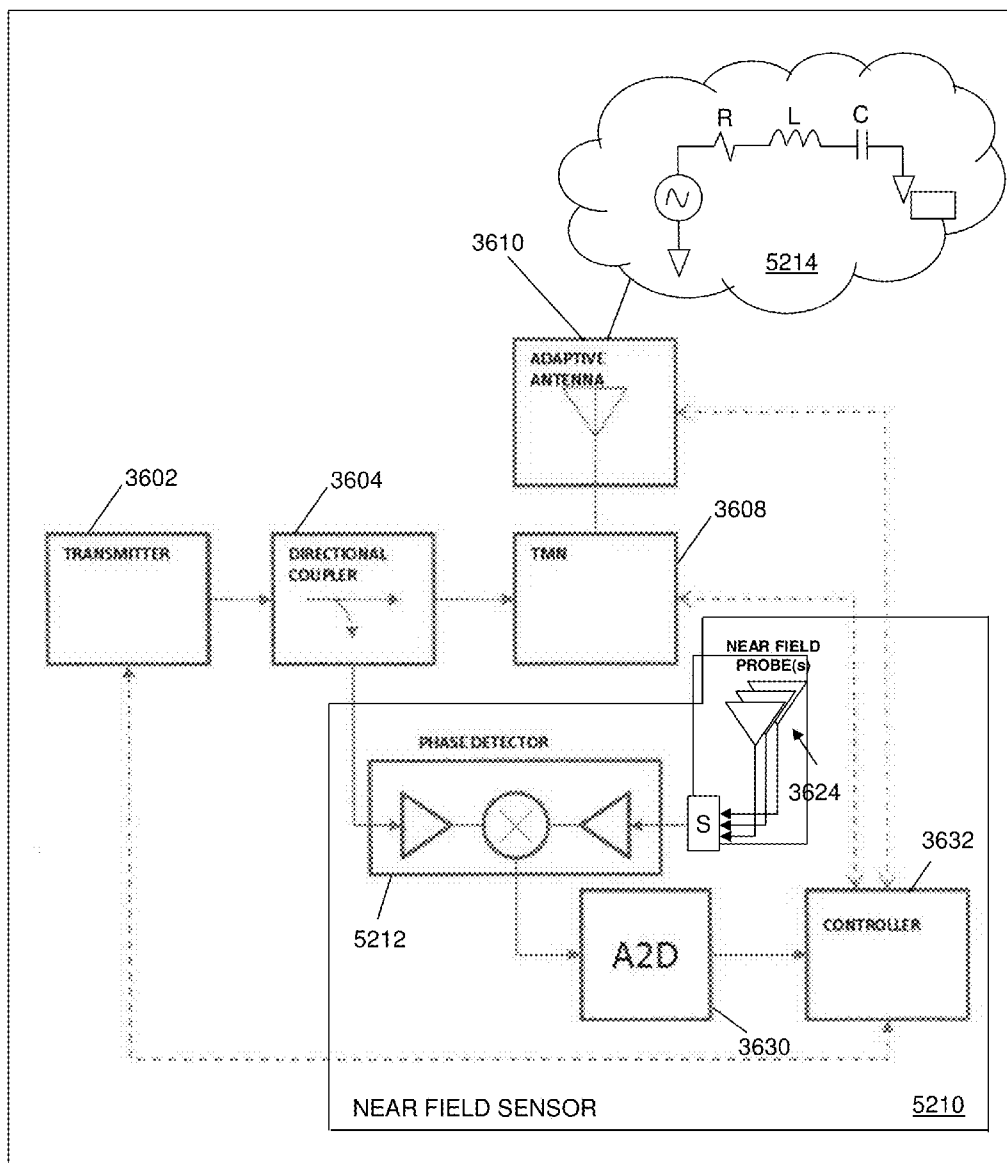


FIG. 52

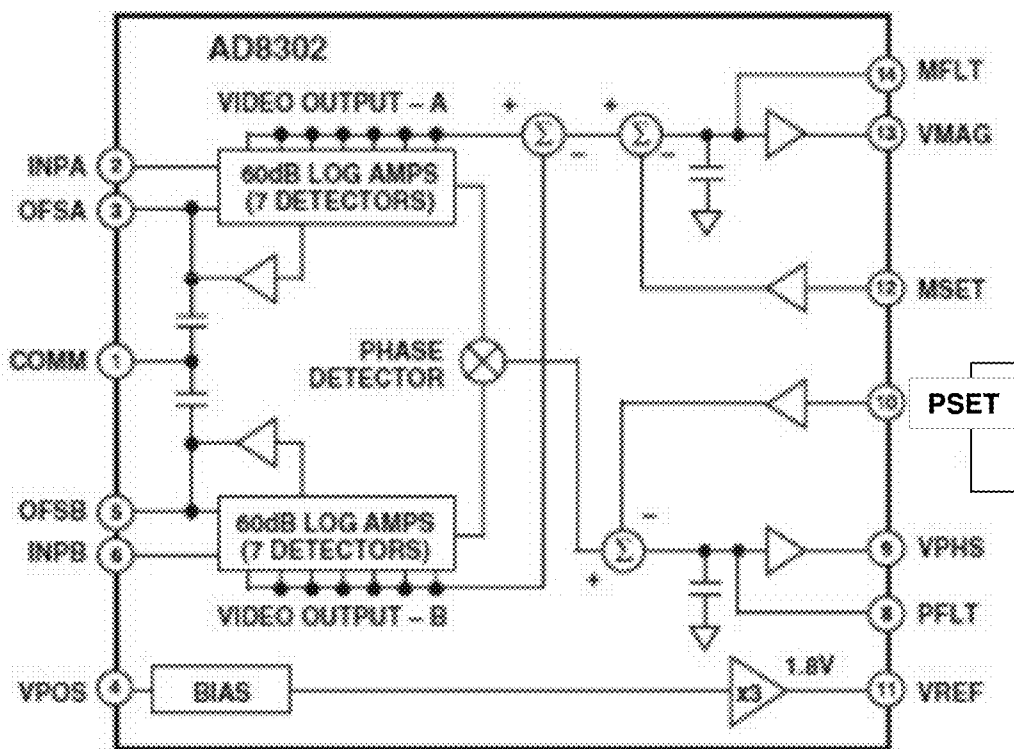
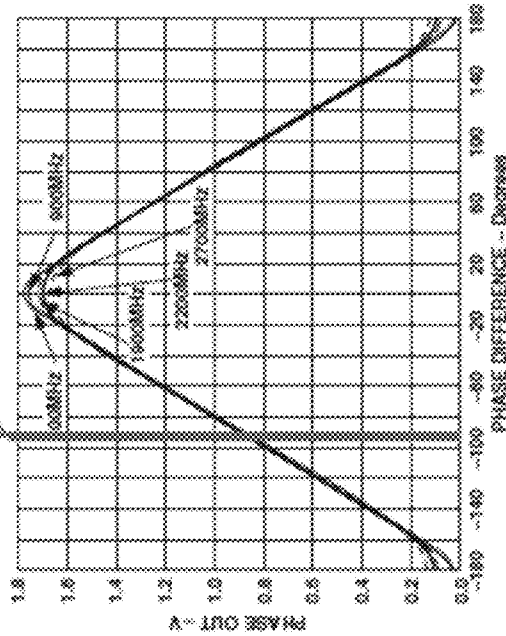


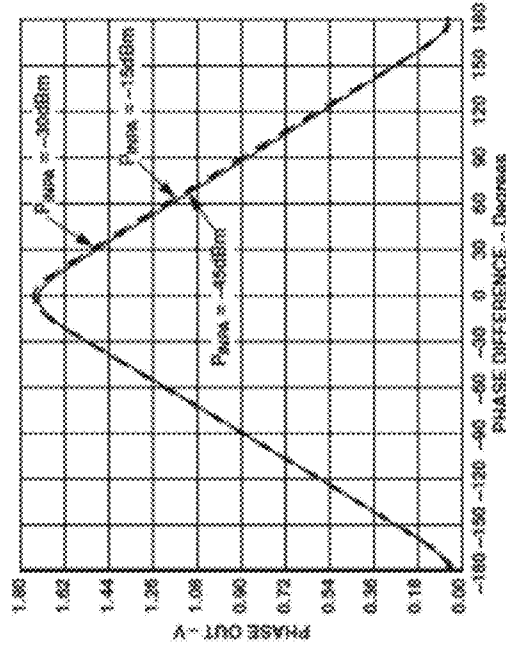
FIG. 53

Phase error versus frequency and power level

Possible operating point Φ_0 : set phase offset to this point for antenna phase = 0

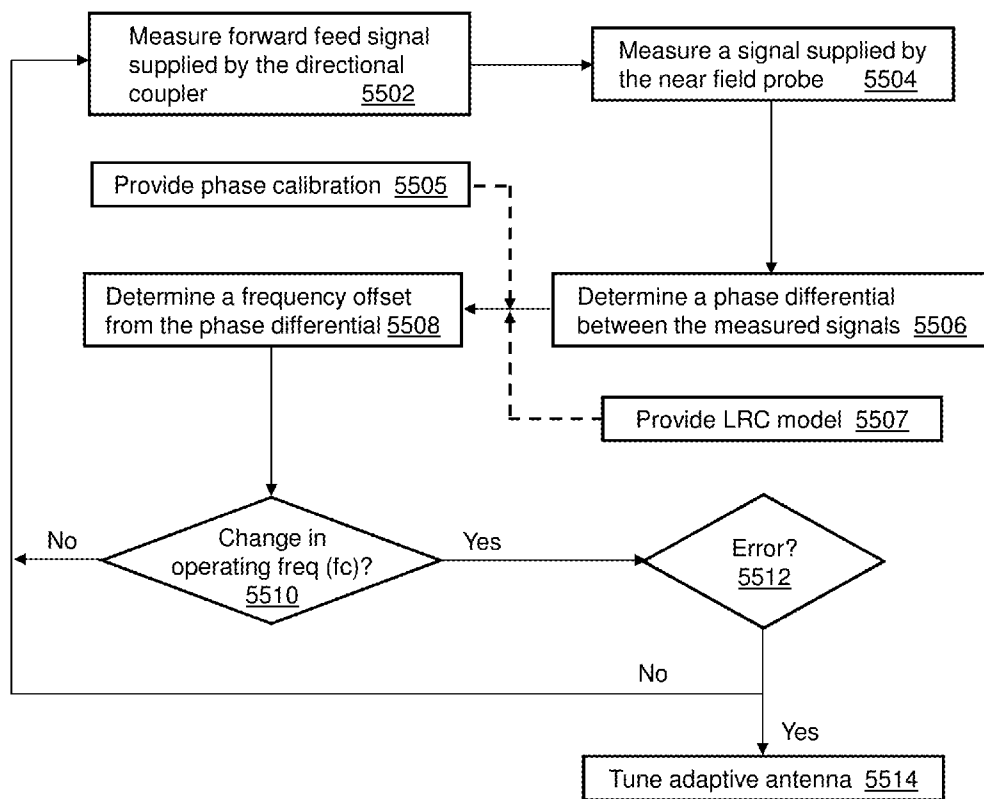


TPC 25. Phase Output (VPHS) vs. Input Phase Difference, Input Levels -30 dBm, Frequencies 100 MHz, 900 MHz, 1900 MHz, 2200 MHz, Supply 5 V, 2700 MHz



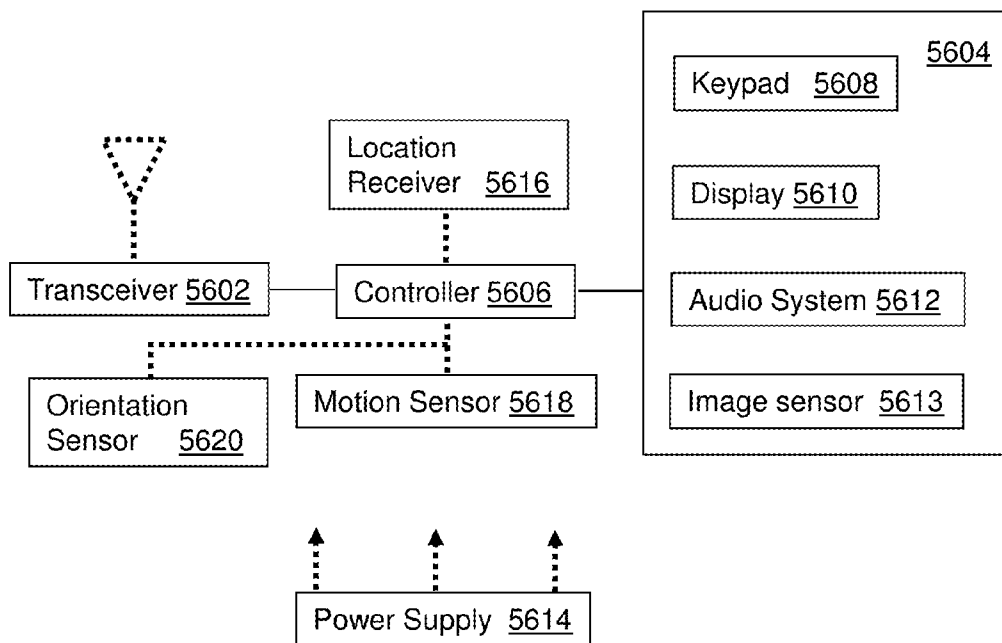
TPC 42. Phase Output vs. Input Phase Difference, $P_{INPA} = P_{INPB}$, $P_{INPA} = P_{INPB} + 15\text{ dB}$, $P_{INPA} = P_{INPB} - 15\text{ dB}$, Frequency 900 MHz

FIG. 54



5500

FIG. 55



5600
FIG. 56

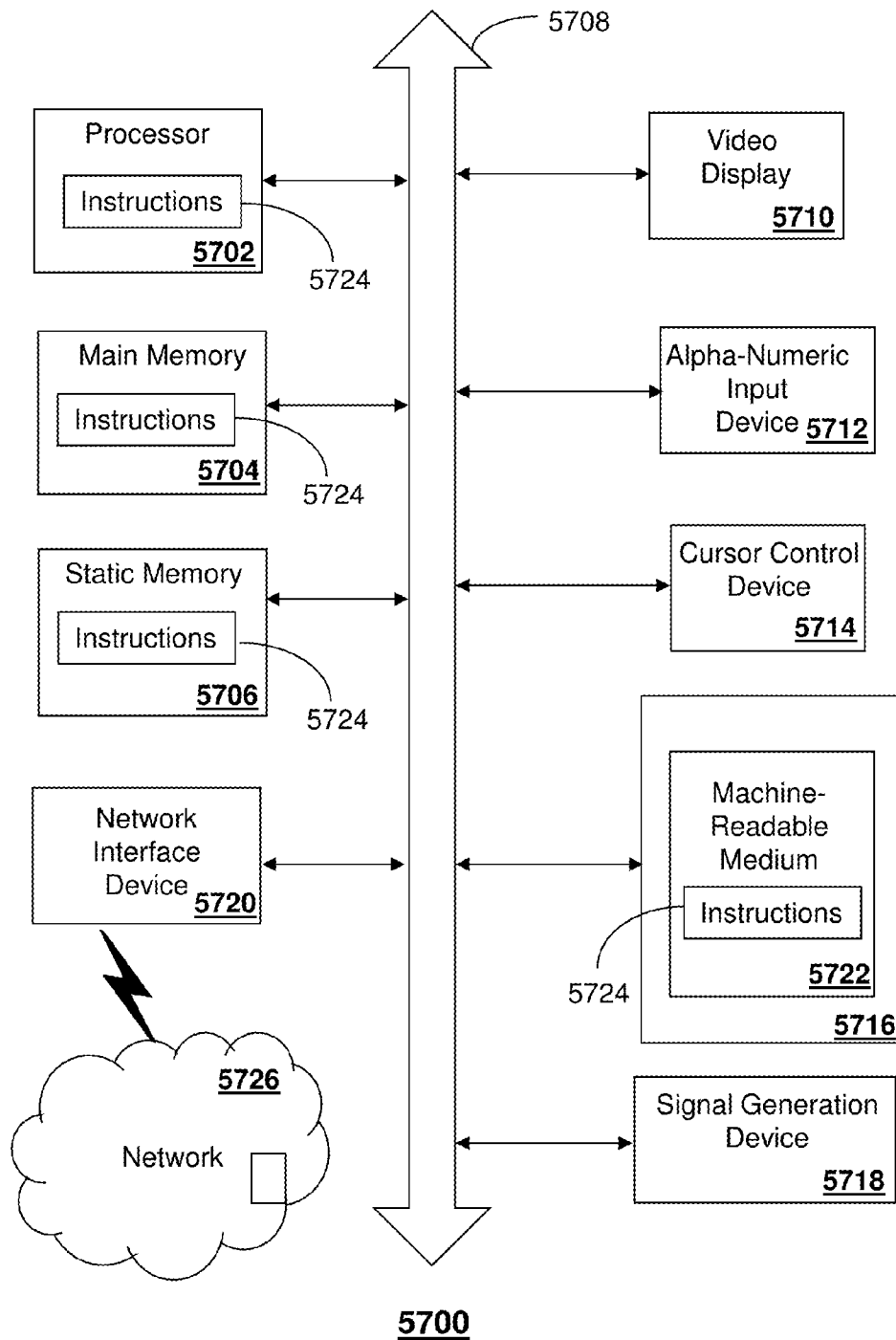


FIG. 57

ANTENNA STRUCTURES AND METHODS THEREOF

CROSS REFERENCE TO RELATED APPLICATIONS

[0001] The present application claims the benefit of priority to U.S. Provisional Application No. 61/896,233 filed on Oct. 28, 2013, which is hereby incorporated herein by reference in its entirety.

[0002] The present application claims the benefit of priority to U.S. Provisional Application No. 61/932,831 filed on Jan. 29, 2014, which is hereby incorporated herein by reference in its entirety.

[0003] The present application claims the benefit of priority to U.S. Provisional Application No. 61/941,888 filed on Feb. 19, 2014, which is hereby incorporated herein by reference in its entirety.

FIELD OF THE DISCLOSURE

[0004] The present disclosure relates generally to antenna structures and methods thereof for determining a frequency offset based on a phase measurement.

BACKGROUND

[0005] It is common for communications devices to have multiple antennas that are packaged close together (e.g., less than a quarter of a wavelength apart) and that can operate simultaneously within the same frequency band. Common examples of such communications devices include portable communications products such as cellular handsets, personal digital assistants (PDAs), and wireless networking devices or data cards for personal computers (PCs). Many system architectures (such as Multiple Input Multiple Output (MIMO)) and standard protocols for mobile wireless communications devices (such as 802.11n for wireless LAN, and 3G and 4G data communications such as 802.16e (WiMAX), HSDPA, 1xEVDO, and LTE) may require multiple antennas operating simultaneously.

BRIEF DESCRIPTION OF THE DRAWINGS

[0006] Reference will now be made to the accompanying drawings, which are not necessarily drawn to scale, and wherein:

[0007] FIG. 1A illustrates an antenna structure with two parallel dipoles;

[0008] FIG. 1B illustrates current flow resulting from excitation of one dipole in the antenna structure of FIG. 1A;

[0009] FIG. 1C illustrates a model corresponding to the antenna structure of FIG. 1A;

[0010] FIG. 1D is a graph illustrating scattering parameters for the FIG. 1C antenna structure;

[0011] FIG. 1E is a graph illustrating the current ratios for the FIG. 1C antenna structure;

[0012] FIG. 1F is a graph illustrating gain patterns for the FIG. 1C antenna structure;

[0013] FIG. 1G is a graph illustrating envelope correlation for the FIG. 1C antenna structure;

[0014] FIG. 2A illustrates an antenna structure with two parallel dipoles connected by connecting elements in accordance with one or more embodiments of the disclosure;

[0015] FIG. 2B illustrates a model corresponding to the antenna structure of FIG. 2A;

[0016] FIG. 2C is a graph illustrating scattering parameters for the FIG. 2B antenna structure;

[0017] FIG. 2D is a graph illustrating scattering parameters for the FIG. 2B antenna structure with lumped element impedance matching at both ports;

[0018] FIG. 2E is a graph illustrating the current ratios for the FIG. 2B antenna structure;

[0019] FIG. 2F is a graph illustrating gain patterns for the FIG. 2B antenna structure;

[0020] FIG. 2G is a graph illustrating envelope correlation for the FIG. 2B antenna structure;

[0021] FIG. 3A illustrates an antenna structure with two parallel dipoles connected by meandered connecting elements in accordance with one or more embodiments of the disclosure;

[0022] FIG. 3B is a graph showing scattering parameters for the FIG. 3A antenna structure;

[0023] FIG. 3C is a graph illustrating current ratios for the FIG. 3A antenna structure;

[0024] FIG. 3D is a graph illustrating gain patterns for the FIG. 3A antenna structure;

[0025] FIG. 3E is a graph illustrating envelope correlation for the FIG. 3A antenna structure;

[0026] FIG. 4 illustrates an antenna structure with a ground or counterpoise in accordance with one or more embodiments of the disclosure;

[0027] FIG. 5 illustrates a balanced antenna structure in accordance with one or more embodiments of the disclosure;

[0028] FIG. 6A illustrates an antenna structure in accordance with one or more embodiments of the disclosure;

[0029] FIG. 6B is a graph showing scattering parameters for the FIG. 6A antenna structure for a particular dipole width dimension;

[0030] FIG. 6C is a graph showing scattering parameters for the FIG. 6A antenna structure for another dipole width dimension;

[0031] FIG. 7 illustrates an antenna structure fabricated on a printed circuit board in accordance with one or more embodiments of the disclosure;

[0032] FIG. 8A illustrates an antenna structure having dual resonance in accordance with one or more embodiments of the disclosure;

[0033] FIG. 8B is a graph illustrating scattering parameters for the FIG. 8A antenna structure;

[0034] FIG. 9 illustrates a tunable antenna structure in accordance with one or more embodiments of the disclosure;

[0035] FIGS. 10A and 10B illustrate antenna structures having connecting elements positioned at different locations along the length of the antenna elements in accordance with one or more embodiments of the disclosure;

[0036] FIGS. 10C and 10D are graphs illustrating scattering parameters for the FIGS. 10A and 10B antenna structures, respectively;

[0037] FIG. 11 illustrates an antenna structure including connecting elements having switches in accordance with one or more embodiments of the disclosure;

[0038] FIG. 12 illustrates an antenna structure having a connecting element with a filter coupled thereto in accordance with one or more embodiments of the disclosure;

[0039] FIG. 13 illustrates an antenna structure having two connecting elements with filters coupled thereto in accordance with one or more embodiments of the disclosure;

[0040] FIG. 14 illustrates an antenna structure having a tunable connecting element in accordance with one or more embodiments of the disclosure;

[0041] FIG. 15 illustrates an antenna structure mounted on a PCB assembly in accordance with one or more embodiments of the disclosure;

[0042] FIG. 16 illustrates another antenna structure mounted on a PCB assembly in accordance with one or more embodiments of the disclosure;

[0043] FIG. 17 illustrates an alternate antenna structure that can be mounted on a PCB assembly in accordance with one or more embodiments of the disclosure;

[0044] FIG. 18A illustrates a three mode antenna structure in accordance with one or more embodiments of the disclosure;

[0045] FIG. 18B is a graph illustrating the gain patterns for the FIG. 18A antenna structure;

[0046] FIG. 19 illustrates an antenna and power amplifier combiner application for an antenna structure in accordance with one or more embodiments of the disclosure;

[0047] FIGS. 20A and 20B illustrate a multimode antenna structure useable, e.g., in a WiMAX USB or ExpressCard/34 device in accordance with one or more further embodiments of the subject disclosure.

[0048] FIG. 20C illustrates a test assembly used to measure the performance of the antenna of FIGS. 20A and 20B.

[0049] FIGS. 20D to 20J illustrate test measurement results for the antenna of FIGS. 20A and 20B.

[0050] FIGS. 21A and 21B illustrate a multimode antenna structure useable, e.g., in a WiMAX USB dongle in accordance with one or more alternate embodiments of the subject disclosure.

[0051] FIGS. 22A and 22B illustrate a multimode antenna structure useable, e.g., in a WiMAX USB dongle in accordance with one or more alternate embodiments of the subject disclosure.

[0052] FIG. 23A illustrates a test assembly used to measure the performance of the antenna of FIGS. 21A and 21B.

[0053] FIGS. 23B to 23K illustrate test measurement results for the antenna of FIGS. 21A and 21B.

[0054] FIG. 24 is a schematic block diagram of an antenna structure with a beam steering mechanism in accordance with one or more embodiments of the subject disclosure.

[0055] FIGS. 25A to 25G illustrate test measurement results for the antenna of FIG. 25A.

[0056] FIG. 26 illustrates the gain advantage of an antenna structure in accordance with one or more embodiments of the subject disclosure as a function of the phase angle difference between feedpoints.

[0057] FIG. 27A is a schematic diagram illustrating a simple dual-band branch line monopole antenna structure.

[0058] FIG. 27B illustrates current distribution in the FIG. 27A antenna structure.

[0059] FIG. 27C is a schematic diagram illustrating a spurline band stop filter.

[0060] FIGS. 27D and 27E are test results illustrating frequency rejection in the FIG. 27A antenna structure.

[0061] FIG. 28 is a schematic diagram illustrating an antenna structure with a band-rejection slot in accordance with one or more embodiments of the subject disclosure.

[0062] FIG. 29A illustrates an alternate antenna structure with a band-rejection slot in accordance with one or more embodiments of the subject disclosure.

[0063] FIGS. 29B and 29C illustrate test measurement results for the FIG. 29A antenna structure.

[0064] FIG. 30 depicts an illustrative embodiment of an antenna structure in accordance with one or more embodiments;

[0065] FIG. 31 depicts an illustrative embodiment of a multiband antenna structure in accordance with one or more embodiments;

[0066] FIGS. 32A and 32B illustrate tuning using discrete selection of inductance to select antenna fundamental resonance frequency in accordance with one or more embodiments;

[0067] FIGS. 33A and 33B illustrate tuning using discrete selection of inductance to select fundamental resonance frequency where a separate but co-located high band element is shown with feed points F1H and F2H that allows for compatibility with RF transceiver front end designs requiring separate low- and mid- or low- and high-band connections to the antenna in accordance with one or more embodiments;

[0068] FIGS. 34A and 34B illustrate tuning and filtering using discrete selection of inductance to select antenna fundamental resonance frequency in accordance with one or more embodiments;

[0069] FIGS. 35A and 35B illustrate tuning and filtering using discrete selection of inductance to select fundamental resonance frequency in accordance with one or more embodiments;

[0070] FIGS. 36A-36B depict illustrative embodiments of a near field sensor;

[0071] FIG. 37 depicts illustrative embodiments for placement of the near field sensor as a probe;

[0072] FIG. 38 depicts illustrative embodiments of environmental use cases applied to the antenna structure of FIG. 27;

[0073] FIG. 39 depicts illustrative embodiments of return loss and efficiency plots according to the environmental use cases of FIG. 38;

[0074] FIG. 40 depicts illustrative embodiments of Smith charts according to the environmental use cases of FIG. 38;

[0075] FIG. 41 depicts illustrative embodiments of magnitude and phase plots associated with one of the probes;

[0076] FIG. 42 depicts illustrative embodiments of magnitude and phase plots associated with one of the probes;

[0077] FIG. 43 depicts illustrative embodiments of phase vs. antenna frequency shift plots of the probes;

[0078] FIG. 44 depicts illustrative embodiments of probe power shift vs. antenna radiated power shift plots of the probes;

[0079] FIG. 45 depicts illustrative embodiments of an antenna structure and probe placements;

[0080] FIG. 46 depicts illustrative embodiments of a free space resonance tuning use a Ltune (a tuning variable);

[0081] FIG. 47 depicts illustrative embodiments of efficiency gain by tuning of the antenna structure based on measurements of one of the probes of the antenna structure of FIG. 45;

[0082] FIG. 48 depicts illustrative embodiments of efficiency gain by tuning of the antenna structure based on measurements of a different one of the probes of the antenna structure of FIG. 45;

[0083] FIG. 49 depicts an illustrative embodiment of a near field sensor;

[0084] FIG. 50 depicts an illustrative embodiment of the near field sensor of FIG. 49 on a printed circuit board;

[0085] FIG. 51 depicts an illustrative embodiment of a first method that can be applied to the subject disclosure;

[0086] FIG. 52 depicts an illustrative embodiment of a near field sensor;

[0087] FIG. 53 depicts an illustrative embodiment of a phase detector;

[0088] FIG. 54 depict illustrative phase error versus frequency and power level plots resulting from the near field sensor embodiment of FIG. 52;

[0089] FIG. 55 depicts an illustrative embodiment of a second method that can be applied to the subject disclosure;

[0090] FIG. 56 depicts an illustrative embodiment of a communication device; and

[0091] FIG. 57 is a diagrammatic representation of a machine in the form of a computer system within which a set of instructions, when executed, may cause the machine to perform any one or more of the methods described herein.

DETAILED DESCRIPTION

[0092] The subject disclosure describes, among other things, illustrative embodiments for monitoring changes in an operating frequency of an antenna and adjusting the operating frequency of the antenna to mitigate such changes. Other embodiments are described in the subject disclosure.

[0093] One embodiment of the subject disclosure includes a method for measuring, by a circuit, from a first probe a first magnitude of radiated energy by an antenna, where the first probe is placed near the antenna, obtaining, by the circuit, a second magnitude of a signal supplied to the antenna, comparing, by the circuit, the first and the second magnitudes, detecting, by the circuit, an offset in an operating frequency of the antenna based on a difference between the first and the second magnitudes, and adjusting, by the circuit, the operating frequency of the antenna to mitigate the offset in the operating frequency of the antenna.

[0094] One embodiment of the subject disclosure includes an antenna structure having a first antenna element for receiving and transmitting radio frequency signals within an operating frequency range, a first aperture tuner for adjusting an operating frequency of the antenna element, and a first near field sensor for sensing radiated energy from the first antenna element. The first near field sensor, the first antenna element, and the first aperture tuner can be coupled to a circuit that performs operations comprising measuring from the first near field sensor a first magnitude of radiated energy by the first antenna element, obtaining a second magnitude of a signal supplied to the first antenna element, comparing the first and the second magnitudes, detecting a change in an operating frequency of the first antenna element based on a difference between the first and the second magnitudes, and directing the first aperture tuner to adjust the operating frequency of the first antenna element to counter the change in the operating frequency of the first antenna element.

[0095] One embodiment of the subject disclosure includes a communication device having a near field sensor coupled to the antenna structure, and a circuit coupled to the antenna structure and the near field sensor. The circuit can perform operations including measuring from the near field sensor a first magnitude of radiated energy by the antenna structure, obtaining a second magnitude of a signal supplied to the antenna structure by a transmitter circuit, comparing the first and the second magnitudes, detecting an offset in an operating frequency of the antenna structure based on a difference

between the first and the second magnitudes, and adjusting the operating frequency of the antenna structure to mitigate the offset.

[0096] One embodiment of the subject disclosure includes a method for measuring, by a circuit, from a first probe a first phase of radiated energy by an antenna, wherein the first probe is placed near the antenna, measuring, by the circuit, from a second probe a second phase of a transmit signal supplied to the antenna, wherein the second probe is placed in a transmission path of the transmit signal, comparing, by the circuit, the first and the second phases to generate a phase differential, detecting, by the circuit, an offset in an operating frequency of the antenna based on the phase differential, and adjusting, by the circuit, the operating frequency of the antenna to mitigate the offset in the operating frequency of the antenna.

[0097] One embodiment of the subject disclosure includes an antenna structure including a first antenna element, a first aperture tuner for adjusting an operating frequency of the antenna element, a probe, and a first near field sensor for sensing radiated energy from the first antenna element. The first near field sensor and the first aperture tuner can be coupled to a circuit that performs operations including measuring from the first near field sensor a first phase of radiated energy by the first antenna element, measuring from the probe a second phase of a first signal supplied to the first antenna element, comparing the first and the second phases to generate a first phase differential, detecting a change in an operating frequency of the first antenna element based on the phase differential, and directing the first aperture tuner to adjust the operating frequency of the first antenna element according to the first phase differential.

[0098] One embodiment of the subject disclosure includes a communication device having an antenna structure, a near field sensor, a probe, and a circuit coupled to the antenna structure and the near field sensor. The circuit can perform operations including measuring from the near field sensor a first signal representing radiated energy from the antenna structure, measuring from the probe a second signal supplied to the antenna structure, determining a phase differential from a first phase of the first signal and a second phase of the second signal, detecting a frequency offset of the antenna structure based on the phase differential, and adjusting an operating frequency of the antenna structure to mitigate the frequency offset.

[0099] Antenna structures in accordance with various embodiments of the disclosure are particularly useful in communications devices that require multiple antennas to be packaged close together (e.g., less than a quarter of a wavelength apart), including in devices where more than one antenna is used simultaneously and within the same frequency band or multiple frequency bands in cases where carrier aggregation is required. Common examples of such devices in which the antenna structures can be used include portable communications products such as cellular handsets, PDAs, smart phones, tablets, and wireless networking devices or data cards for PCs or other equipment integrated communication devices such as automobiles, trucks, or other vehicle categories. The antenna structures are also useful with system architectures such as MIMO and standard protocols for mobile wireless communications devices (such as 802.11n for wireless LAN, and 3G and 4G data communications such as 802.16e (WiMAX), HSDPA, 1xEVDO, LTE) that require multiple antennas operating simultaneously. The

embodiments of the subject disclosure can be applied to future generations of wireless communication protocols such as 5G.

[0100] FIGS. 1A-1G illustrate the operation of an antenna structure **100**. FIG. 1A schematically illustrates the antenna structure **100** having two parallel antennas, in particular parallel dipoles **102**, **104**, of length L . The dipoles **102**, **104** are separated by a distance d , and are not connected by any connecting element. The dipoles **102**, **104** have a fundamental resonant frequency that corresponds approximately to $L=\lambda/2$. Each dipole is connected to an independent transmit/receive system, which can operate at the same frequency. This system connection can have the same characteristic impedance z_0 for both antennas, which in this example is 50 ohms.

[0101] When one dipole is transmitting a signal, some of the signal being transmitted by the dipole will be coupled directly into the neighboring dipole. The maximum amount of coupling generally occurs near the half-wave resonant frequency of the individual dipole and generally increases as the separation distance d is made smaller. For example, for $d<\lambda/3$, the magnitude of coupling is greater than 0.1 or -10 dB, and for $d<\lambda/8$, the magnitude of the coupling is greater than -5 dB.

[0102] It is desirable to have no coupling (i.e., complete isolation) or to reduce the coupling (i.e., at least reduced isolation) between the antennas. If the coupling is, e.g., -10 dB, 10 percent of the transmit power is lost due to that amount of power being directly coupled into the neighboring antenna. There may also be detrimental system effects such as saturation or desensitization of a receiver connected to the neighboring antenna or degradation of the performance of a transmitter connected to the neighboring antenna. Currents induced on the neighboring antenna distort the gain pattern compared to that generated by an individual dipole. This effect is known to reduce the correlation between the gain patterns produced by the dipoles. Thus, while coupling may provide some pattern diversity, it has detrimental system impacts as described above.

[0103] Because of the close coupling, the antennas do not act independently and can be considered an antenna system having two pairs of terminals or ports that correspond to two different gain patterns. Use of either port involves substantially the entire structure including both dipoles. The parasitic excitation of the neighboring dipole enables diversity to be achieved at close dipole spacing, but currents excited on the dipole pass through the source impedance, and therefore manifest mutual coupling between ports.

[0104] FIG. 1C illustrates a model dipole pair corresponding to the antenna structure **100** shown in FIG. 1 used for simulations. In this example, the dipoles **102**, **104** have a square cross section of $1\text{ mm}\times 1\text{ mm}$ and length (L) of 56 mm. These dimensions yield a center resonant frequency of 2.45 GHz when attached to a 50-ohm source. The free-space wavelength at this frequency is 122 mm. A plot of the scattering parameters S_{11} and S_{21} for a separation distance (d) of 10 mm, or approximately $\lambda/12$, is shown in FIG. 1D. Due to symmetry and reciprocity, $S_{22}=S_{11}$ and $S_{12}=S_{21}$. For simplicity, only S_{11} and S_{21} are shown and discussed. In this configuration, the coupling between dipoles as represented by S_{21} reaches a maximum of -3.7 dB.

[0105] FIG. 1E shows the ratio (identified as “Magnitude I_2/I_1 ” in the figure) of the vertical current on dipole **104** of the antenna structure to that on dipole **102** under the condition in which port **106** is excited and port **108** is passively termi-

nated. The frequency at which the ratio of currents (dipole **104**/dipole **102**) is a maximum corresponds to the frequency of 180 degree phase differential between the dipole currents and is just slightly higher in frequency than the point of maximum coupling shown in FIG. 1D.

[0106] FIG. 1F shows azimuthal gain patterns for several frequencies with excitation of port **106**. The patterns are not uniformly omni-directional and change with frequency due to the changing magnitude and phase of the coupling. Due to symmetry, the patterns resulting from excitation of port **108** would be the mirror image of those for port **106**. Therefore, the more asymmetrical the pattern is from left to right, the more diverse the patterns are in terms of gain magnitude.

[0107] Calculation of the correlation coefficient between patterns provides a quantitative characterization of the pattern diversity. FIG. 1G shows the calculated correlation between port **106** and port **108** antenna patterns. The correlation is much lower than is predicted by Clark’s model for ideal dipoles. This is due to the differences in the patterns introduced by the mutual coupling.

[0108] FIGS. 2A-2F illustrate the operation of an exemplary two port antenna structure **200** in accordance with one or more embodiments of the disclosure. The two port antenna structure **200** includes two closely-spaced resonant antenna elements **202**, **204** and provides both low pattern correlation and low coupling between ports **206**, **208**. FIG. 2A schematically illustrates the two port antenna structure **200**. This structure is similar to the antenna structure **100** comprising the pair of dipoles shown in FIG. 1B, but additionally includes horizontal conductive connecting elements **210**, **212** between the dipoles on either side of the ports **206**, **208**. The two ports **206**, **208** are located in the same locations as with the FIG. 1 antenna structure. When one port is excited, the combined structure exhibits a resonance similar to that of the unattached pair of dipoles, but with a significant reduction in coupling and an increase in pattern diversity.

[0109] An exemplary model of the antenna structure **200** with a 10 mm dipole separation is shown in FIG. 2B. This structure has generally the same geometry as the antenna structure **100** shown in FIG. 1C, but with the addition of the two horizontal connecting elements **210**, **212** electrically connecting the antenna elements slightly above and below the ports. This structure shows a strong resonance at the same frequency as unattached dipoles, but with very different scattering parameters as shown in FIG. 2C. There is a deep drop-out in coupling, below -20 dB, and a shift in the input impedance as indicated by S_{11} . In this example, the best impedance match (S_{11} minimum) does not coincide with the lowest coupling (S_{21} minimum). A matching network can be used to improve the input impedance match and still achieve very low coupling as shown in FIG. 2D. In this example, a lumped element matching network comprising a series inductor followed by a shunt capacitor was added between each port and the structure.

[0110] FIG. 2E shows the ratio (indicated as “Magnitude I_2/I_1 ” in the figure) of the current on dipole element **204** to that on dipole element **202** resulting from excitation of port **206**. This plot shows that below the resonant frequency, the currents are actually greater on dipole element **204**. Near resonance, the currents on dipole element **204** begin to decrease relative to those on dipole element **202** with increasing frequency. A point of low coupling (2.44 GHz in this case) occurs near the frequency where currents on both dipole elements are generally equal in magnitude. At this frequency,

the phase of the currents on dipole element **204** lag those of dipole element **202** by approximately 160 degrees.

[0111] Unlike the FIG. 1C dipoles without connecting elements, the currents on antenna element **204** of the FIG. 2B combined antenna structure **200** are not forced to pass through the terminal impedance of port **208**. Instead a resonant mode is produced where the current flows down antenna element **204**, across the connecting element **210**, **212**, and up antenna element **202** as indicated by the arrows shown on FIG. 2A. (Note that this current flow is representative of one half of the resonant cycle; during the other half, the current directions are reversed). The resonant mode of the combined structure features the following: (1) the currents on antenna element **204** largely bypass port **208**, thereby allowing for high isolation between the ports **206**, **208**, and (2) the magnitude of the currents on both antenna elements **202,204** are approximately equal, which allows for dissimilar and uncorrelated gain patterns as described in further detail below.

[0112] Because the magnitude of currents is nearly equal on the antenna elements, a much more directional pattern is produced (as shown on FIG. 2F) than in the case of the FIG. 1C antenna structure **100** with unattached dipoles. When the currents are equal, the condition for nulling the pattern in the x (or phi=0) direction is for the phase of currents on dipole **204** to lag those of dipole **202** by the quantity $\pi n - kd$ (where $k=2\pi/\lambda$, and λ is the effective wavelength). Under this condition, fields propagating in the phi=0 direction from dipole **204** will be 180 degrees out of phase with those of dipole **202**, and the combination of the two will therefore have a null in the phi=0 direction.

[0113] In the model example of FIG. 2B, d is 10 mm or an effective electrical length of $\lambda/12$. In this case, kd equates $\pi/6$ or 30 degrees, and so the condition for a directional azimuthal radiation pattern with a null towards phi=0 and maximum gain towards phi=180 is for the current on dipole **204** to lag those on dipole **202** by 150 degrees. At resonance, the currents pass close to this condition (as shown in FIG. 2E), which explains the directionality of the patterns. In the case of the excitation of port **204**, the radiation patterns are the mirror opposite of those of FIG. 2F, and maximum gain is in the phi=0 direction. The difference in antenna patterns produced from the two ports has an associated low predicted envelope correlation as shown on FIG. 2G. Thus the combined antenna structure has two ports that are isolated from each other and produce gain patterns of low correlation.

[0114] Accordingly, the frequency response of the coupling is dependent on the characteristics of the connecting elements **210**, **212**, including their impedance and electrical length. In accordance with one or more embodiments of the disclosure, the frequency or bandwidth over which a desired amount of isolation can be maintained is controlled by appropriately configuring the connecting elements. One way to configure the cross connection is to change the physical length of the connecting element. An example of this is shown by the multimode antenna structure **300** of FIG. 3A where a meander has been added to the cross connection path of the connecting elements **310**, **312**. This has the general effect of increasing both the electrical length and the impedance of the connection between the two antenna elements **302**, **304**. Performance characteristics of this structure including scattering parameters, current ratios, gain patterns, and pattern correlation are shown on FIGS. 3B, 3C, 3D, and 3E, respectively. In this embodiment, the change in physical length has not significantly altered the resonant frequency of the structure, but

there is a significant change in S21, with larger bandwidth and a greater minimum value than in structures without the meander. Thus, it is possible to optimize or improve the isolation performance by altering the electrical characteristic of the connecting elements.

[0115] Exemplary multimode antenna structures in accordance with various embodiments of the disclosure can be designed to be excited from a ground or counterpoise **402** (as shown by antenna structure **400** in FIG. 4), or as a balanced structure (as shown by antenna structure **500** in FIG. 5). In either case, each antenna structure includes two or more antenna elements (**402**, **404** in FIG. 4, and **502**, **504** in FIG. 5) and one or more electrically conductive connecting elements (**406** in FIG. 4, and **506**, **508** in FIG. 5). For ease of illustration, only a two-port structure is illustrated in the example diagrams. However, it is possible to extend the structure to include more than two ports in accordance with various embodiments of the disclosure. A signal connection to the antenna structure, or port (**418**, **412** in FIGS. 4 and **510**, **512** in FIG. 5), is provided at each antenna element. The connecting element provides electrical connection between the two antenna elements at the frequency or frequency range of interest. Although the antenna is physically and electrically one structure, its operation can be explained by considering it as two independent antennas. For antenna structures not including a connecting element such as antenna structure **100**, port **106** of that structure can be said to be connected to antenna **102**, and port **108** can be said to be connected to antenna **104**. However, in the case of this combined structure such as antenna structure **400**, port **418** can be referred to as being associated with one antenna mode, and port **412** can be referred to as being associated with another antenna mode.

[0116] The antenna elements are designed to be resonant at the desired frequency or frequency range of operation. The lowest order resonance occurs when an antenna element has an electrical length of one quarter of a wavelength. Thus, a simple element design is a quarter-wave monopole in the case of an unbalanced configuration. It is also possible to use higher order modes. For example, a structure formed from quarter-wave monopoles also exhibits dual mode antenna performance with high isolation at a frequency of three times the fundamental frequency. Thus, higher order modes may be exploited to create a multiband antenna. Similarly, in a balanced configuration, the antenna elements can be complementary quarter-wave elements as in a half-wave center-fed dipole. However, the antenna structure can also be formed from other types of antenna elements that are resonant at the desired frequency or frequency range. Other possible antenna element configurations include, but are not limited to, helical coils, wideband planar shapes, chip antennas, meandered shapes, loops, and inductively shunted forms such as Planar Inverted-F Antennas (PIFAs).

[0117] The antenna elements of an antenna structure in accordance with one or more embodiments of the disclosure need not have the same geometry or be the same type of antenna element. The antenna elements should each have resonance at the desired frequency or frequency range of operation.

[0118] In accordance with one or more embodiments of the disclosure, the antenna elements of an antenna structure have the same geometry. This is generally desirable for design simplicity, especially when the antenna performance requirements are the same for connection to either port.

[0119] The bandwidth and resonant frequencies of the combined antenna structure can be controlled by the bandwidth and resonance frequencies of the antenna elements. Thus, broader bandwidth elements can be used to produce a broader bandwidth for the modes of the combined structure as illustrated, e.g., in FIGS. 6A, 6B, and 6C. FIG. 6A illustrates a multimode antenna structure 600 including two dipoles 602, 604 connected by connecting elements 606, 608. The dipoles 602, 604 each have a width (W) and a length (L) and are spaced apart by a distance (d). FIG. 6B illustrates the scattering parameters for the structure having exemplary dimensions: W=1 mm, L=57.2 mm, and d=10 mm. FIG. 6C illustrates the scattering parameters for the structure having exemplary dimensions: W=10 mm, L=50.4 mm, and d=10 mm. As shown, increasing W from 1 mm to 10 mm, while keeping the other dimensions generally the same, results in a broader isolation bandwidth and impedance bandwidth for the antenna structure.

[0120] It has also been found that increasing the separation between the antenna elements increases the isolation bandwidth and the impedance bandwidth for an antenna structure.

[0121] In general, the connecting element is in the high-current region of the combined resonant structure. It may therefore be desirable for the connecting element to have a high conductivity.

[0122] The ports are located at the feed points of the antenna elements as they would be if they were operated as separate antennas. Matching elements or structures may be used to match the port impedance to the desired system impedance.

[0123] In accordance with one or more embodiments of the disclosure, the multimode antenna structure can be a planar structure incorporated, e.g., into a printed circuit board, as shown as FIG. 7. In this example, the antenna structure 700 includes antenna elements 702, 704 connected by a connecting element 706 at ports 708, 710. The antenna structure is fabricated on a printed circuit board substrate 712. The antenna elements shown in the figure are simple quarter-wave monopoles. However, the antenna elements can be any geometry that yields an equivalent effective electrical length.

[0124] In accordance with one or more embodiments of the disclosure, antenna elements with dual resonant frequencies can be used to produce a combined antenna structure with dual resonant frequencies and hence dual operating frequencies. FIG. 8A shows an exemplary model of a multimode dipole structure 800 where the dipole antenna elements 802, 804 are split into two fingers 806, 808 and 810, 812, respectively, of unequal length. The dipole antenna elements have resonant frequencies associated with each the two different finger lengths and accordingly exhibit a dual resonance. Similarly, the multimode antenna structure using dual-resonant dipole arms exhibits two frequency bands where high isolation (or small S21) is obtained as shown in FIG. 8B.

[0125] In accordance with one or more embodiments of the disclosure, a multimode antenna structure 900 shown in FIG. 9 is provided having variable length antenna elements 902, 904 forming a tunable antenna. This may be done by changing the effective electrical length of the antenna elements by a controllable device such as an RF switch 906, 908 at each antenna element 902, 904. In this example, the switch may be opened (by operating the controllable device) to create a shorter electrical length (for higher frequency operation) or closed to create a longer electrical length (for lower frequency operation). The operating frequency band for the antenna

structure 900, including the feature of high isolation, can be tuned by tuning both antenna elements in concert. This approach may be used with a variety of methods of changing the effective electrical length of the antenna elements including, e.g., using a controllable dielectric material, loading the antenna elements with a variable capacitor such as a micro-electromechanical systems (MEMs) device, varactor, or tunable dielectric capacitor, and switching on or off parasitic elements.

[0126] In accordance with one or more embodiments of the disclosure, the connecting element or elements provide an electrical connection between the antenna elements with an electrical length approximately equal to the electrical distance between the elements. Under this condition, and when the connecting elements are attached at the port ends of the antenna elements, the ports are isolated at a frequency near the resonance frequency of the antenna elements. This arrangement can produce nearly perfect isolation at particular frequency.

[0127] Alternately, as previously discussed, the electrical length of the connecting element may be increased to expand the bandwidth over which isolation exceeds a particular value. For example, a straight connection between antenna elements may produce a minimum S21 of -25 dB at a particular frequency and the bandwidth for which S21 < -10 dB may be 100 MHz. By increasing the electrical length, a new response can be obtained where the minimum S21 is increased to -15 dB but the bandwidth for which S21 < -10 dB may be increased to 150 MHz.

[0128] Various other multimode antenna structures in accordance with one or more embodiments of the disclosure are possible. For example, the connecting element can have a varied geometry or can be constructed to include components to vary the properties of the antenna structure. These components can include, e.g., passive inductor and capacitor elements, resonator or filter structures, or active components such as phase shifters.

[0129] In accordance with one or more embodiments of the disclosure, the position of the connecting element along the length of the antenna elements can be varied to adjust the properties of the antenna structure. The frequency band over which the ports are isolated can be shifted upward in frequency by moving the point of attachment of the connecting element on the antenna elements away from the ports and towards the distal end of the antenna elements. FIGS. 10A and 10B illustrate multimode antenna structures 1000, 1002, respectively, each having a connecting element electrically connected to the antenna elements. In the FIG. 10A antenna structure 1000, the connecting element 1004 is located in the structure such that the gap between the connecting element 1004 and the top edge of the ground plane 1006 is 3 mm. FIG. 10C shows the scattering parameters for the structure showing that high isolation is obtained at a frequency of 1.15 GHz in this configuration. A shunt capacitor/series inductor matching network is used to provide the impedance match at 1.15 GHz. FIG. 10D shows the scattering parameters for the structure 1002 of FIG. 10B, where the gap between the connecting element 1008 and the top edge 1010 of the ground plane is 19 mm. The antenna structure 1002 of FIG. 10B exhibits an operating band with high isolation at approximately 1.50 GHz.

[0130] FIG. 11 schematically illustrates a multimode antenna structure 1100 in accordance with one or more further embodiments of the disclosure. The antenna structure

1100 includes two or more connecting elements **1102**, **1104**, each of which electrically connects the antenna elements **1106**, **1108**. (For ease of illustration, only two connecting elements are shown in the figure. It should be understood that use of more than two connecting elements is also contemplated.) The connecting elements **1102**, **1104** are spaced apart from each other along the antenna elements **1106**, **1108**. Each of the connecting elements **1102**, **1104** includes a switch **1112**, **1110**. Peak isolation frequencies can be selected by controlling the switches **1110**, **1112**. For example, a frequency f_1 can be selected by closing switch **1110** and opening switch **1112**. A different frequency f_2 can be selected by closing switch **1112** and opening switch **1110**.

[0131] FIG. 12 illustrates a multimode antenna structure **1200** in accordance with one or more alternate embodiments of the disclosure. The antenna structure **1200** includes a connecting element **1202** having a filter **1204** operatively coupled thereto. The filter **1204** can be a low pass or band pass filter selected such that the connecting element connection between the antenna elements **1206**, **1208** is only effective within the desired frequency band, such as the high isolation resonance frequency. At higher frequencies, the structure will function as two separate antenna elements that are not coupled by the electrically conductive connecting element, which is open circuited.

[0132] FIG. 13 illustrates a multimode antenna structure **1300** in accordance with one or more alternate embodiments of the disclosure. The antenna structure **1300** includes two or more connecting elements **1302**, **1304**, which include filters **1306**, **1308**, respectively. (For ease of illustration, only two connecting elements are shown in the figure. It should be understood that use of more than two connecting elements is also contemplated.) In one possible embodiment, the antenna structure **1300** has a low pass filter **1308** on the connecting element **1304** (which is closer to the antenna ports) and a high pass filter **1306** on the connecting element **1302** in order to create an antenna structure with two frequency bands of high isolation, i.e., a dual band structure.

[0133] FIG. 14 illustrates a multimode antenna structure **1400** in accordance with one or more alternate embodiments of the disclosure. The antenna structure **1400** includes one or more connecting elements **1402** having a tunable element **1406** operatively connected thereto. The antenna structure **1400** also includes antenna elements **1408**, **1410**. The tunable element **1406** alters the delay or phase of the electrical connection or changes the reactive impedance of the electrical connection. The magnitude of the scattering parameters S_{21} / S_{12} and a frequency response are affected by the change in electrical delay or impedance and so an antenna structure can be adapted or generally optimized for isolation at specific frequencies using the tunable element **1406**.

[0134] FIG. 15 illustrates a multimode antenna structure **1500** in accordance with one or more alternate embodiments of the disclosure. The multimode antenna structure **1500** can be used, e.g., in a WiMAX USB dongle. The antenna structure **1500** can be configured for operation, e.g., in WiMAX bands from 2300 to 2700 MHz.

[0135] The antenna structure **1500** includes two antenna elements **1502**, **1504** connected by a conductive connecting element **1506**. The antenna elements include slots to increase the electrical length of the elements to obtain the desired operating frequency range. In this example, the antenna structure is optimized for a center frequency of 2350 MHz. The length of the slots can be reduced to obtain higher center

frequencies. The antenna structure is mounted on a printed circuit board assembly **1508**. A two-component lumped element match is provided at each antenna feed.

[0136] The antenna structure **1500** can be manufactured, e.g., by metal stamping. It can be made, e.g., from 0.2 mm thick copper alloy sheet. The antenna structure **1500** includes a pickup feature **1510** on the connecting element at the center of mass of the structure, which can be used in an automated pick-and-place assembly process. The antenna structure is also compatible with surface-mount reflow assembly.

[0137] FIG. 16 illustrates a multimode antenna structure **1600** in accordance with one or more alternate embodiments of the disclosure. As with antenna structure **1500** of FIG. 15, the antenna structure **1600** can also be used, e.g., in a WiMAX USB dongle. The antenna structure can be configured for operation, e.g., in WiMAX bands from 2300 to 2700 MHz.

[0138] The antenna structure **1600** includes two antenna elements **1602**, **1604**, each comprising a meandered monopole. The length of the meander determines the center frequency. The exemplary design shown in the figure is optimized for a center frequency of 2350 MHz. To obtain higher center frequencies, the length of the meander can be reduced.

[0139] A connecting element **1606** electrically connects the antenna elements. A two-component lumped element match is provided at each antenna feed.

[0140] The antenna structure can be fabricated, e.g., from copper as a flexible printed circuit (FPC) mounted on a plastic carrier **1608**. The antenna structure can be created by the metalized portions of the FPC. The plastic carrier provides mechanical support and facilitates mounting to a PCB assembly **1610**. Alternatively, the antenna structure can be formed from sheet-metal.

[0141] FIG. 17 illustrates a multimode antenna structure **1700** in accordance with another embodiment of the disclosure. This antenna design can be used, e.g., for USB, Express 34, and Express 54 data card formats. The exemplary antenna structure shown in the figure is designed to operate at frequencies from 2.3 to 6 GHz. The antenna structure can be fabricated, e.g., from sheet-metal or by FPC over a plastic carrier **1702**.

[0142] FIG. 18A illustrates a multimode antenna structure **1800** in accordance with another embodiment of the disclosure. The antenna structure **1800** comprises a three mode antenna with three ports. In this structure, three monopole antenna elements **1802**, **1804**, **1806** are connected using a connecting element **1808** comprising a conductive ring that connects neighboring antenna elements. The antenna elements are balanced by a common counterpoise, or sleeve **1810**, which is a single hollow conductive cylinder. The antenna has three coaxial cables **1812**, **1814**, **1816** for connection of the antenna structure to a communications device. The coaxial cables **1812**, **1814**, **1816** pass through the hollow interior of the sleeve **1810**. The antenna assembly may be constructed from a single flexible printed circuit wrapped into a cylinder and may be packaged in a cylindrical plastic enclosure to provide a single antenna assembly that takes the place of three separate antennas. In one exemplary arrangement, the diameter of the cylinder is 10 mm and the overall length of the antenna is 56 mm so as to operate with high isolation between ports at 2.45 GHz. This antenna structure can be used, e.g., with multiple antenna radio systems such as MIMO or 802.11N systems operating in the 2.4 to 2.5 GHz bands. In addition to port to port isolation, each port advantageously produces a different gain pattern as shown on FIG. 18B. While

this is one specific example, it is understood that this structure can be scaled to operate at any desired frequency. It is also understood that methods for tuning, manipulating bandwidth, and creating multiband structures described previously in the context of two-port antennas can also apply to this multipoint structure.

[0143] While the above embodiment is shown as a true cylinder, it is possible to use other arrangements of three antenna elements and connecting elements that produce the same advantages. This includes, but is not limited to, arrangements with straight connections such that the connecting elements form a triangle, or another polygonal geometry. It is also possible to construct a similar structure by similarly connecting three separate dipole elements instead of three monopole elements with a common counterpoise. Also, while symmetric arrangement of antenna elements advantageously produces equivalent performance from each port, e.g., same bandwidth, isolation, impedance matching, it is also possible to arrange the antenna elements asymmetrically or with unequal spacing depending on the application.

[0144] FIG. 19 illustrates use of a multimode antenna structure **1900** in a combiner application in accordance with one or more embodiments of the disclosure. As shown in the figure, transmit signals may be applied to both antenna ports of the antenna structure **1900** simultaneously. In this configuration, the multimode antenna can serve as both antenna and power amplifier combiner. The high isolation between antenna ports restricts interaction between the two amplifiers **1902**, **1904**, which is known to have undesirable effects such as signal distortion and loss of efficiency. Optional impedance matching at **1906** can be provided at the antenna ports.

[0145] FIGS. 20A and 20B illustrate a multimode antenna structure **2000** in accordance with one or more alternate embodiments of the subject disclosure. The antenna structure **2000** can also be used, e.g., in a WiMAX USB or Express-Card/34 device. The antenna structure can be configured for operation, e.g., in WiMAX bands from 2300 to 6000 MHz.

[0146] The antenna structure **2000** includes two antenna elements **2001**, **2004**, each comprising a broad monopole. A connecting element **2002** electrically connects the antenna elements. Slots (or other cut-outs) **2005** are used to improve the input impedance match above 5000 MHz. The exemplary design shown in the figure is optimized to cover frequencies from 2300 to 6000 MHz.

[0147] The antenna structure **2000** can be manufactured, e.g., by metal stamping. It can be made, e.g., from 0.2 mm thick copper alloy sheet. The antenna structure **2000** includes a pickup feature **2003** on the connecting element **2002** generally at the center of mass of the structure, which can be used in an automated pick-and-place assembly process. The antenna structure is also compatible with surface-mount reflow assembly. Feed points **2006** of the antenna provide the points of connection to the radio circuitry on a PCB, and also serve as a support for structural mounting of the antenna to the PCB. Additional contact points **2007** provide structural support.

[0148] FIG. 20C illustrates a test assembly **2010** used to measure the performance of antenna **2000**. The figure also shows the coordinate reference for far-field patterns. Antenna **2000** is mounted on a 30×88 mm PCB **2011** representing an ExpressCard/34 device. The grounded portion of the PCB **2011** is attached to a larger metal sheet **2012** (having dimensions of 165×254 mm in this example) to represent a coun-

terpoise size typical of a notebook computer. Test ports **2014**, **2016** on the PCB **2011** are connected to the antenna through 50-ohm striplines.

[0149] FIG. 20D shows the VSWR measured at test ports **2014**, **2016**. FIG. 20E shows the coupling (S21 or S12) measured between the test ports. The VSWR and coupling are advantageously low across the broad range of frequencies, e.g., 2300 to 6000 MHz. FIG. 20F shows the measured radiation efficiency referenced from the test ports **2014** (Port 1), **2016** (Port 2). FIG. 20G shows the calculated correlation between the radiation patterns produced by excitation of test port **2014** (Port 1) versus those produced by excitation of test port **2016** (Port 2). The radiation efficiency is advantageously high while the correlation between patterns is advantageously low at the frequencies of interest. FIG. 20H shows far field gain patterns by excitation of test port **2014** (Port 1) or test port **2016** (Port 2) at a frequency of 2500 MHz. FIGS. 20I and 20J show the same pattern measurements at frequencies of 3500 and 5200 MHz, respectively. The patterns resulting from test port **2014** (Port 1) are different and complementary to those of test port **2016** (Port 2) in the $\phi=0$ or XZ plane and in the $\theta=90$ or XY plane.

[0150] FIGS. 21A and 21B illustrate a multimode antenna structure **2100** in accordance with one or more alternate embodiments of the subject disclosure. The antenna structure **2100** can also be used, e.g., in a WiMAX USB dongle. The antenna structure can be configured for operation, e.g., in WiMAX bands from 2300 to 2400 MHz.

[0151] The antenna structure **2100** includes two antenna elements **2102**, **2104**, each comprising a meandered monopole. The length of the meander determines the center frequency. Other tortuous configurations such as, e.g., helical coils and loops, can also be used to provide a desired electrical length. The exemplary design shown in the figure is optimized for a center frequency of 2350 MHz. A connecting element **2106** (shown in FIG. 21B) electrically connects the antenna elements **2102**, **2104**. A two-component lumped element match is provided at each antenna feed.

[0152] The antenna structure can be fabricated, e.g., from copper as a flexible printed circuit (FPC) **2103** mounted on a plastic carrier **2101**. The antenna structure can be created by the metalized portions of the FPC **2103**. The plastic carrier **2101** provides mounting pins or pips **2107** for attaching the antenna to a PCB assembly (not shown) and pips **2105** for securing the FPC **2103** to the carrier **2101**. The metalized portion of **2103** includes exposed portions or pads **2108** for electrically contacting the antenna to the circuitry on the PCB.

[0153] To obtain higher center frequencies, the electrical length of the elements **2102**, **2104** can be reduced. FIGS. 22A and 22B illustrate a multimode antenna structure **2200**, the design of which is optimized for a center frequency of 2600 MHz. The electrical length of the elements **2202**, **2204** is shorter than that of elements **2102**, **2104** of FIGS. 21A and 21B because metallization at the end of the elements **2202**, **2204** has been removed, and the width of the of the elements at feed end has been increased.

[0154] FIG. 23A illustrates a test assembly **2300** using antenna **2100** of FIGS. 21A and 21B along with the coordinate reference for far-field patterns. FIG. 23B shows the VSWR measured at test ports **2302** (Port 1), **2304** (Port 2). FIG. 23C shows the coupling (S21 or S12) measured between the test ports **2302** (Port 1), **2304** (Port 2). The VSWR and coupling are advantageously low at the frequencies of inter-

est, e.g., 2300 to 2400 MHz. FIG. 23D shows the measured radiation efficiency referenced from the test ports. FIG. 23E shows the calculated correlation between the radiation patterns produced by excitation of test port 2302 (Port 1) versus those produced by excitation of test port 2304 (Port 2). The radiation efficiency is advantageously high while the correlation between patterns is advantageously low at the frequencies of interest. FIG. 23F shows far field gain patterns by excitation of test port 2302 (Port 1) or test port 2304 (Port 2) at a frequency of 2400 MHz. The patterns resulting from test port 2302 (Port 1) are different and complementary to those of test port 2304 (Port 2) in the $\phi=0$ or XZ plane and in the $\theta=90$ or XY plane.

[0155] FIG. 23G shows the VSWR measured at the test ports of assembly 2300 with antenna 2200 in place of antenna 2100. FIG. 23H shows the coupling (S21 or S12) measured between the test ports. The VSWR and coupling are advantageously low at the frequencies of interest, e.g. 2500 to 2700 MHz. FIG. 23I shows the measured radiation efficiency referenced from the test ports. FIG. 23J shows the calculated correlation between the radiation patterns produced by excitation of test port 2302 (Port 1) versus those produced by excitation of test port 2304 (Port 2). The radiation efficiency is advantageously high while the correlation between patterns is advantageously low at the frequencies of interest. FIG. 23K shows far field gain patterns by excitation of test port 2302 (Port 1) or test port 2304 (Port 2) at a frequency of 2600 MHz. The patterns resulting from test port 2302 (Port 1) are different and complementary to those of test port 2304 (Port 2) in the $\phi=0$ or XZ plane and in the $\theta=90$ or XY plane.

[0156] One or more further embodiments of the subject disclosure are directed to techniques for beam pattern control for the purpose of null steering or beam pointing. When such techniques are applied to a conventional array antenna (comprising separate antenna elements that are spaced at some fraction of a wavelength), each element of the array antenna is fed with a signal that is a phase shifted version of a reference signal or waveform. For a uniform linear array with equal excitation, the beam pattern produced can be described by the array factor F, which depends on the phase of each individual element and the inter-element element spacing d.

$$F = A_0 \sum_{n=0}^{N-1} \exp[jn(\beta d \cos \theta + \alpha)]$$

[0157] where $\beta=2\pi/\lambda$, N=Total # of elements, α =phase shift between successive elements, and θ =angle from array axis

[0158] By controlling the phase α to a value α_r , the maximum value of F can be adjusted to a different direction θ_r , thereby controlling the direction in which a maximum signal is broadcast or received.

[0159] The inter-element spacing in conventional array antennas is often on the order of $1/4$ wavelength, and the antennas can be closely coupled, having nearly identical polarization. It is advantageous to reduce the coupling between elements, as coupling can lead to several problems in the design and performance of array antennas. For example, problems such as pattern distortion and scan blindness (see Stutzman, Antenna Theory and Design, Wiley 1998, pgs 122-128 and 135-136, and 466-472) can arise from excessive inter-ele-

ment coupling, as well as a reduction of the maximum gain attainable for a given number of elements.

[0160] Beam pattern control techniques can be advantageously applied to all multimode antenna structures described herein having antenna elements connected by one or more connecting elements, which exhibit high isolation between multiple feedpoints. The phase between ports at the high isolation antenna structure can be used for controlling the antenna pattern. It has been found that a higher peak gain is achievable in given directions when the antenna is used as a simple beam-forming array as a result of the reduced coupling between feedpoints. Accordingly, greater gain can be achieved in selected directions from a high isolation antenna structure in accordance with various embodiments that utilizes phase control of the carrier signals presented to its feed terminals.

[0161] In handset applications where the antennas are spaced at much less than $1/4$ wavelength, mutual coupling effects in conventional antennas reduce the radiation efficiency of the array, and therefore reduce the maximum gain achievable.

[0162] By controlling the phase of the carrier signal provided to each feedpoint of a high isolation antenna in accordance with various embodiments, the direction of maximum gain produced by the antenna pattern can be controlled. A gain advantage of, e.g., 3 dB obtained by beam steering is advantageous particularly in portable device applications where the beam pattern is fixed and the device orientation is randomly controlled by the user. As shown, e.g., in the schematic block diagram of FIG. 24, which illustrates a pattern control apparatus 2400 in accordance with various embodiments, a relative phase shift α is applied by a phase shifter 2402 to the RF signals applied to each antenna feed 2404, 2408. The signals are fed to respective antenna ports of antenna structure 2410.

[0163] The phase shifter 2402 can comprise standard phase shift components such as, e.g., electrically controlled phase shift devices or standard phase shift networks.

[0164] FIGS. 25A-25G provide a comparison of antenna patterns produced by a closely spaced 2-D conventional array of dipole antennas and a 2-D array of high isolation antennas in accordance with various embodiments of the subject disclosure for different phase differences α between two feeds to the antennas. In FIGS. 25A-25G, curves are shown for the antenna patterns at $\theta=90$ degrees. The solid lines in the figures represents the antenna pattern produced by the isolated feed single element antenna in accordance with various embodiments, while the dashed lines represent the antenna pattern produced by two separate monopole conventional antennas separated by a distance equal to the width of the single element isolated feed structure. Therefore, the conventional antenna and the high isolation antenna are of generally equivalent size.

[0165] In all cases shown in the figures, the peak gain produced by the high isolation antenna in accordance with various embodiments produces a greater gain margin when compared to the two separate conventional dipoles, while providing azimuthal control of the beam pattern. This behavior makes it possible to use the high isolation antenna in transmit or receive applications where additional gain is needed or desired in a particular direction. The direction can be controlled by adjusting the relative phase between the drivepoint signals. This may be particularly advantageous for portable devices needing to direct energy toward a receive

point such as, e.g., a base station. The combined high isolation antenna offers greater advantage when compared to two single conventional antenna elements when phased in a similar fashion.

[0166] As shown in FIG. 25A, the combined dipole in accordance with various embodiments shows greater gain in a uniform azimuth pattern ($\theta=90$) for $\alpha=0$ (zero degrees phase difference).

[0167] As shown in FIG. 25B, the combined dipole in accordance with various embodiments shows greater peak gain (at $\phi=0$) with a non-symmetric azimuthal pattern ($\theta=90$ plot for $\alpha=30$ (30 degrees phase difference between feedpoints)).

[0168] As shown in FIG. 25C, the combined dipole in accordance with various embodiments shows greater peak gain (at $\phi=0$) with a shifted azimuthal pattern ($\theta=90$ plot for $\alpha=60$ (60 degrees phase difference between feedpoints)).

[0169] As shown in FIG. 25D, the combined dipole in accordance with various embodiments shows even greater peak gain (at $\phi=0$) with a shifted azimuthal pattern ($\theta=90$ plot for $\alpha=90$ (90 degrees phase difference between feedpoints)).

[0170] As shown in FIG. 25E, the combined dipole in accordance with various embodiments shows greater peak gain (at $\phi=0$) with a shifted azimuthal pattern ($\theta=90$ plot greater backlobe (at $\phi=180$) for $\alpha=120$ (120 degrees phase difference between feedpoints)).

[0171] As shown in FIG. 25F, the combined dipole in accordance with various embodiments shows greater peak gain (at $\phi=0$) with a shifted azimuthal pattern ($\theta=90$ plot), even greater backlobe (at $\phi=180$) for $\alpha=150$ (150 degrees phase difference between feedpoints)).

[0172] As shown in FIG. 25G, the combined dipole in accordance with various embodiments shows greater peak gain (at $\phi=0$ & 180) with a double lobed azimuthal pattern ($\theta=90$ plot) for $\alpha=180$ (180 degrees phase difference between feedpoints)).

[0173] FIG. 26 illustrates the ideal gain advantage if the combined high isolation antenna in accordance with one or more embodiments over two separate dipoles as a function of the phase angle difference between the feedpoints for a two feedpoint antenna array.

[0174] Further embodiments of the subject disclosure are directed to multimode antenna structures that provide increased high isolation between multi-band antenna ports operating in close proximity to each other at a given frequency range. In these embodiments, a band-rejection slot is incorporated in one of the antenna elements of the antenna structure to provide reduced coupling at the frequency to which the slot is tuned.

[0175] FIG. 27A schematically illustrates a simple dual-band branch line monopole antenna 2700. The antenna 2700 includes a band-rejection slot 2702, which defines two branch resonators 2704, 2706. The antenna is driven by signal generator 2708. Depending on the frequency at which the antenna 2700 is driven, various current distributions are realized on the two branch resonators 2704, 2706.

[0176] The physical dimensions of the slot 2702 are defined by the width W_s and the length L_s as shown in FIG. 27A. When the excitation frequency satisfies the condition of $L_s=l_0/4$, the slot feature becomes resonant. At this point the current distribution is concentrated around the shorted section of the slot, as shown in FIG. 27B.

[0177] The currents flowing through the branch resonators 2704, 2706 are approximately equal and oppositely directed

along the sides of the slot 2702. This causes the antenna structure 2700 to behave in a similar manner to a spurline band stop filter 2720 (shown schematically in FIG. 27C), which transforms the antenna input impedance down significantly lower than the nominal source impedance. This large impedance mismatch results in a very high VSWR, shown in FIGS. 27D and 27E, and as a result leads to the desired frequency rejection.

[0178] This band-rejection slot technique can be applied to an antenna system with two (or more) antennas elements operating in close proximity to each other where one antenna element needs to pass signals of a desired frequency and the other does not. In one or more embodiments, one of the two antenna elements includes a band-rejection slot, and the other does not. FIG. 28 schematically illustrates an antenna structure 2800, which includes a first antenna element 2802, a second antenna element 2804, and a connecting element 2806. The antenna structure 2800 includes ports 2808 and 2810 at antenna elements 2802 and 2804, respectively. In this example, a signal generator drives the antenna structure 2802 at port 2808, while a meter is coupled to the port 2810 to measure current at port 2810. It should be understood, however, that either or both ports can be driven by signal generators. The antenna element 2802 includes a band-rejection slot 2812, which defines two branch resonators 2814, 2816. In this embodiment, the branch resonators comprise the main transmit section of the antenna structure, while the antenna element 2804 comprises a diversity receive portion of the antenna structure.

[0179] Due to the large mismatch at the port of the antenna element 2802 with the band-reject slot 2812, the mutual coupling between it and the diversity receive antenna element 2804, which is actually matched at the slot resonant frequency will be quite small and will result in relatively high isolation.

[0180] FIG. 29A is a perspective view of a multimode antenna structure 2900 comprising a multi-band diversity receive antenna system that utilizes the band-rejection slot technique in the GPS band in accordance with one or more further embodiments of the subject disclosure. (The GPS band is 1575.42 MHz with 20 MHz bandwidth.) The antenna structure 2900 is formed on a flex film dielectric substrate 2902, which is formed as a layer on a dielectric carrier 2904. The antenna structure 2900 includes a GPS band rejection slot 2906 on the primary transmit antenna element 2908 of the antenna structure 2900. The antenna structure 2900 also includes a diversity receive antenna element 2910, and a connecting element 2912 connecting the diversity receive antenna element 2910 and the primary transmit antenna element 2908. A GPS receiver (not shown) is connected to the diversity receive antenna element 2910. In order to generally minimize the antenna coupling from the primary transmit antenna element 2908 and to generally maximize the diversity antenna radiation efficiency at these frequencies, the primary antenna element 2908 includes the band-rejection slot 2906 and is tuned to an electrical quarter wave length near the center of the GPS band. The diversity receive antenna element 2910 does not contain such a band rejection slot, but comprises a GPS antenna element that is properly matched to the main antenna source impedance so that there will be generally maximum power transfer between it and the GPS receiver. Although both antenna elements 2908, 2910 co-exist in close proximity, the high VSWR due to the slot 2906 at the primary transmit antenna element 2908 reduces the coupling

to the primary antenna element source resistance at the frequency to which the slot **2906** is tuned, and therefore provides isolation at the GPS frequency between both antenna elements **2908**, **2910**. The resultant mismatch between the two antenna elements **2908**, **2910** within the GPS band is large enough to decouple the antenna elements in order to meet the isolation requirements for the system design as shown in FIGS. **29B** and **29C**.

[0181] In the antenna structures described herein in accordance with various embodiments of the subject disclosure, the antenna elements and the connecting elements can form a single integrated radiating structure such that a signal fed to either port excites the entire antenna structure to radiate as a whole, rather than separate radiating structures. As such, the techniques described herein provide isolation of the antenna ports without the use of decoupling networks at the antenna feed points.

[0182] Other embodiments disclosed herein are directed to an antenna that separates the fundamental (low band) resonance from the high band resonance by using two separate structures, which are connected at the feedpoint—thus accomplishing the goal of achieving a MIMO or Diversity antenna with each feed exhibiting a multiband capability, and whereby each feed is optimally isolated from the opposite feed. By way of a non-limiting illustration, in some implementations, high band frequencies can range from 1710 to 2170 MHz, and low band frequencies can range from 698 to 960 MHz.

[0183] In one or more embodiments of the antenna structures described in the subject disclosure, electrical currents flowing through neighboring antenna elements **3002** and **3004** (see FIG. **30**) can be configured to be similar in magnitude, such that an antenna mode excited by one antenna port (e.g., Port 1) is approximately electrically isolated from an antenna mode excited by another antenna port (e.g., Port 2) at a given desired signal frequency range. In one embodiment, this can be accomplished by configuring antennas **3002** and **3004** with a connecting element **3006** to enable common and difference mode currents, which when summed together result in some or a substantial amount of isolation between ports 1 and 2. Configuring an antenna structure to control differential and common mode current to cause isolation between any number of antenna ports can be applied to any of the antenna embodiments described herein.

[0184] FIG. **31** illustrates an exemplary multiband antenna **3100** in accordance with one or more embodiments. The antenna **3100** can include a low band structure comprising two low band antenna elements **3102**, **3104** connected by a connecting element **3106**. A fixed or variable reactive element **3126** such as a fixed or variable inductor L is provided in the connecting element **3106** to provide control (reduction) of the mutual coupling between feedpoints for the low band element by varying the electrical length of the connecting element **3106** in accordance with the disclosures of U.S. Pat. No. 7,688,273, the disclosure of which is incorporated by reference herein in its entirety. Similarly, a connecting element **3116** can be provided between the high band antenna elements **3112**, **3114**. A fixed or variable reactive element **3136** such as a fixed or variable inductor L can be provided in the connecting element **3116** to provide control (reduction) of the mutual coupling between feedpoints for the low band element by varying the electrical length of the connecting element **3116** in accordance with the disclosures of U.S. Pat. No. 7,688,273.

[0185] The high band structure comprising two high band antenna elements **3112**, **3114** can be connected to the low band structure at feed points f_1 , f_2 . Two filters **3142** and **3144** are provided in the high band antenna elements **3112**, **3114** for blocking low band frequencies, thereby isolating the high band antenna elements **3112**, **3114** from the low band antenna elements **3102**, **3104**. The filters **3142** and **3144** can be passive or programmable pass band filters. In the present illustration the filters **3142** and **3144** can represent high pass filters implemented with a capacitor and/or other components to achieve desired high pass filtering characteristics. To achieve similar isolation with the low band structure, the low band antenna elements **3102**, **3104** can be configured with filters **3152**, **3154** to block high band frequencies, thereby isolating the high band antenna elements **3112**, **3114** from the low band antenna elements **3102**, **3104**. The filters **3152**, **3154** can be passive or programmable pass band filters. In the present illustration the filters **3152**, **3154** can represent low pass filters implemented with reactive and passive components that achieve desired low pass filtering characteristics.

[0186] By having a structure associated with low band resonance and a separate structure associated with high band resonance, the low band structure can be advantageously designed or optimized independently of the high band structure and vice-versa. A further advantage is that the low band or high band structures may separately take on different antenna design realizations, e.g., monopole, loop, Planar Inverted “F” antenna (PIFA), etc. allowing the designer to select the best option for the electrical and mechanical design requirements. In one exemplary embodiment, the low band structure may be a monopole, while the high band structure may be a PIFA.

[0187] A separate network is provided for each structure. The low band structure can use a fixed or variable inductive bridge **3126** as an interconnecting element **3106**. The high band element is fed from the common feedpoint, but with a high pass network **3142**, **3144**—the simplest being a series capacitor with low reactance at the high band frequencies and higher reactance at the low band frequencies. In addition, the low band antenna elements **3102**, **3104** can be configured with variable reactive components **3122**, **3124** to perform aperture tuning which enables shifting of the low band resonance frequency of the low band structure. The reactive components **3122**, **3124** can be independently controlled so that the resonance frequency of low band antenna element **3102** can be independently controlled from the low band resonance frequency of low band antenna element **3104**. The reactive components **3122**, **3124** can be represented by switched inductors which can be aggregated or reduced to vary the electrical length of the low band antenna elements **3102**, **3104**, respectively.

[0188] Similarly, the high band antenna elements **3112**, **3114** can be configured with variable reactive components **3132**, **3134** to perform aperture tuning which enables shifting of the high band resonance frequency of the high band structure. The reactive components **3132**, **3134** can be independently controlled so that the resonance frequency of high band antenna element **3112** can be independently controlled from the high band resonance frequency of high band antenna element **3114**. The reactive components **3132**, **3134** can also be represented by switched inductors which can be aggregated or reduced to vary the electrical length of the high band antenna elements **3112**, **3114**, respectively.

[0189] The aforementioned structures, enable high band tuning to be performed relatively independent of low band tuning, providing a simpler design process and better performance than antennas not having such separate structures. Other more complex networks may also be used advantageously to separate the interdependence of the high and low band structures still using a common feedpoint for a MIMO branch such as shown in FIG. 31. The method illustrated in FIG. 31 is not limited to 2x2, 2x1 MIMO or 2 feed antennas used for diversity applications, and may be extended to higher branch order MIMO antennas, e.g., 3x3, etc.

[0190] A number of factors affect antenna performance in a hand held mobile communication device. While these factors are related, they generally fall into one of three categories; antenna size, mutual coupling between multiple antennas, and device usage models. The size of an antenna is dependent on three criteria; bandwidth of operation, frequency of operation, and required radiation efficiency. Bandwidth requirements have obviously increased as they are driven by FCC frequency allocations in the US and carrier roaming agreements around the world. Different regions use different frequency bands, now with over 40 E-UTRA band designations—many overlapping but requiring world capable wireless devices to typically cover a frequency range from 698 to 2700 MHz.

[0191] A simple relationship exists between the bandwidth, size, and radiation efficiency for the fundamental or lowest frequency resonance of a physically small antenna.

$$\frac{\Delta f}{f} \propto \left(\frac{a}{\lambda}\right)^3 \eta^{-1} \quad (1)$$

[0192] Here a is the radius of a sphere containing the antenna and its associated current distribution. Since a is normalized to the operating wavelength, the formula may be interpreted as “fractional bandwidth is proportional to the wavelength normalized modal volume”. The radiation efficiency η is included as a factor on the right side of (1), indicating that greater bandwidth, is achievable by reducing the efficiency. Radio frequency currents exist not only on the antenna element but also on the attached conductive structure or “counterpoise”. For instance, mobile phone antennas in the 698-960 MHz bands use the entire PCB as a radiating structure so that the physical size of the antenna according to (1) is actually much larger than what appears to be the “antenna”. The “antenna” may be considered a resonator that is electromagnetically coupled to the PCB so that it excites currents over the entire conductive structure or chassis. Most smartphones exhibit conductive chassis dimensions of approximately 70x130 mm, which from an electromagnetic modal analysis predicts a fundamental mode near 1 GHz suggesting that performance bandwidth degrades progressively at lower excitation frequencies. The efficiency-bandwidth trade-off is complex requiring E-M simulation tools for accurate prediction. Results indicate that covering 698-960 MHz (Bands 12, 13, 17, 18, 19, 20, 5 and 8) with a completely passive antenna with desirable antenna size and geometry becomes difficult without making sacrifices in radiation efficiency.

[0193] Factors determining the achievable radiation efficiency are not entirely obvious, as the coupling coefficient between the “antenna” and the chassis; radiative coupling to lossy components on the PCB; dielectric absorption in plastic housing, coupling to co-existing antennas; as well as losses

from finite resistance within the “antenna” resonator structure, all play a part. In most cases, the requirements imposed by operators suggest minimum radiation efficiencies of 40-50%, so that meeting a minimum TRP requirement essentially requires tradeoffs between the power amplifier (PA) output and the achievable antenna efficiency. In turn, poor efficiency at the antenna translates to less battery life, as the PA must compensate for the loss.

[0194] Prior to concerns over band aggregation, wireless devices operated on one band at a time with need to change when roaming. Consequently, the required instantaneous bandwidth would be considerably less than that required to address worldwide compatibility. Take a 3G example for instance, where operation in band 5 from (824-894 MHz) compared to operation in bands 5 plus 8 (824-960 MHz). Then, add the requirements for band 13 and band 17 and the comparison becomes more dramatic—824-960 vs. 698-960 MHz. This becomes a problematic as legacy phone antennas support pentaband operation but only bands 5 and band 8. Given equation (1) several choices exist. The most obvious would be to increase the antenna system size, (i.e. the antenna and phone chassis footprint) and/or to reduce the radiation efficiency. Since 4G smartphones require 2 antennas, neither approach is necessarily desirable from an industrial design standpoint, although it is possible to cover the 700-2200 MHz bands with a completely passive antenna in a space allocation of 6.5x10x60 mm.

[0195] Various alternative antenna configurations are the following: limit the antenna(s) instantaneous bandwidth within current antenna space allocations to allow use of 1 or more antennas without compromising the industrial design (Antenna Supplier motivation); make the antenna(s) smaller to achieve a compact and sleek device with greater functionality by limiting the instantaneous bandwidth with same or improved antenna efficiency (OEM motivation); improve the antenna efficiency, and therefore the network performance by controlling the antenna instantaneous frequency/tuning (Operator motivation); make the antenna agile to adapt to different usage models (OEM/User/Operator motivation); or combinations of the above.

[0196] The simplest approach can be to limit the instantaneous operation to a single band to satisfy the protocol requirements for a single region. To satisfy the roaming requirements, the antenna could be made frequency agile on a band-by-band basis. This approach represents the most basic type of “state-tuned” antenna.

[0197] Various embodiments disclosed herein are directed to an antenna that separates the fundamental (low band) resonance from the high band resonance by using two separate structures, which are connected at the feedpoint—thus accomplishing the goal of achieving a MIMO or Diversity antenna with each feed exhibiting a multiband capability, and whereby each feed is optimally isolated from the opposite feed. By way of non-limiting example, in some implementations, high band frequencies can range from 1710 to 2700 MHz, and low band frequencies can range from 500 to 960 MHz.

[0198] The exemplary embodiments allow for tuning of the first resonance of the antenna to accommodate multiple operational bands depending on a tuning state, and broadband operation on the high bands (e.g., 1710-2170 MHz, or 1710-2700 MHz) independent of the low band tuning state.

[0199] Referring to FIG. 32A, an example is shown that is illustrative of single low band-multiple high band aggrega-

tion compatibility. The high band radiation efficiency in this case can remain essentially the same independent of the low band tuning state, but the low band resonance frequency is able to be tuned in discrete frequency increments according to the equivalent electrical length, as selected by the series inductance L_{var} which is shown in FIG. 32B. The variable inductance can be created using discrete reactive elements such as inductors and a switching mechanism such as an SP4T switch. The configuration as shown yields 3 different inductances depending on which state the switch is in: (state 1) $L_{VAR}=L_3+L_4+L_5$ (switch connects to pole 1 or 4); (state 2) $L_{VAR}=L_{path2}||L_3+L_4+L_5$ or approximately L_4+L_5 (switch connects to pole 2); or (state 3) $L_{VAR}=L_{path3}||(L_3+L_4)+L_5$ OR approximately L_5 (switch connects to pole 3). In this embodiment, L_{path2} and L_{path3} refer to the equivalent inductances of the circuit paths through the switch. Keeping the inductors close to the switch can minimize or otherwise reduce the path inductances such that the discrete inductors are essentially shorted out by the switch.

[0200] The antenna incorporates a main structure that has a fundamental resonance at the lowest frequency band. The solution employs a multiband antenna having 3 low band tuning states as shown in FIG. 32B. State 1 includes a low band (fundamental) resonance suited for LTE 700 (698-742 MHz) operation; State 2 includes a low band resonance suited to GSM 850 (824-894 MHz) operation, and state 3 a low band resonance suited to GSM 900 (880-960 MHz).

[0201] The high band resonance (1710-2170 MHz) can be reasonably independent of the tuning state for the low band by nature of the separation of the low and high band radiating elements from the feedpoints. The low band tuning can be accomplished by switching different reactive components in between the feedpoint and the radiating structure. The high band operation of the antenna can be governed primarily by the auxiliary radiating section at the terminus of the capacitor opposite the feedpoint. The capacitor functions primarily as a high pass filter to decouple the feedpoint from the high and low bands portions of the antenna. In this way, signals at different operating bands can be directed to the appropriate radiating section of the combined antenna. The high band resonance can be determined in part by the electrical length of the high band portion of the antenna (indicated in the illustration by horizontal conductive segments). In other embodiments, the capacitor may be a highpass, bandpass, or tunable filter. In a similar manner, the path from the feedpoint to the low band radiating portion of the antenna may include a low pass, bandpass or tunable filter.

[0202] Tuning can be accomplished using a switching device such one capable of SP4T operation. In one embodiment, a solid state silicon-based FET switch can be used in each leg of the antenna to alter the series inductance presented to the antenna feedpoint, thereby lowering the resonant frequency as a function of the amount of inductance added. Although inductors are used in this embodiment, other reactive components may also be used for the purpose of altering the electrical length of the low band portion of the antenna radiating structure including capacitive elements. The switch may be of various types such as a mechanical MEMS type device, a voltage/current controlled variable device, and so forth. The switch may also be configured with multiple poles and with any throw capability needed to select the number of tuning states required for antenna operation. The number of throws can establish the number of tuning states possible, which in turn is dictated by the number of frequency bands to

be supported. While three states are shown in the illustrated embodiment, any number of states can be utilized corresponding to any number of frequency bands or ranges. In one embodiment, a pair of adjustable reactive elements (e.g., fixed inductors coupled with switching mechanisms) can be coupled with corresponding pairs of feedpoints, and the tuning can be performed by settings each of the adjustable reactive elements to the same tuning state among the group of tuning states.

[0203] Referring to FIG. 33A, a separate but co-located high band element is shown with feed points F1H and F2H that allows for compatibility with RF transceiver front end designs requiring separate low- and mid- or low- and high-band connections to the antenna. The variable inductance can be created using discrete inductors and a SP4T switch as shown. The configuration as shown yields 3 different inductances depending on which state the switch is in: (state 1) $L_{VAR}=L_3+L_4+L_5$ (switch connects to pole 1 or 4); (state 2) $L_{VAR}=L_{path2}||L_3+L_4+L_5$ or approximately L_4+L_5 (switch connects to pole 2); or (state 3) $L_{VAR}=L_{path3}||(L_3+L_4)+L_5$ OR approx. L_5 (switch connects to pole 3). L_{path2} and L_{path3} refer to the equivalent inductances of the circuit paths through the switch. Keeping the inductors close to the switch minimizes the path inductances such that the discrete inductors are essentially shorted out by the switch.

[0204] The exemplary antennas can provide better radiation efficiency and/or smaller size compared to an untuned antenna by nature of the tuning to each band of operation separately. The reactive elements (e.g., inductors and their associated inductance) can establish the electrical length of the low band elements, and therefore can provide for adjusting the low band resonance (tuning) Referring additionally to FIGS. 34A-35B, antenna structures that enable tuning to each band of operation separately while also providing for desired filtering through use of low-pass-filters and high-pass-filters as illustrated.

[0205] Further, the fundamental mode associated of the antenna low band resonance can be tuned by adjustment of the electrical length of the low band portion of the antenna via reactive elements which may exhibit either inductive or capacitive characteristics. As illustrated in FIG. 32A, discrete inductors are shown in a series connection between the antenna feed points and the radiating element end plates on the each side of the antenna, thereby increasing the equivalent electrical length. The use of separate or discrete components is intended to be illustrative of the principle, but by no means limiting to scope of the subject disclosure. In one or more embodiments, the techniques and/or components of the exemplary embodiments described herein that provide for antenna tuning can be utilized in conjunction with techniques and/or components described with respect to U.S. Pat. No. 7,688,273. In one or more embodiments, the techniques and/or components of the exemplary embodiments described herein that provide for antenna tuning can be utilized in conjunction with techniques and/or components described with respect to U.S. patent application Ser. No. 14/266,053, entitled "Antenna Structures and Methods Thereof", filed on Apr. 30, 2014, under attorney docket number 5000-0191 (2013-03B).

[0206] FIG. 36A depicts an illustrative embodiment of a near field sensor 3620 utilized with other RF components of a communication device 3600. In one embodiment near field sensor 3620 can comprise a first log detector 3622 that receives signals from a directional coupler 3604, a second log

detector **3626** that receives signals from a near field probe **3624**. In another embodiment, such as shown in FIG. **36B**, the near field sensor **3620** can comprise a single log detector **3626** that receives signals from one or more near field probes **3624** selectable by a switch **3625**. Instead of relying on a directional coupler **3604** such as shown in FIG. **36A**, the controller **3632** of FIG. **36B** can be configured to determine a magnitude of a forward feed signal supplied by the transmitter **3602** based on a known state of the transmitter **3602**, which can be determined from a look-up table. That is, the controller **3632** may be aware that the transmitter **3602** has been configured to transmit at a desired magnitude as a result of configuring components of the transmitter **3602** such as an amplifier or otherwise. The controller **3632** can utilize a look-up table comprising magnitudes indexed according to known states of the transmitter **3602**, or can determine the magnitude of a transmit signal based on an algorithm implemented by the controller **3632**. The look-up table can be created by characterizing the transmitter **3602** in a lab or manufacturing setting. Accordingly, the embodiments that follow can be based on either the embodiments of FIG. **36A** or **36B**.

[0207] The near field probe **3624** can be a small trace of metal serving as a miniature antenna that can receive radiated energy from an adaptive antenna **3610** and which can have a very small parasitic effect (if any) on the adaptive antenna **3610**, thereby unaffected the original operating characteristics of the adaptive antenna **3610**. The near field probe **3624** can be located on a printed circuit board (PCB), a housing assembly component or some other suitable location of the communication device **3600** that enables placement of the near field probe **3624** at a particular perspective of the adaptive antenna **3610**. As depicted in FIGS. **36A** and **36B**, more than one near field probe **3624** can be used at various location of the communication device **3600** as will be described below.

[0208] The output signals of the first and second log detectors **3622** and **3626** can be supplied to a difference circuit **3628** that produces a difference signal supplied to an analog to digital converter (A2D) **3630**, which in turn supplies a digital value to a controller **3632** for processing. The difference signal represents a difference in magnitude between the signals supplied by the first and second log detectors **3622** and **3626**. The signal supplied by the first log detector **3622** can represent a measure of a forward feed signal supplied by an RF transmitter **3602**. The difference in magnitude between the forward feed signal and the signal measured by the near field probe **3624** can be used to detect a change in a resonance frequency of the adaptive antenna **3610**. In the embodiment of FIG. **36B**, the controller **3632** would be supplied a digital value from the A2D **3630** that corresponds only to the magnitude of the near field signal generated by the log detector **3626**. The controller **3632** in turn can obtain a digital representation of the magnitude of the forward feed (or transmit) signal supplied by the transmitter **3602** by retrieving a magnitude value from a look-up table based on a known state of the transmitter **3602** or it can obtain it by way of a computational approach that determines the magnitude from the known state of the transmitter **3602**. Once the forward feed magnitude is determined, the controller **3632** can determine a difference between the forward feed and near field signal magnitudes using digital signal processing techniques, and thereby detect a change in a resonance frequency of the adaptive antenna **3610**.

[0209] The adaptive antenna **3610** can be an antenna structure such as any of the embodiments described above. For

instance, the adaptive antenna **3610** can be represented by one of the embodiments of FIGS. **31-35**, which enable programming of the resonant frequency of the antenna. If the detected change of the resonance frequency of the adaptive antenna **3610** is determined to be undesirable based on the difference signals supplied by the A2D **3630**, the adaptive antenna **3610** can be tuned by the controller **3632** by changing the electrical length of the antenna by reconfiguring the structure of the antenna (e.g., adding or removing antenna components), by adding or removing reactive components such as the embodiments of FIGS. **32B**, **33B**, **34B** and **35B**, or changing the reactance of a component of the antenna (e.g., a variable capacitor or variable inductor). As the adaptive antenna **3610** is tuned by the controller **3632**, the controller **3632** can also be configured to program a matching network **3608** or supply the tuning data of the adaptive antenna **3610** to a separate controller of the matching network to enable programming of the match network to adapt to changes applied to the adaptive antenna **3610** while tuning its resonant frequency. It is noted that the near field sensor **3620** as described herein can be used with other antenna structures not described in the subject disclosure.

[0210] What follows is an illustrative algorithm for tuning the adaptive antenna **3610** based on near field rf power measurements. We begin by assuming the adaptive antenna **3610** is tunable with a total of N states. The adaptive antenna **3610** can be set to a particular state, k, based on operating conditions such as a band of operation. The A2D **3630** provides the controller **3632** a relative power measurement, Y, at a specific transmit frequency in use. In one embodiment, an objective is to improve Y. To do this, the k is stepped at time interval, τ , and the response of Y is used to determine if the state should be incremented, decremented, or kept the same. The time τ may be chosen to be longer than a response time of other power control loops used by the communication device **3600** and/or other network operations that may be dependent on the transmit power level from the communication device **3600**. With this in mind, a tuning algorithm can be described as follows:

[0211] Let k_0 be the nominal setting for the state value
 [0212] Let the value of k alternate between k_0 , k_0+1 and k_0-1 :

[0213] $k(n\tau)=k_0+\cos(n\pi/2)$, where n is the number of time increments

[0214] For each state, measure the probe response $Y(n\tau)$

[0215] Calculate the slope, $m=dY/dk$

[0216] Calculate the running average \bar{m} , over M time intervals,

$$\bar{m}=\sum_{r=n-M}^n m(r\tau)$$

[0217] Compare \bar{m} to a threshold δ to determine whether to change the state

[0218] If $\bar{m} \geq \delta$ $k=k-1$

[0219] If $\bar{m} \leq -\delta$ $k=k+1$

[0220] If $|\bar{m}| < \delta$ k is unchanged

[0221] In an embodiment where multiple near field probes **3624** are used, the above algorithm can be changed so that delta measurements of Y are averaged over time. Averaging delta Y readings can increase the reliability of the measurement. In one embodiment, the controller **3632** can select an individual near field probe **3624** using a programmable multiplexer (S) **3625**. The controller **3632** can then apply the above algorithm using only those near field probes **3624** that provide a delta Y with desirable results. This approach can be applied to each near field probe **3624** until one or more near

field probes 3624 are identified as providing desirable tuning results of the adaptive antenna 3610. The controller 3632 can then average the delta Y magnitudes measured for each near field probe 3624, or select only one of the identified near field probes 3624 for tuning the adaptive antenna 3610. In a multi-antenna system where the transmitter 3602 can transmit from any one of a plurality of adaptive antennas 3610, the near field sensor 3620 can be configured to choose a near field probe 3624 closest to the antenna used during transmission for performing the above algorithm. In another embodiment, if for a selected near field probe 3624 the near field sensor 3620 is not performing due to unrepresentative information supplied by the selected near field probe 3624 (e.g., a user's finger is changing the performance of the selected near field probe 3624) then the controller 3632 can be adapted to avoid the identified near field probe 3624 and perform averaging from other probes unaffected by the environment effect.

[0222] In other embodiments averaging can be performed for more than one near field probe 3624 associated with a single adaptive antenna. In yet another embodiment, multiple near field probes 3624 can be placed on each radiating element of an antenna (high band, mid band, and low band near field probes). In another embodiment, one near field probe can be used per radiating element of an antenna. In yet another embodiment, a pad of an integrated circuit (IC) can be used as a near field probe 3624 of an antenna.

[0223] Multiple near field probes 3624 can be used at different locations of the communication device 3600 using a multiplexer 3625 to select between near field probes 3624 to get a measurement of radiated energy of the adaptive antenna 3610 from different perspectives (e.g., bottom, top, sides). FIG. 37 provides a placement illustration of six near field probes 3624 on a printed circuit board. The near field probes 3624 of FIG. 37 are sized to yield -30 dB of coupling with the antenna structure shown. Low band simulations were performed on an antenna structure with a PCB ground of 110 mm×60 mm. FIG. 38 depicts six use cases applied to the circuit board of FIG. 37. The gray sections of each use case represent body tissue or steel. The simulation further assumed a 2 mm air gap between a furthest model element and a log material.

[0224] FIG. 39 depicts return loss plots (S11) for steel and body tissue and their respective efficiencies for each use case. Compared with free space, the resonant frequency of the antenna shifts from free space from -150 to +60 MHz. The efficiency changes from -18 to -2 dB. The Smith charts of FIG. 40 depict steel and body tissue plots of all probes for all use cases. FIG. 41 depicts magnitude and phase response of probe 2 which is closest to an end of the antenna. FIG. 42 depicts the magnitude and phase response of probe 4 which is to the left of the antenna. In this latter embodiment, the response is not well behaved, which illustrates that not all probe locations may provide optimal results. FIG. 43 depicts phase shift versus antenna frequency shift plots for probe 2. These plots show that the phase shift experienced at probe 2 correlates with an observed frequency shift. The sensitivity is about 0.24 degrees per MHz. FIG. 44 depicts power shift versus antenna radiated power shift plots for probe 2. These plots show that the magnitude shift experienced at probe 2 correlates worst with an observed power shift. Probe 7 (opposite end of ground) correlates best with the radiated power shift. The sensitivity is about 0.28 degrees per radiated power shift.

[0225] FIGS. 45-48 depict simulations for an aperture tuned antenna model. FIG. 45 depicts two embodiments having near field probes placed near and far from an antenna located at one end of a PCB having dimensions of 60 mm×126 mm. The antenna is designed for a low band nominal frequency of 860 MHz. A variable inductor (Ltune) can be changed to shift the resonant frequency of the antenna. The models shown in FIG. 45 can be used to determine how much improvement can be made by changing Ltune in several loading scenarios.

[0226] FIG. 46 depicts free space resonance tuning using Ltune. Return loss (S11) is presented in the pots of FIG. 46 as a function of the value of Ltune. The simulations assume in free space a nominal setting of L=5.6 nH at a resonant frequency of 860 MHz. The simulation methodology included running each of the models of FIG. 45 with all of the loading cases shown in FIG. 38. The value of Ltune is then swept for each loading case. A determination is then made of the maximum radiated power at the desired operating frequency (fc) over the sweep of Ltune. The maximum radiated power is then compared based on metrics such as maximizing a magnitude of S21 (power coupled to the near field probe), minimizing a magnitude of S11, and normalizing S21 phase to 0 degrees (the normalized phase is the measured S21 phase minus the reference phase delay at resonance center determined from the free space model or by the actual phase when the antenna is tuned to the desired frequency).

[0227] FIG. 47 depicts an efficiency gain by optimization of tuning for the case of the near field probe nearest the antenna in FIG. 45. FIG. 47 shows an improvement in radiated power from 0 to 2.2 dB depending on loading case. It is further observed that an ideal optimization of S21 or S11 results in nearly the same gain as optimizing on radiated power itself. It is also observed that optimizing on S21 phase also works well except in five of the six loading cases. FIG. 48 depicts an efficiency gain by optimization of tuning for the case of the probe opposite the antenna in FIG. 45. FIG. 48 shows again that optimization of S21 or S11 are reliable. However, in this case, optimizing on S21 phase works poorly in the situation where near field probe is far from the antenna.

[0228] FIG. 49 depicts an illustrative implementation of a near field sensor. In one embodiment, the near field sensor can comprise a transmission line coupled to a directional coupler, an RF IC (e.g., an Analog Devices AD8302) powered by a battery for measuring amplitude and phase between a forward feed signal supplied by the directional coupler, and a signal supplied by the near field probe. The magnitude and phase measured by the RF IC can be supplied to a controller that performs algorithmic steps as described earlier for detecting a change in a desire frequency of the antenna. RF paths AB and AC can be configured to 90 degrees of path difference for nominal free space, which is the center of the measurement range for phase of the RF IC. RF paths AB and AC can be set to ~30 dB path loss, the center of the input range being -30 dBm. FIG. 50 depicts a PCB layout of the near field sensor.

[0229] It is noted that any of the adaptive antenna embodiments described in the subject disclosure can be applied to multiple MIMO configuration (2×2, 4×4, etc.) or diversity configurations. It is further noted that adaptive antenna embodiments described in the subject disclosure can be applied to multiband antenna structures. In such configurations, the subject disclosure enables support for carrier aggregation of multiple bands for simultaneous transmission or

reception in MIMO or diversity configurations, while maintaining at least some isolation between antenna ports.

[0230] FIG. 51 depicts an illustrative embodiment of a method 5100 that can be applied to the embodiments of the subject disclosure. The method 5100 can begin at step 5102 where circuitry (such as a log detector) can be used to measure a magnitude of a forward feed signal supplied by a directional coupler coupled to an adaptive antenna by way of a matching network. At step 5104 a near field probe can be used to measure a magnitude of radiated energy from the adaptive antenna. At step 5106 a difference between the magnitude of the forward feed signal and the radiated energy of the antenna can be determined. At step 5110 a determination can be made whether the difference in magnitude results in a change in the operating frequency (fc) of the adaptive antenna. If there is no change (or an insignificant change) in the operating frequency (fc) is detected, method 5100 can be adapted for repeating subsequent iterations of method 5100 beginning from step 5102. If the change in the operating frequency (fc) is considered significant, at step 5112 a frequency offset error can be determined according to the difference in magnitude determined at step 5106.

[0231] If the frequency offset error is considered insignificant, method 5100 can be repeated in subsequent iterations beginning from step 5102. If, however, the frequency offset error is considered undesirable (or unacceptable), at step 5114 the adaptive antenna can be tuned by, for example, varying the electrical length of the antenna based on an Ltune value calculated from the difference in magnitude between the forward feed signal and the radiated energy of the antenna. The Ltune value can be used to configure a switched array of inductors such as shown in FIGS. 32B, 33B, 34B and 35B. Alternatively, a tuning value can be calculated from the difference in magnitude between the forward feed signal and the radiated energy of the antenna, which can be used to tune one or more programmable variable reactive elements (such as one or more variable capacitors, one or more variable inductors, or combinations thereof) coupled to the antenna that reconfigure the electrical length of the antenna, and thereby change the operating frequency of the antenna to a desirable frequency.

[0232] FIG. 52 depicts another illustrative embodiment of a near field sensor 5210. In this embodiment, the near field sensor 5210 can be configured to perform operations including measuring phase changes in signals radiated by the adaptive antenna 3610 using one or more near field probes 3624, measuring a phase of a forward feed signal using a directional coupler 3604, determining a phase offset between the phase radiated energy emitted by the adaptive antenna 3610 and the phase of the forward feed signal supplied to the adaptive antenna 3610 using a phase detector 5212, and tuning the operating frequency of the adaptive antenna 3610 according to the phase offset using the controller 3632. FIG. 53 depicts a phase detector from Analog Devices™ (AD8302), which can be used in the subject disclosure. The phase detector of FIG. 53 can be used for measuring gain/loss and phase up to a frequency of 2.7 GHz. The phase detector includes dual demodulating log amps with a phase detector input range of -60 dBm to 0 dBm in a 50 Ohm system.

[0233] In one embodiment, an inductive, capacitive, and resistive (LRC) model (such as shown by reference 5214) of an unloaded adaptive antenna 3610 can be characterized by an antenna supplier. The LRC characteristics of the adaptive antenna 3610 can be characterized at a time of manufacture of

the adaptive antenna 3610. Characterization and/or factory measurements can be stored in a look-up table (or hardcoded) in an algorithm executed by a controller or ASIC design for calculating a frequency offset measurement to perform tuning of the adaptive antenna 3610. A phase calibration measurement can also be performed on a detector chain (directional coupler 3604, phase detector 5212, near field antennas 3624) to remove phase measurement error in the algorithm. Phase calibration may depend on frequency of operation of the adaptive antenna 3610. Accordingly, a phase calibration look-up table can be implemented that is frequency dependent to accommodate changes in calibration based on frequency of operation of the adaptive antenna 3610.

[0234] In one embodiment, the impedance of the LRC model 5214 can be described by the following equation:

$$Z = R + j\omega L + \frac{1}{j\omega C}$$

[0235] where $\omega=2\pi f$ and f is frequency. The complex power delivered can be described by the equation:

$$S = \frac{V^2}{R + j\omega L + \frac{1}{j\omega C}} = \frac{V^2}{R + j\left(\omega L - \frac{1}{\omega C}\right)} = \frac{R - j\left(\omega L - \frac{1}{\omega C}\right)}{R^2 + \left(\omega L - \frac{1}{\omega C}\right)^2} * V^2$$

[0236] Based on the above equation, phase of S can be determined according to equation:

$$\phi = \text{atan}\left(\frac{\frac{1}{\omega C} - \omega L}{R}\right)$$

[0237] When $\phi=0$, the antenna model 5214 is at resonance.

[0238] Solving for ω :

$$\begin{aligned} \omega^2 L + R * \tan\phi * \omega - \frac{1}{C} &= 0 \\ \omega(\phi) &= \frac{-R * \tan\phi + \sqrt{R^2 * \tan^2\phi + \frac{4L}{C}}}{2L} \\ f(\phi) &= \frac{\omega(\phi)}{2\pi} \end{aligned}$$

[0239] From the above equations, the following conditions can be assessed:

[0240] If $f_{\text{operation}(op)} = f_{\text{resonance}(r)}$, then $\phi=0$, and $\omega=1/\sqrt{LC}=\omega_0$

[0241] If $f_{op} < f_r$, then $\phi > 0$, and $\omega < 1/\sqrt{LC}$

[0242] If $f_{op} > f_r$, then $\phi < 0$

[0243] Based on the above observations, one embodiment of an algorithm for detecting a change in an operating frequency of the adaptive antenna 3610 can comprise the following steps:

[0244] Phase detector 5212 measures a differential phase ϕ

[0245] The controller 3632 can then calculate a measured frequency according to $\omega_{measured}=f(\theta)$

[0246] The controller 3632 knows the desired frequency ω_{target}

[0247] The controller 3632 can then calculate a relative scaling error in the measured versus the target frequency $\alpha_{offset}=\omega_{measured}/\omega_{target}$

[0248] As noted earlier, a phase calibration measurement can be performed on the detector chain to remove phase measurement error. This can be factored into calculating the α_{offset}

[0249] α_{offset} may be integrated or averaged over a time interval or a number of samples to reduce noise or sensitivity to transients shorter than desired time interval

[0250] Also described earlier, the antenna resonance can be modeled according to $\omega_0=1/\sqrt{LC}$

[0251] To correct a detected offset in frequency back to a target frequency (ω_{target}), the present operating frequency ($\omega_{measured}$) can be multiplied by $1/\alpha_{offset}$

[0252] Removing the offset can be accomplished by tuning L or C of the antenna. As noted earlier, the LC modeling of the antenna can be characterized in a lab setting, during manufacturing, or by other suitable means. An aperture tuner using a switch array of inductors such as shown in FIGS. 32B-35B can be used to tune the adaptive antenna 3610. Tunable capacitive devices can also be used in place of the tunable inductors or combinations thereof

[0253] To remove the detected frequency offset, the adaptive antenna 3610 can be tuned such that the product of LC is changed by a factor of α_{offset}^2 to return $\omega_{measured}$ to ω_{target} .

[0254] The plots of FIG. 54 depict phase error versus frequency and power level of the phase detector (AD8302 shown in FIG. 53). To improve the accuracy of phase detection data provided by the phase detector to the controller, the phase detector can be utilized in a configuration whereby a phase delay from a near field probe is set using a length of delay line such that an RF signal reaching the phase detector input from the near field probe is approximately 90 degrees out of phase with an RF signal reaching another phase detector input from the directional coupler under nominal conditions, taken as a free space condition. In another embodiment, the delay line can be instead applied to the RF signal supplied by the directional coupler.

[0255] FIG. 55 depicts an illustrative embodiment of a method 5500 for frequency offset detection and tuning based on phase measurements. Method 5500 can begin with step 5502 in which a forward feed signal (e.g., a transmit signal supplied by the transmitter 3602) is measured by way of the directional coupler 3604 and supplied to the phase detector 5212. Similarly, at step 5504, the near field probe 3624 can supply a measure of a signal representing radiated energy from the adaptive antenna 3610. As noted in other embodiments, a switch, such as shown in FIG. 52, can be used to select from a plurality of near field probes 3624 to provide measurements of radiated energy from the adaptive antenna 3610 from multiple positions of the probes. The controller 3632 can selectively use multiple measurements from one or more near field probes 3624 to improve the accuracy of the algorithm.

[0256] At step 5506, the phase detector 5212 can generate a phase differential based on the phase of the signals mea-

sured at steps 5502 and 5504. A digital representation of the phase differential is then supplied by the A2D 3630 to the controller 3632 for calculating a frequency offset (α_{offset}). The controller 3632 at step 5505 can retrieve phase calibration data from a look-up table based on a target frequency of operation or a measured frequency of operation. In one embodiment the look-up table can further depend on an open loop state of the antenna and use case information such as whether a communication device utilizing the antenna structure of the subject disclosure is being held by a user's hand, whether the communication device is in a position next to a user's ear, and so on. The phase calibration data can be used to adjust calibration errors in the phase differential. To calculate a frequency offset as described above, the controller 3632 can also retrieve from a look-up table at step 5507 an LRC model of the adaptive antenna 3610, which may also be frequency dependent. The calibration data and the LRC model can be stored in a memory of a communication device that integrates the embodiments of FIG. 52. At step 5510, the controller 3632 can determine whether a change in frequency from a desired target frequency has occurred. A change in frequency can be determined when, for example, α_{offset} is greater than or less than unity (i.e., 1).

[0257] At step 5512, the controller 3632 can be configured to make a determination whether the frequency offset is significant enough to warrant retuning of the measured operating frequency of the adaptive antenna 3610. To avoid excessive retuning of the adaptive antenna 3610, the controller 3632 can be configured to compare α_{offset} to a range of thresholds. For example, when $\alpha_{offset}>1$, α_{offset} can be compared to a first threshold. The first threshold can represent an acceptable frequency overshoot range of the frequency measured ($\omega_{measured}$) above the target frequency (ω_{target}). Similarly, when $\alpha_{offset}<1$, α_{offset} can be compared to a second threshold. The second threshold can represent an acceptable frequency undershoot range of the frequency measured ($\omega_{measured}$) below the target frequency (ω_{target}). The first and second thresholds can be based on specifications provided by a network provider. Thus, when the frequency measured exceeds the first threshold or is below the second threshold, the controller 3632 can proceed to step 5514 where it retunes the adaptive antenna 3610 as previously described in the subject disclosure to bring α_{offset} closer to unity.

[0258] It is further noted that more than two thresholds (e.g., two thresholds for detecting large offsets and two additional thresholds for detecting smaller offsets) can be used to enable a determination when a coarse tuning versus a fine tuning of the adaptive antenna 3610 is required.

[0259] In another embodiment of the subject disclosure, method 5500 of FIG. 55 can be adapted to use a first look-up table that maps a detected phase output voltage to a frequency shift, and a second lookup table that maps antenna tuning states to the frequency shift determined from the first look-up table. Accordingly, when the controller 3632 reads a voltage signal from the phase detector 5212 in digital format provided by the A2D 3630, the controller 3632 proceeds to look up a frequency shift in the first look-up table, then utilizes the frequency shift to index through the second look-up table to obtain one or more state increments to shift the frequency of the antenna to a desired state. The one or more state increments can represent an adjustment of the electrical length of the adaptive antenna 3610 utilizing an array of selectable inductors such as shown in FIGS. 32B-35B.

[0260] In also noted that the methods depicted in FIGS. 51 and 55 can be combined to further enhance frequency offset detection and retuning. For example, in one embodiment delta averages of Y can be compared to delta averages of α_{offset} and such comparisons can be used to estimate a frequency offset. In another embodiment, delta averages of Y can be correlated to expected delta averages of α_{offset} which can be recorded in a look-up table. Similarly, delta averages of α_{offset} can be correlated to expected delta averages of Y, which can be recorded in a look-up table. The look-up tables can in turn be used for validation of a frequency offset calculation. Other suitable techniques can be used to compare the results of one algorithm against the other for validation of measurements.

[0261] RF magnitude detection (embodiment of FIG. 51) and RF phase detection (embodiment of FIG. 54) can be used together to provide improved antenna frequency tuning. The RF magnitude detection provides a direct measurement of radiated power. Phase detection yields an instantaneous estimate of the amount of frequency error, and hence the amount of correction needed. In one embodiment the frequency error estimate determined from phase detection may be used to calculate a specific amount of frequency shift and direction for the next iterative step in the magnitude detection algorithm. Thus phase detection algorithm of FIG. 54 can enable the RF magnitude algorithm of FIG. 51 to close in on a desired frequency of operation.

[0262] In one embodiment, an iterative algorithm for mitigating a frequency offset can utilize both magnitude and phase readings as described in the subject disclosure to determine an error estimate. The error estimate can be based on a weighted combination of both magnitude (mbar) and phase (α_{offset}) offsets, with the algorithm seeking to reduce the combined error estimate instead of relying on either the magnitude or phase error estimates individually.

[0263] In one embodiment, a look-up table can be used that is indexed by a transmit power and a frequency band of operation known to the controller 3632. The look-up table can include a list of expected differential phase measurements produced by the phase detector 5212 at a known transmit power and frequency band, which can be measured when for the adaptive antenna 3610 is operating in an optimal environment (e.g., free space). In cases where a use case of a communication device utilizing the adaptive antenna 3610 can be determined (e.g., communication device held next to a user's ear, communication device held in user's hand away from the user's head, etc.), the look-up table can be further enhanced to provide expected differential phase measurements based on the combination of transmit power, frequency band and use case. The look-up table of differential phase measurements can be determined in a lab setting, during manufacturing, or in other suitable controlled environments for characterizing a front-end transmission circuit such as shown in FIG. 52. Inherent in the differential phase measurements of the look-up table would be any phase error produced by any of the devices in the front-end transmission circuit of FIG. 52 at a given frequency and transmit power. The look-up table can thus be used to compare differential phase error measurements produced by the phase detector 5212 while a communication device is in use versus an expected differential phase error provided by the look-up table at a given transmit power and frequency band known to the controller 3632.

[0264] The difference between a differential phase measurement produced by the phase detector 5212 while the communication device is in use and an expected differential phase error obtained from the look-up table can be used by the controller 3632 to determine a frequency offset of the adaptive antenna 3610. An additional look-up table indexed by the determined frequency offset can be used to determine incremental tuning steps for controlling an aperture tuner of the adaptive antenna 3610 to reduce the frequency offset. The algorithm associated with this embodiment can be used as an approach for coarse frequency tuning of the adaptive antenna 3610, while determining a change in the operating frequency of the adaptive antenna 3610 based on a measure of α_{offset} as described earlier can be used for fine tuning the operating frequency of the adaptive antenna 3610.

[0265] In yet another embodiment, frequency tuning of the adaptive antenna 3610 based on any of the embodiments of the subject disclosure can be coordinated with adaptive tuning of a matching network coupled to the adaptive antenna 3610. For instance, while tuning a frequency of the adaptive antenna 3610, an algorithm for tuning the matching network can be maintained in abeyance until such time as the frequency tuning is finished. Similarly, while the controller 3632 is tuning a matching network, an algorithm for frequency tuning can be placed in abeyance until the match tuner is finished. Additionally, switching between match tuning and frequency tuning algorithms can be triggered by thresholds of optimization and/or timers that limit a time for each algorithm to perform its function. To stabilize match tuning and frequency tuning algorithms, a desirable range of optimization of both algorithms can be established so that the combination of the algorithms achieves a common goal and tuning of either a match or frequency offset reaches a point of stability.

[0266] FIG. 56 depicts an illustrative embodiment of a communication device 5600. The communication device 5600 can comprise a wireline and/or wireless transceiver 5602 (herein transceiver 5602), a user interface (UI) 5604, a power supply 5614, a location receiver 5616, a motion sensor 5618, an orientation sensor 5620, and a controller 5606 for managing operations thereof. The transceiver 5602 can support short-range or long-range wireless access technologies such as Bluetooth, ZigBee, WiFi, DECT, or cellular communication technologies, just to mention a few. Cellular technologies can include, for example, CDMA-1X, UMTS/HSDPA, GSM/GPRS, TDMA/EDGE, EV/DO, WiMAX, SDR, LTE, as well as other next generation wireless communication technologies as they arise. The transceiver 5602 can also be adapted to support circuit-switched wireline access technologies (such as PSTN), packet-switched wireline access technologies (such as TCP/IP, VoIP, etc.), and combinations thereof. The transceiver 5602 can be adapted to utilize any of the aforementioned adaptive antenna embodiments described above singly or in any combination.

[0267] The UI 5604 can include a depressible or touch-sensitive keypad 5608 with a navigation mechanism such as a roller ball, a joystick, a mouse, or a navigation disk for manipulating operations of the communication device 5600. The keypad 5608 can be an integral part of a housing assembly of the communication device 5600 or an independent device operably coupled thereto by a tethered wireline interface (such as a USB cable) or a wireless interface supporting for example Bluetooth. The keypad 5608 can represent a numeric keypad commonly used by phones, and/or a QWERTY keypad with alphanumeric keys. The UI 5604 can

further include a display **5610** such as monochrome or color LCD (Liquid Crystal Display), OLED (Organic Light Emitting Diode) or other suitable display technology for conveying images to an end user of the communication device **5600**. In an embodiment where the display **5610** is touch-sensitive, a portion or all of the keypad **5608** can be presented by way of the display **5610** with navigation features.

[0268] The display **5610** can use touch screen technology to also serve as a user interface for detecting user input. As a touch screen display, the communication device **5600** can be adapted to present a user interface with graphical user interface (GUI) elements that can be selected by a user with a touch of a finger. The touch screen display **5610** can be equipped with capacitive, resistive or other forms of sensing technology to detect how much surface area of a user's finger has been placed on a portion of the touch screen display. This sensing information can be used to control the manipulation of the GUI elements or other functions of the user interface. The display **5610** can be an integral part of the housing assembly of the communication device **5600** or an independent device communicatively coupled thereto by a tethered wireline interface (such as a cable) or a wireless interface.

[0269] The UI **5604** can also include an audio system **5612** that utilizes audio technology for conveying low volume audio (such as audio heard in proximity of a human ear) and high volume audio (such as speakerphone for hands free operation). The audio system **5612** can further include a microphone for receiving audible signals of an end user. The audio system **5612** can also be used for voice recognition applications. The UI **5604** can further include an image sensor **5613** such as a charged coupled device (CCD) camera for capturing still or moving images.

[0270] The power supply **5614** can utilize common power management technologies such as replaceable and rechargeable batteries, supply regulation technologies, and/or charging system technologies for supplying energy to the components of the communication device **5600** to facilitate long-range or short-range portable applications. Alternatively, or in combination, the charging system can utilize external power sources such as DC power supplied over a physical interface such as a USB port or other suitable tethering technologies.

[0271] The location receiver **5616** can utilize location technology such as a global positioning system (GPS) receiver capable of assisted GPS for identifying a location of the communication device **5600** based on signals generated by a constellation of GPS satellites, which can be used for facilitating location services such as navigation. The motion sensor **5618** can utilize motion sensing technology such as an accelerometer, a gyroscope, or other suitable motion sensing technology to detect motion of the communication device **5600** in three-dimensional space. The orientation sensor **5620** can utilize orientation sensing technology such as a magnetometer to detect the orientation of the communication device **5600** (north, south, west, and east, as well as combined orientations in degrees, minutes, or other suitable orientation metrics).

[0272] The communication device **5600** can use the transceiver **5602** to also determine a proximity to a cellular, WiFi, Bluetooth, or other wireless access points by sensing techniques such as utilizing a received signal strength indicator (RSSI) and/or signal time of arrival (TOA) or time of flight (TOF) measurements. The controller **5606** can utilize computing technologies such as a microprocessor, a digital signal processor (DSP), programmable gate arrays, application spe-

cific integrated circuits, and/or a video processor with associated storage memory such as Flash, ROM, RAM, SRAM, DRAM or other storage technologies for executing computer instructions, controlling, and processing data supplied by the aforementioned components of the communication device **400**.

[0273] Other components not shown in FIG. **56** can be used in one or more embodiments of the subject disclosure. For instance, the communication device **5600** can include a reset button (not shown). The reset button can be used to reset the controller **5606** of the communication device **5600**. In yet another embodiment, the communication device **5600** can also include a factory default setting button positioned, for example, below a small hole in a housing assembly of the communication device **5600** to force the communication device **5600** to re-establish factory settings. In this embodiment, a user can use a protruding object such as a pen or paper clip tip to reach into the hole and depress the default setting button. The communication device **400** can also include a slot for adding or removing an identity module such as a Subscriber Identity Module (SIM) card. SIM cards can be used for identifying subscriber services, executing programs, storing subscriber data, and so forth.

[0274] The communication device **5600** as described herein can operate with more or less of the circuit components shown in FIG. **56**. These variant embodiments can be used in one or more embodiments of the subject disclosure.

[0275] It should be understood that devices described in the exemplary embodiments can be in communication with each other via various wireless and/or wired methodologies. The methodologies can be links that are described as coupled, connected and so forth, which can include unidirectional and/or bidirectional communication over wireless paths and/or wired paths that utilize one or more of various protocols or methodologies, where the coupling and/or connection can be direct (e.g., no intervening processing device) and/or indirect (e.g., an intermediary processing device such as a router).

[0276] FIG. **57** depicts an exemplary diagrammatic representation of a machine in the form of a computer system **5700** within which a set of instructions, when executed, may cause the machine to perform any one or more of the embodiments described above. One or more instances of the machine can utilize the aforementioned adaptive antenna embodiments singly or in any combination. In some embodiments, the machine may be connected (e.g., using a network **5726**) to other machines. In a networked deployment, the machine may operate in the capacity of a server or a client user machine in server-client user network environment, or as a peer machine in a peer-to-peer (or distributed) network environment.

[0277] The machine may comprise a server computer, a client user computer, a personal computer (PC), a tablet PC, a smart phone, a laptop computer, a desktop computer, a control system, a network router, switch or bridge, or any machine capable of executing a set of instructions (sequential or otherwise) that specify actions to be taken by that machine. It will be understood that a communication device of the subject disclosure includes broadly any electronic device that provides voice, video or data communication. Further, while a single machine is illustrated, the term "machine" shall also be taken to include any collection of machines that individually or jointly execute a set (or multiple sets) of instructions to perform any one or more of the methods discussed herein.

[0278] The computer system 5700 may include a processor (or controller) 5702 (e.g., a central processing unit (CPU), a graphics processing unit (GPU), or both), a main memory 5704 and a static memory 5706, which communicate with each other via a bus 5708. The computer system 5700 may further include a display unit 5710 (e.g., a liquid crystal display (LCD), a flat panel, or a solid state display). The computer system 5700 may include an input device 5712 (e.g., a keyboard), a cursor control device 5714 (e.g., a mouse), a disk drive unit 5716, a signal generation device 5718 (e.g., a speaker or remote control) and a network interface device 5720. In distributed environments, the embodiments described in the subject disclosure can be adapted to utilize multiple display units 5710 controlled by two or more computer systems 5700. In this configuration, presentations described by the subject disclosure may in part be shown in a first of the display units 5710, while the remaining portion is presented in a second of the display units 5710.

[0279] The disk drive unit 5716 may include a tangible computer-readable storage medium 5722 on which is stored one or more sets of instructions (e.g., software 5724) embodying any one or more of the methods or functions described herein, including those methods illustrated above. The instructions 5724 may also reside, completely or at least partially, within the main memory 5704, the static memory 5706, and/or within the processor 5702 during execution thereof by the computer system 5700. The main memory 5704 and the processor 5702 also may constitute tangible computer-readable storage media.

[0280] Dedicated hardware implementations including, but not limited to, application specific integrated circuits, programmable logic arrays and other hardware devices that can likewise be constructed to implement the methods described herein. Application specific integrated circuits and programmable logic array can use downloadable instructions for executing state machines and/or circuit configurations to implement embodiments of the subject disclosure. Applications that may include the apparatus and systems of various embodiments broadly include a variety of electronic and computer systems. Some embodiments implement functions in two or more specific interconnected hardware modules or devices with related control and data signals communicated between and through the modules, or as portions of an application-specific integrated circuit. Thus, the example system is applicable to software, firmware, and hardware implementations.

[0281] In accordance with various embodiments of the subject disclosure, the operations or methods described herein are intended for operation as software programs or instructions running on or executed by a computer processor or other computing device, and which may include other forms of instructions manifested as a state machine implemented with logic components in an application specific integrated circuit or field programmable gate array. Furthermore, software implementations (e.g., software programs, instructions, etc.) including, but not limited to, distributed processing or component/object distributed processing, parallel processing, or virtual machine processing can also be constructed to implement the methods described herein. It is further noted that a computing device such as a processor, a controller, a state machine or other suitable device for executing instructions to perform operations or methods may perform such operations directly or indirectly by way of one or more intermediate devices directed by the computing device.

[0282] While the tangible computer-readable storage medium 5722 is shown in an example embodiment to be a single medium, the term “tangible computer-readable storage medium” should be taken to include a single medium or multiple media (e.g., a centralized or distributed database, and/or associated caches and servers) that store the one or more sets of instructions. The term “tangible computer-readable storage medium” shall also be taken to include any non-transitory medium that is capable of storing or encoding a set of instructions for execution by the machine and that cause the machine to perform any one or more of the methods of the subject disclosure.

[0283] The term “tangible computer-readable storage medium” shall accordingly be taken to include, but not be limited to: solid-state memories such as a memory card or other package that houses one or more read-only (non-volatile) memories, random access memories, or other re-writable (volatile) memories, a magneto-optical or optical medium such as a disk or tape, or other tangible media which can be used to store information. Accordingly, the disclosure is considered to include any one or more of a tangible computer-readable storage medium, as listed herein and including art-recognized equivalents and successor media, in which the software implementations herein are stored.

[0284] Although the present specification describes components and functions implemented in the embodiments with reference to particular standards and protocols, the disclosure is not limited to such standards and protocols. Each of the standards for Internet and other packet switched network transmission (e.g., TCP/IP, UDP/IP, HTML, HTTP) represent examples of the state of the art. Such standards are from time-to-time superseded by faster or more efficient equivalents having essentially the same functions. Wireless standards for device detection (e.g., RFID), short-range communications (e.g., Bluetooth, WiFi, Zigbee), and long-range communications (e.g., WiMAX, GSM, CDMA, LTE) can be used by computer system 5700.

[0285] The illustrations of embodiments described herein are intended to provide a general understanding of the structure of various embodiments, and they are not intended to serve as a complete description of all the elements and features of apparatus and systems that might make use of the structures described herein. Many other embodiments will be apparent to those of skill in the art upon reviewing the above description. The exemplary embodiments can include combinations of features and/or steps from multiple embodiments. Other embodiments may be utilized and derived therefrom, such that structural and logical substitutions and changes may be made without departing from the scope of this disclosure. Figures are also merely representational and may not be drawn to scale. Certain proportions thereof may be exaggerated, while others may be minimized. Accordingly, the specification and drawings are to be regarded in an illustrative rather than a restrictive sense.

[0286] Although specific embodiments have been illustrated and described herein, it should be appreciated that any arrangement calculated to achieve the same purpose may be substituted for the specific embodiments shown. This disclosure is intended to cover any and all adaptations or variations of various embodiments. Combinations of the above embodiments, and other embodiments not specifically described herein, can be used in the subject disclosure.

[0287] The Abstract of the Disclosure is provided with the understanding that it will not be used to interpret or limit the

scope or meaning of the claims. In addition, in the foregoing Detailed Description, it can be seen that various features are grouped together in a single embodiment for the purpose of streamlining the disclosure. This method of disclosure is not to be interpreted as reflecting an intention that the claimed embodiments require more features than are expressly recited in each claim. Rather, as the following claims reflect, inventive subject matter lies in less than all features of a single disclosed embodiment. Thus the following claims are hereby incorporated into the Detailed Description, with each claim standing on its own as a separately claimed subject matter.

[0288] It is to be understood that although the disclosure has been described above in terms of particular embodiments, the foregoing embodiments are provided as illustrative only, and do not limit or define the scope of the disclosure.

[0289] Various other embodiments, including but not limited to the following, are also within the scope of the claims. For example, the elements or components of the various multimode antenna structures described herein may be further divided into additional components or joined together to form fewer components for performing the same functions. For example, the antenna elements and the connecting element or elements that are part of a multimode antenna structure may be combined to form a single radiating structure having multiple feed points operatively coupled to a plurality of antenna ports or feed points.

[0290] It is further noted that the low band and high band antennae structures described in the subject disclosure may be different or dissimilar antenna types, such as, for example, monopole, PIFA, loop, dielectric or other structures known in the art. It is also noted that the embodiments described herein may represent other sub-frequency ranges such as, for example, low band, mid band, and high band. Accordingly, the antenna structures described herein may have differing antenna types, and differing frequency ranges.

[0291] Having described embodiments of the present disclosure, it should be apparent that modifications can be made without departing from the spirit and scope of the disclosure.

What is claimed is:

1. A method, comprising:
 - measuring, by a circuit, from a first probe a first phase of radiated energy by an antenna, wherein the first probe is placed near the antenna;
 - measuring, by the circuit, from a second probe a second phase of a transmit signal supplied to the antenna, wherein the second probe is placed in a transmission path of the transmit signal;
 - comparing, by the circuit, the first and the second phases to generate a phase differential;
 - detecting, by the circuit, an offset in an operating frequency of the antenna based on the phase differential; and
 - adjusting, by the circuit, the operating frequency of the antenna to mitigate the offset in the operating frequency of the antenna.
2. The method of claim 1, wherein the detecting of the offset in the operating frequency comprises determining the offset according to a reactive profile of the antenna and the phase differential.
3. The method of claim 2, further comprising retrieving the reactive profile of the antenna from a look-up table.
4. The method of claim 3, wherein the frequency of the antenna is adjusted by modifying an electrical length of the antenna, wherein the difference between the first and the second phases is proportional to the offset in the operating

frequency of the antenna, wherein the second probe comprises a directional coupler, and wherein the offset in the operating frequency of the antenna is caused by the antenna being exposed to an environmental effect.

5. The method of claim 1, wherein a third probe is placed near the antenna to form a plurality of near field probes.

6. The method of claim 5, further comprising:

- measuring a plurality of phases of the radiated energy from the plurality of near field probes; and
- monitoring the plurality of phases measured to improve an accuracy of one of the comparing step, the detecting step, the adjusting step, or any combination thereof.

7. The method of claim 1, wherein the antenna comprises an aperture tuner to adjust a resonant frequency range of the antenna, and wherein the adjusting of the operating frequency of the antenna is performed by supplying a signal to the aperture tuner.

8. The method of claim 7, wherein the aperture tuner comprises a variable reactive element to adjust the resonant frequency range of the antenna.

9. The method of claim 7, wherein the aperture tuner comprises a switchable array of reactive elements to adjust the resonant frequency range of the antenna.

10. The method of claim 7, wherein the aperture tuner comprises one of a variable capacitor, a variable inductor, or a combination thereof.

11. An antenna structure, comprising:

- a first antenna element;
- a first aperture tuner for adjusting an operating frequency of the antenna element;
- a probe; and
- a first near field sensor for sensing radiated energy from the first antenna element, wherein the first near field sensor and the first aperture tuner are coupled to a circuit that performs operations comprising:
 - measuring from the first near field sensor a first phase of radiated energy by the first antenna element;
 - measuring from the probe a second phase of a first signal supplied to the first antenna element;
 - comparing the first and the second phases to generate a first phase differential;
 - detecting a change in an operating frequency of the first antenna element based on the phase differential; and
 - directing the first aperture tuner to adjust the operating frequency of the first antenna element according to the first phase differential.

12. The antenna structure of claim 11, wherein the probe comprises a directional coupler coupled to a path that supplies the first signal to the first antenna element.

13. The antenna structure of claim 11, wherein the detecting of the change in the operating frequency of the first antenna element comprises determining the change in the operating frequency of the first antenna element according to a reactive profile of the antenna.

14. The antenna structure of claim 13, further comprising retrieving the reactive profile from a look-up table.

15. The antenna structure of claim 14, wherein the look-up table is indexed according to the operating frequency of the first antenna element.

16. The antenna structure of claim 11, wherein the first antenna element is adjusted by modifying an electrical length of the antenna element using the first aperture tuner, and

wherein the first phase differential is proportional to the change in the operating frequency of the first antenna element.

17. The antenna structure of claim 11, further comprising a second antenna element.

18. The antenna structure of claim 17, wherein the first antenna element is coupled to the second antenna element by way of a coupling element, and wherein the coupling element causes differential currents and common mode currents flowing through the first antenna element and the second antenna element to combine in a manner that increases signal isolation between a first port of the first antenna element and a second port of the second antenna element.

19. The antenna structure of claim 17, further comprising: a second near field sensor; and

a second aperture tuner, wherein the second antenna element is coupled to the second near field sensor and the second aperture tuner, and wherein the operations further comprise:

measuring from the second near field sensor a third phase of radiated energy by the second antenna element;

measuring a fourth phase of a second signal supplied to the second antenna element;

comparing the third and the fourth phases to generate a second phase differential;

detecting a change in a second operating frequency of the second antenna element based on the second differential phase; and

directing the second aperture tuner to adjust the second operating frequency of the second antenna element according to the second phase differential.

20. The antenna structure of claim 17, wherein the first antenna element and the second antenna element are config-

ured for one of a multiple-input and multiple-output (MIMO) or a diversity antenna configuration.

21. A communication device, comprising:

an antenna structure;

a near field sensor;

a probe; and

a circuit coupled to the near field sensor and probe, wherein the circuit performs operations comprising:

measuring from the near field sensor a first signal representing radiated energy from the antenna structure;

measuring from the probe a second signal supplied to the antenna structure;

determining a phase differential from a first phase of the first signal and a second phase of the second signal;

detecting a frequency offset of the antenna structure based on the phase differential; and

adjusting an operating frequency of the antenna structure to mitigate the frequency offset.

22. The communication device of claim 21, wherein the operating frequency of the antenna structure is adjusted by modifying an electrical length of the antenna structure.

23. The communication device of claim 22, wherein the electrical length is modified with one of a first device having tunable capacitance, a second device having a tunable inductance, or a combination thereof.

24. The communication device of claim 21, wherein the probe comprises a directional coupler coupled to a signal path of the signal.

25. The communication device of claim 21, wherein the communication device comprises one of a cellular telephone or a wireless access point.

* * * * *